THESIS

LANDSLIDE HAZARD ZONATION BASED ON DETERMINISTIC METHOD USING OUTCROP-BASED GEOLOGICAL STRENGTH INDEX (GSI) SYSTEM A CASE STUDY IN KAYANGAN CATCHMENT, KULON PROGO REGENCY, YOGYAKARTA PROVINCE, INDONESIA

Thesis submitted to the Double Degree M.Sc. Programme,
Gadjah Mada University and Faculty of Geo-Information Science and Earth Observation, University of Twente in partial fulfilment of the requirement
for the degree of Master of Science in Geo-Information
for Spatial Planning and Risk Management

By:

Bagus Haryono

UGM : 09/292238/PMU/06158

ITC : 24610-AES

Supervisors :

Dr. Danang Sri Hadmoko, M.Sc. (UGM)

Dr. Dhruba Pikha Shrestha (ITC)

DOUBLE DEGREE M.Sc. PROGRAMME
GADJAH MADA UNIVERSITY
FACULTY OF GEO-INFORMATION SCIENCE
AND EARTH OBSERVATION (ITC)
UNIVERSITY OF TWENTE
2011

THESIS

LANDSLIDE HAZARD ZONATION BASED ON DETERMINISTIC METHOD USING OUTCROP-BASED GEOLOGICAL STRENGTH INDEX (GSI) SYSTEM A CASE STUDY IN KAYANGAN CATCHMENT, KULON PROGO REGENCY, YOGYAKARTA PROVINCE, INDONESIA

By:

Bagus Haryono

UGM : 09/292238/PMU/06158

ITC : 24610-AES

Has been approved in Yogyakarta

On ... February 2011

By Thesis Assessment Board :

Supervisor 1 :

Dr. Danang Sri Hadmoko, M.Sc.

ITC Examiner 1 :

Prof. Dr. Victor Jetten

Supervisor 2 :

Dr. Dhruba Pikha Shrestha

ITC Examiner 2 :

Drs. Tom Loran

This thesis has been accepted as one of the requirements
To obtain a Master's degree
Date 22 MAR 2011

Program Director of
Geo-Information for Spatial
Planning and Risk Management

Prof. Dr. H.A. Sudibyakto, M.S.

On be half of Director
Vice Director for Academic Affairs,
Development and Cooperation

Prof. Ir. Suryo Purwono, MA.Sc., Ph.D.

dedicated to :

Celvy Sulistiyaning Darmawati
Lintang Pinilih and his sister

..... my constant inspiration .....

DISCLAIMER

This document describes work undertaken as part of a program of study at the Double Degree International Program of Geo-Information for Spatial Planning and Risk Management, a Joint Educational Program of Gadjah Mada University, Indonesia and Faculty of Geo-Information Science and Earth Observation, University of Twente, the Netherlands. All views and opinions expressed therein remain the sole responsibility of the author, and do not necessarily represent those of the institute.

Yogyakarta, February 2011

Bagus Haryono

ABSTRACT

In Indonesia that has tropical climate, landslide becomes one of damaging natural disasters. It causes disadvantages such as properties damages and victims of people. The occurence of landslide is very common due to intense rainfall, steep slope on the hilly or mountainous areas, and weak geological formations. Kayangan Catchment, Kulon Progo Regency, Yogyakarta Province, has weathered lihological formation, hilly and steeply sloped area that experiences the landslide occurrences. Due to the impact of landslide, disaster management must be done especially in providing the landslide hazard information. This data is very important to predict the probability of occurence and estimate the potential of losses. This research intends to find out landslide hazard zones of Kayangan Catchment based on deterministic method using outcrop-based Geological Strength Index (GSI) System.

Deterministic method is one of the methods in landslide hazard zonation by means of slope stability analysis. This method uses safety factor (SF) with Mohr-Coulomb failure criteria as the basis in defining the susceptibility of an area. The equation of this criteria uses cohesion (c) and angle of friction (Φ) as the parameters in calculation.

Outcrop-based Geological Strength Index (GSI) system as the way to assess the characteristic of regolith in terms of lithology, surface condition (weathering) and discontinuity (blockiness) of rock mass was performed to obtain cohesion and friction angle data as the parameters used in slope stability assessment. In this research, it was performed by using Ilwis software.

The results reveals the best accurate landslide hazard map shows moderate level of accuracy where the degree of fit (DF) in high hazard level = 54.86%, in moderate level = 44.28% and in low level = 0.86%. It shows a moderate performance of accuracy of landslide hazard map. Therefore the method can be considered reliable in landslide hazard zonation.

Keywords : landslide, hazard, deterministic method, geological strength index (GSI) system, slope stability, Ilwis, Kulon Progo.

INTISARI

Di Indonesia yang memiliki iklim tropik, tanah longsor menjadi satu dari bencana-bencana alam yang merusak. Tanah longsor menyebabkan kerugian-kerugian seperti kerusakan-kerusakan bangunan dan korban-korban manusia. Kejadian tanah longsor sangat umum terjadi yang disebabkan oleh curah hujan tinggi, lereng yang terjal pada daerah-daerah perbukitan atau pegunungan, dan formasi geologi yang lemah. Daerah Aliran Sungai (DAS) Kayangan, Kabupaten Kulon Progo, Provinsi Daerah Istimewa Yogyakarta memiliki formasi batuan yang lapuk, daerah berbukit dan berlereng terjal yang mengalami kejadian-kejadian tanah longsor. Karena dampak tanah longsor tersebut, manajemen bencana harus dijalankan khususnya dalam penyediaan informasi bahaya tanah longsor. Data ini merupakan data yang sangat penting untuk memperkirakan kemungkinan kejadian dan memperkirakan potensi kerugiannya. Research ini bermaksud untuk memperoleh zona-zona bahaya tanah longsor di DAS Kayangan dengan metode deterministik yang menggunakan sistem indeks kekuatan geologi (*Geological Strength Index*/GSI) berdasarkan singkapan batuan di permukaan. Metode deterministik merupakan salah satu dari metode dalam zonasi bahaya tanah longsor dengan cara analisis kestabilan lereng. Metode ini menggunakan faktor keamanan (*safety factor*) dengan kriteria kegagalan lereng Mohr-Coulomb sebagai dasar dalam menentukan kerawanan suatu wilayah. Rumus dari kriteria ini menggunakan kohesi (*c*) dan sudut gesek (*friction angle/Φ*) sebagai parameter dalam perhitungannya. Sistem indeks kekuatan geologi berdasarkan singkapan batuan permukaan sebagai cara untuk menguji karakteristik *regolith* dalam hal jenis batuan, kondisi permukaan/pelapukan dan diskontinuitas dari masa batuan, dikerjakan untuk memperoleh data kohesi dan sudut gesek sebagai parameter yang dipakai dalam pengujian kestabilan lereng. Dalam penelitian ini, pengujian kestabilan lereng tersebut dikerjakan dengan menggunakan software Ilwis. Hasil penelitian menunjukkan bahwa peta bahaya longsor dengan akurasi terbaik memiliki akurasi tingkat menengah di mana derajat kesesuaian (*degree of fit*) di tingkat bahaya tinggi = 54,86%, di tingkat bahaya menengah = 44,28%, dan di tingkat bahaya rendah = 0,86%. Hal tersebut menunjukkan akurasi dengan performa menengah dari peta bahaya tanah longsor. Oleh karena itu, metode ini dapat dipertimbangkan layak dalam zonasi bahaya tanah longsor.

Kata-kata kunci : tanah longsor, bahaya, metode deterministik, sistem indeks kekuatan geologi (geological strength index/GSI), kestabilan lereng, Ilwis, Kulon Progo.

ACKNOWLEDGEMENT

It want to say thank to all who contributed to my study especially my thesis since it has indeed been a collaborative effort of many and it would not have been possible for me to finish it without the valuable inputs and comments. Herewith, I gratefully acknowledge and give thanks to each one of them:

To Bappenas and Netherlands Education Centre, for providing a scholarship to pursue higher education in Gadjah Mada University (GMU), Yogyakarta and Faculty of Geo-Information Science and Earth Observation (ITC), University of Twente, Enschede, the Netherlands.

To Government of Rembang Regency, for giving me permission to continue my study, especially to my employer Dinas Energi Dan Sumber Daya Mineral Kabupaten Rembang, and my officemates for their support.

To my supervisors: Dr. Danang Sri Hadmoko, M.Sc., for his attention and support, Dr. Dhruba Pikha Shrestha, for the intensive long distance guidance. Their immeasurable assistance, suggestions, inputs and comments allow to work to come to the end.

To all lecturer and staff members in Gadjah Mada University and ITC-University of Twente, for their support and guidance, especially to Prof. Dr. Sudibyakto, M.S., Prof. Dr. Junun Sartohadi, Drs. Robert Voskuil, Dr. David G. Rossiter, and all lecturers that I could not mention individually.

To my Geo-info batch V classmates, for the invaluable and unforgettable help, cooperation, friendship, care, and support during my study.

To my Jokja friends: Fajarianto "serbu" Efendi for accompanying me to be an "obat nyamuk" and to discuss everything about life, Aris "nasib" Budiman, for our daily conversation to become successful man in life.

To my soulmate: Celvy Sulistiyaning Darmawati, for the prayers and patience.

To my son Lintang Pinilih and his sister who is still in her mother's hug, thanks for the inspirations making me tough in completing this study.

To my family: my parents, my brothers and sisters, for their eternal encouragement, hope, and love accompanying me to the end of my study. All of these make me strong to go through this one of the hard periods of my life.

Yogyakarta, February 2011
Bagus Haryono

TABLE OF CONTENTS

LIST OF FIGURES

LIST OF TABLES

CHAPTER 1. INTRODUCTION

1.1. Background

Indonesia is susceptible to many types of natural hazards, such as volcanic eruption, earthquake, and tsunami, because Indonesia is in collision zone of three tectonic plates (Eurasian, India-Australian, and Pacific plates), between two oceans (Pacific and Indian), and between two big continents (Australian and Asian) (Sutikno, 2007; Marfai et al., 2008). Moreover, the multiple effects of physical processes and human agency also contribute to the natural hazards each year. Flood, coastal inundation, subsidence, and landslide are very common due to intense rainfall, earthquakes that occurs frequently, steep slope on the mountainous areas, and weak geological formations.

Indonesia has a tropical climate, with two distinct seasons; monsoon wet and dry. The rainy season is usually from November to April, with some regional variations. Average annual rainfall varies greatly with the lowlands receiving about 1.7 to 3.1 cm and the mountainous regions getting up to 6.1 cm. Average annual temperature is less variable and ranges from 23–32 °C (University of Indonesia, 2007; Case et al., 2007).

According to data from National Disaster Management Agency (BNPB), in Indonesia, during 1998-2009 period, 1,273 people lost their lives, 1,505 injured, 36,503 people had to be evacuated. The damages number are 14,776 houses, 129 public facilities, 339 Km roads, 52,046 Ha plantation and forest (Table 1.1).

Table 1.1. Landslide data of Indonesia from 1998-2009 (BNPB, 2010).

Year	Landslide number	Victims (people)			Damages			
		Death	Injured	Evacuated	Houses (unit)	Public facilities (unit)	Roads (Km)	Plantation/ Forest (Ha)
1998	17	41	32	-	380	4	2	138
1999	8	58	-	-	365	10	-	-
2000	89	167	-	-	1,386	-	-	780
2001	20	15	3	-	175	4	-	2
2002	48	40	51	1,095	1,456	2	-	1,773
2003	69	168	204	10,050	2,314	15	194	45,957
2004	54	131	76	3,965	2,259	19	23	1,498
2005	49	207	32	2,449	1,018	2	100	1,137
2006	72	196	485	9,489	2,392	23	3	110
2007	97	90	78	1,271	974	24	-	-
2008	108	97	350	3,179	956	17	17	216
2009*	70	63	194	5,005	1,101	9	-	435
Total	701	1273	1505	36503	14776	129	339	52046

* : temporary data

Central Java including Yogyakarta Province, Indonesia, suffers from natural hazards such as land subsidence, coastal inundation, flood, volcanic eruption, earthquake, tsunami, and landslide (Figure 1.1). The occurrence of each kind of natural hazard varies according to the intensity of geo-processes (Marfai et al., 2008).

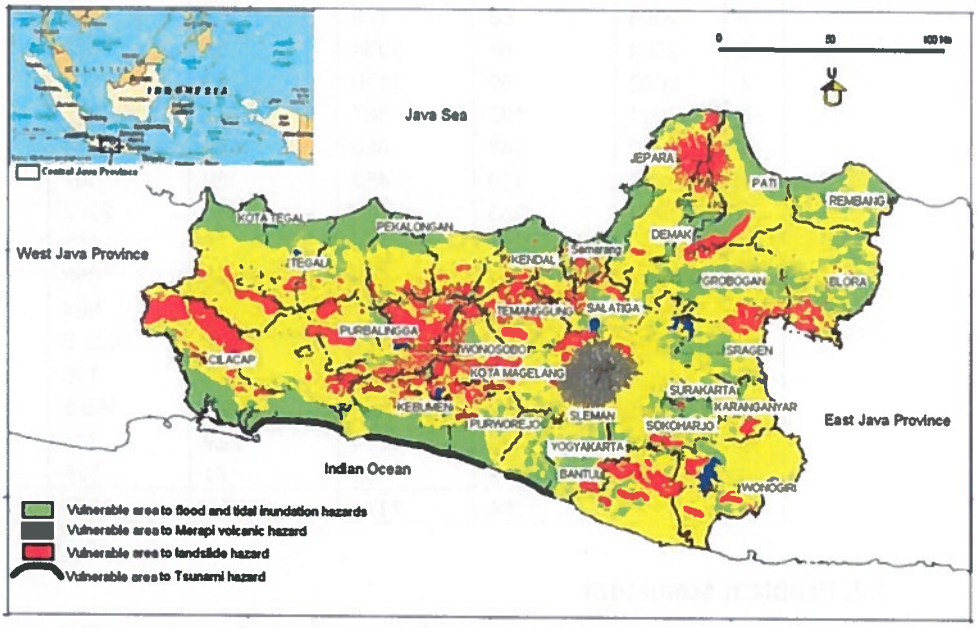

Figure 1.1. Preliminary multi-hazard map of Central Java, landslide hazard in red color (Marfai, et al., 2008).

According to Hadmoko et al. (2010), the death toll by landslides in Java is very high, due to the high frequency of landslide events and the high level of people's vulnerability. During the period of 1990–2005, a thousand of landslide disasters have been reported in Java. During this period, the death toll caused by landslides in Java exceeded 1,112 people and the number of people injured reached 395 (Table 1.2). This vulnerability results mainly from the high density of population and infrastructures located in the disaster prone areas. Landslide disasters also become the major obstacle in development process because their economic losses are relatively high (Guzzetti et al. 1999; Saha and Gupta 2002; Knapen et al., 2006; Hadmoko et al., 2010).

Due to the impact of landslide, disaster management must be done especially in providing the landslide hazard information. This data is very important to predict the probability of occurence and estimate the potential of losses.

Table 1.2. The impact of landslide disasters in Java during the period 1990-2005 to the houses, agricultural land, road and economic activities (Hadmoko, 2006a, b; Hadmoko, et al., 2010).

No	Year	Destruction				
		House completely damages	House partially damages	Agriculture area (Ha)	Road (m)	Estimated economic losses (euros)
1	2005	57	84	27	450	413,500
2	2004	68	179	169	155	650,500
3	2003	59	1354	93	235	1,816,900
4	2002	89	1119	129	607	1,772,100
5	2001	133	387	41	718	1,139,300
6	2000	182	626	1176	334	2,185,400
7	1999	120	459	89	307	1,575,900
8	1998	203	388	198	2362	1,592,200
9	1997	24	305	75	451	634,100
10	1996	131	632	58	858	1,508,800
11	1995	57	217	71	964	762,600
12	1994	125	191	266	1125.5	976,200
13	1993	88	153	221	136	736,600
14	1992	22	720	104.3	165.5	951,150
15	1991	32	264	229	345	603,700
16	1990	118	96	71	326	721,500
Total		**1508**	**7174**	**3017.3**	**9539**	**18,040,450**

1.2. Problem statement

In analysing landslide hazard, different approaches are available which have different reliability due to its accuracy. According to Van Westen (2006), deterministic modelling might give more reliable answers but requires detailed datasets about the spatial variation of parametric values which form the input of the hydrological, geotechnical and slope stability models and the most sensitive parameters are slope gradients (which can be easily be obtained from accurate DEM nowadays) and soil thickness. Those slope gradients and soil thickness are used as the parameters in safety factor calculation in slope stability assessment. The spatial distribution of soil thickness is extremely difficult to measure. Beside of the field measurement process, it is also influenced by the vegetation that covers the soil, slope and weathering condition. Other parameter that is also sensitive for slope stability is water saturation (*m*). This parameter is obtained from the ratio between the height of water table and soil thickness. The existence of water table depends on the porosity and permeability of soil/material in yielding the water.

Although geomorphological models give a certain prediction for soil thickness, its spatial variability is large. The weathering processes in the underlying rocks are factors that are often neglected that inluence the material properties such as cohesion (c) and friction angle (Φ). Those parameters are difficult to measure for many points over large areas and show a high spatial variability. In a GIS environment only the infinite slope stability model with the slip plane parallel to the surface can be used efficiently for larger areas, as landslide models on the catchment scale, with complex or curved slip surfaces, are difficult to implement (Van Westen, 2006).

Deterministic method as one of the methods in landslide hazard zonation by means of slope stability analysis needs to be proved as the reliable method. It uses safety factor (SF) with Mohr-Coulomb failure criteria as the basis in defining the susceptibility of an area. This equation uses cohesion (c) and angle of friction (Φ) as the parameters in calculation which are obtained from laboratorical analysis from hand speciman sample of soil/rock. Actually the laboratory derived c and Φ do not exactly represent the real c and Φ of material observed. In fact there are phenomena that influence their values and should be considered to represent the whole material. Those phenomena in the field are blockiness, and the surface condition of the discontinuities indicated by joint roughness and alteration.

Due to the above mentioned problem, the parameters need to be estimated properly for improving landslide hazard information. Therefore, Geological Strength Index (GSI) system that provides cohesion and friction angle needed in safety factor calculation probably may be the answer of the problem.

Geological Strength Index (GSI) introduced by Hoek (1994), Hoek et al. 1995) and Hoek and Brown (1998) in Hoek et al. (1998) provides a system for estimating the reduction in rock mass strength for different geological conditions as identified by field observations. The rock mass characterisation is straightforward. It is based upon the visual impression of the rock structure, in terms of blockiness, and the surface condition of the discontinuities indicated by joint roughness and alteration. The value of GSI is estimated from the contours given in Table 2.1. The c and Φ can be obtained from the curves of GSI-*mi* (Hoek and Brown, 1997). *mi* is the values of the constant for intact rock by rock group that can be obtained from *mi* modified table (Hoek,

2007). Based on the GSI data, calculation of safety factor using its c and Φ can be more accurate because it represents the whole material/rock mass properties observed.

1.3. Objectives

The main objective of this research was to find out landslide hazard zones of Kayangan Catchment based on deterministic method using outcrop-based Geological Strength Index (GSI) system.

Its specific objectives were :

1. to apply outcrop-based GSI system in collecting data in the field
2. to apply outcrop-based GSI system in obtaining cohesion and friction angle as parameters used in slope stability assessment;
3. to assess the reliability of landslide hazard zonation based on deterministic method using outcrop-based GSI system.

1.4. Research Questions

The results of this research are intended to answer the following research question as a main focus of the discussion :

1. to apply outcrop-based GSI system in collecting data in the field :
   a. How is the applicability of outcrop-based GSI system in collecting data in the field?
   b. Is outcrop-based GSI system suitable to be applied for physical condition in research area?
2. to apply outcrop-based GSI system in obtaining cohesion and friction angle as parameters used in slope stability assessment:
   a. Can outcrop-based GSI data collected from the field be used in obtaining cohesion and friction angle as parameters used in slope stability assessment?
3. to assess the reliability of landslide hazard zonation based on deterministic method using outcrop-based GSI system:
   a. How to perform lanslide hazard zonation based on deterministic method using outcrop-based GSI system?
   b. What is the accuracy of landslide hazard zonation based on deterministic method using outcrop-based GSI system?

c. What kind of scenario does result the best landslide hazard zones based on deterministic method using outcrop-based GSI system?
d. Is deterministic method using outcrop-based GSI system reliable in landslide hazard zonation?
e. Is there any relationship between actual landslides and its GSI data?

1.5. Benefit of The Research

The research may give benefit for purposes to provide a new methodology to assess landslide hazard in a data poor environment and to provide landslide hazard information of area.

CHAPTER 2. LITERATURE REVIEW

2.1. Regolith

2.1.1. Regolith and weathering

The characteristic of regolith is the important thing that controls the occurence of landslide. Its characteristic such as surface condition/weathering grade, structure/discontinuity, and also internal structure of grains influence the internal characteristic of regolith. Cohesion and friction angle are the internal characteristic as product from characteristics mentioned above. Beside of this, mineral content of parent rock mass weathered also influences the weigth of regolith. Those characteristics are used as parameters in slope stability assessment.

Eggleton (2001); Scott & Pain (2009) defined that regolith is the entire unconsolidated or secondarily re-cemented cover that overlies more coherent bedrock and which has been formed by weathering, erosion, transport and/or deposition of the older material. The materials included as regolith are fractured and weathered basement rocks saprolites, soils, organic accumulations, glacial deposits, colluvium, alluvium, evaporitic sediments, aeolian deposits and ground water. Everything from fresh rock to fresh air is called as regolith.

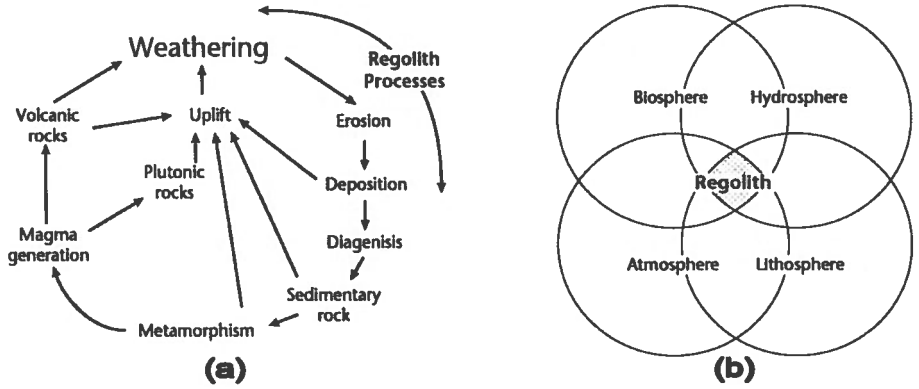

Figure 2.1. (a) Weathering in the geological cycle (after Wilson 2004; Scott & Pain, 2009), (b) The influence of different interactions on regolith (after Taylor and Eggleton 2001; Scott & Pain, 2009).

Weathering is a part of the geological cycle (Figure 2.1), and is generally occurred when rocks are exposed to the atmosphere and the physical

and/or chemical breakdown of component minerals occurs (Scott & Pain, 2009). Physical and chemical processes remove mineral components from their original location and redeposite elsewhere, and when components are subjected to diagenesis, it continue their path in the geological cycle. Regolith processes includes weathering, erosion and deposition processes. Each process involves the interaction between minerals, air and water, which is enhanced in most cases by biota activities.

Water plays a critical role in regolith development even in arid environments and surface and sub-surface flow are themselves modified by the structural make up of the regolith (Scott & Pain, 2009) (Figure 2.2). The figure below shows that water can erode, transport and deposit surface material to the other place.

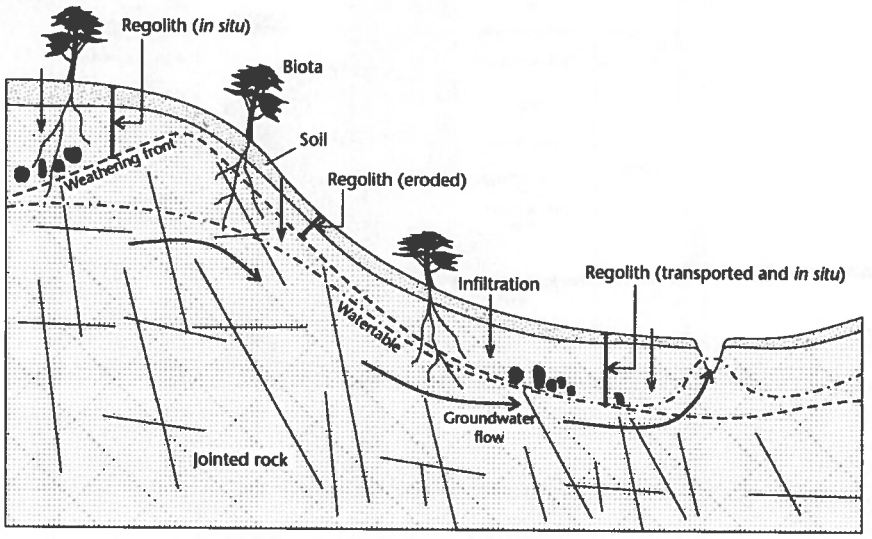

Figure 2.2. The effect of groundwater in regolith processes (after Taylor and Eggleton, 2001; Scott & Pain, 2009).

2.1.2. Structure of the regolith

Structure of regolith profile is one of characteristics of regolith that also controls the landslide occurrence. its structure is a product of a complex interaction of weathering process and erosion process that influences the thickness of regolith. Regolith thickness is one of parameters in slope stability assessment because it is involved in safety factor calculation.

Regolith structure at any particular site depends on the extent to which chemical weathering has transformed the bedrock composition, as well as

the degree of physical and chemical addition and removal of materials (McQueen & Scott in Scott & Pain, 2009).

A well-developed vertical zonation profiles may include from depth to surface (McQueen & Scott in Scott & Pain, 2009) (Figure 2.3.a):

- a zone of partially weathered bedrock that retains the primary rock fabric
- a clay-rich or sandy plasmic/arenose zone in which the primary rock fabric has been destroyed
- a ferruginous mottled zone; a ferruginous, bauxitic or siliceous duricrust/residuum
- a soil layer
- a surface lag of chemically and physically resistant materials.

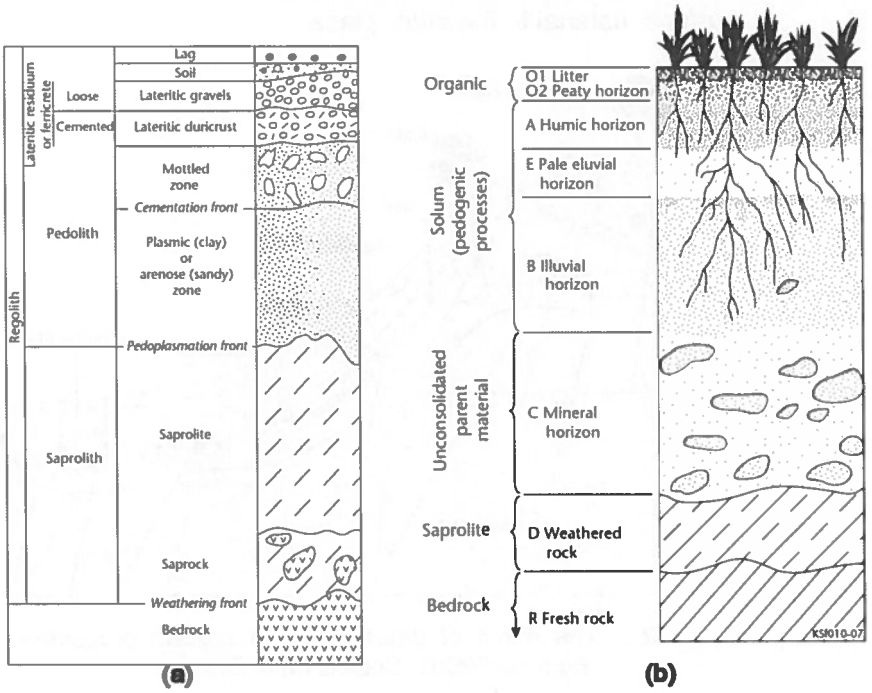

Figure 2.3. (a) Idealised regolith profile (after Eggleton 2001; McQueen & Scott in Scott & Pain, 2009), (b) An idealised soil profile (after Butt *et al.* 2005; McQueen & Scott in Scott & Pain, 2009).

According to McQueen & Scott (in Scott & Pain, 2009), the saprolith is the zone in which the primary rock fabric is preserved and the zone in which the parent fabric has been destroyed, new fabrics formed or soil developed is termed the pedolith. Weathering occurs from the top of profile down to the weathering front defined as the boundary between fresh rock and saprolith that shows some sign of chemical weathering of rock. Due to

bedrock type and landscape setting, various parts of this mature zonation may be absent, eroded or buried., Generally there is significant lateral variation in the regolith and its chemical structure across a landscape (or paleolandscape). These variations may be down to a scale of metres or tens of metres.

Weathering will typically penetrate preferentially and deeper along fractured or more permeable zones (McQueen & Scott; Scott & Pain, 2009). Generally the youngest weathering zone is at the base and the oldest at the top of a profile. Less-weathered blocks (lithorelicts) may be preserved well above the weathering front and even to the surface. The most recently weathered material is importantly that closest to fresh rock. In the saprolith portion, the lower most saprock layer is the least chemically altered zone, with less than 20% of weatherable minerals altered. Generally it will retain the most recent weathering evidence. Alteration of major primary mineral, chemical leaching and the growth of secondary mineral can eventually destroy the primary fabric of rock to produce the pedolith (Figure 2.3.a).

Common soil horizons (Figure 2.3.b; McQueen & Scott in Scott & Pain, 2009) include :

- Litter (or O1): organic matter on the ground surface
- (or O2): fibrous (peaty) or massive organic matter
- A: near-surface mineral horizon containing humified organic matter
- E (or A2): pale, commonly sandy, eluvial horizon with little organic matter. Iron and Mn oxides and clays leached or translocated to lower horizons
- B: illuvial horizons enriched in clay, and/or Fe and Mn oxides and/or organic matter derived from overlying horizons
- C: mineral horizon from which the overlying horizons are presumed to have been derived. It is only slightly affected by pedogenic processes so that remnant geological structures or fabric may be retained
- D: layers below the C horizon unaffected by the pedogenic processes that formed overlying horizons, such as previously formed saprolite or transported overburden
- R: continuous fresh rock.

The horizons of A, E and B are referred to as the solum (McQueen & Scott; Scott & Pain, 2009). This terminology is ideally suited to well-differentiated soils, such as podzols, but less readily applied to arid-zone soils that have weak differentiation of horizon.

Water table is the boundary of dry and wet zones in regolith profile when the pressure of atmosphere is equal to pressure of water. Water table fluctuates following the water that infiltrates through the porous part of regolith and the movement of base flow. The water presence influences the cohesion of regolith because its pressure reduces the cohesion between grains of regolith.

According to McQueen & Scott (in Scott & Pain, 2009), water table is an important chemical and physical boundary within the profile of weathering, marking the interface between water saturation zone and the overlying zone of partial water content. In weathering profiles, in a steady state, the water table will generally occur in the zone of saprock or lower saprolite. Water table position can change seasonally, or over longer time periods, with climate change and landscape evolution (McQueen & Scott; Scott & Pain, 2009). In wetter conditions the water table can rise up through the profile of weathering and in drier conditions, it may progressively fall. The depth from surface to the water table will also depend on the factors of geomorphic setting and local hydrology, including vegetation pumping (McQueen & Scott; Scott & Pain, 2009).

2.2. Geological Strength Index (GSI) System

Geological Strength Index (GSI) system as a visual inspection technique provides the way to assess the characteristic of regolith in terms of lithology, surface condition (weathering) and discontinuity (blockiness) of rock mass that can derive its cohesion and friction angle.

Geological Strength Index (GSI) introduced by Hoek (1994); Hoek, et al. (1995); Hoek and Brown (1998); Hoek, et al. (1998) provides a system for estimating the reduction in rock mass strength for different geological conditions as identified by field observations. The characterisation of rock mass is straightforward and based upon the rock structure visual impression, in terms of blockiness, and the surface condition of the

discontinuities indicated by joint roughness and alteration (Table 2.1). A practical basis provided from the combination of those two parameters is used for describing a wide range of rock mass types, with rock structure which is diversified ranging from very tightly interlocked strong rock fragments to heavily crushed rock masses. Based on the rock mass description, the value of GSI is estimated by using the contours given in Table 2.1. The uniaxial compressive strength (UCS) and the material constant *mi* are determined by laboratory testing or estimated from published tables (Hoek et al., 1998) (Table 2.2,3). In the Hoek and Brown failure criterion, the *mi* value reflects the frictional characteristics of the component minerals and grains of the intact rock (Marinos et al., 2006). The shear strength of the rock mass, defined by the angle of internal friction Φ and cohesion c, are estimated by using the curves plotted in Table 2.4.
Geological strength index is based upon an assessment of the lithology, structure and condition of discontinuity surfaces in the rock mass and estimated from visual examination of the rock mass exposed in outcrops, in surface excavations such as road cuts and in tunnel faces and borehole cores (Marinos et al., 2005). By combining the two fundamental parameters of the geological process, the blockiness of the mass and the conditions of discontinuities, the GSI respects the main geological constraints that govern a formation and is thus a geologically sound index that is simple to apply in the field (Marinos et al., 2005).

Note that attempts to "quantify" the GSI classification to satisfy the perception that "engineers are happier with numbers" are interesting but have to be applied with caution (Cai et al., 2004; Sonmez and Ulusay, 1999; Marinos et al., 2005). The quantification processes used are related to the frequency and orientation of discontinuities and are limited to rock masses in which these numbers can easily be measured. In tectonically disturbed rock masses in which the structural fabric has been destroyed, the quantifications do not work well. In such rock masses, Marinos et al. (2005) recommend the use of the original qualitative approach based on careful visual observations.

Table 2.1. Characterisation of blocky rock masses on the basis of interlocking and joint conditions (Hoek, 2007).

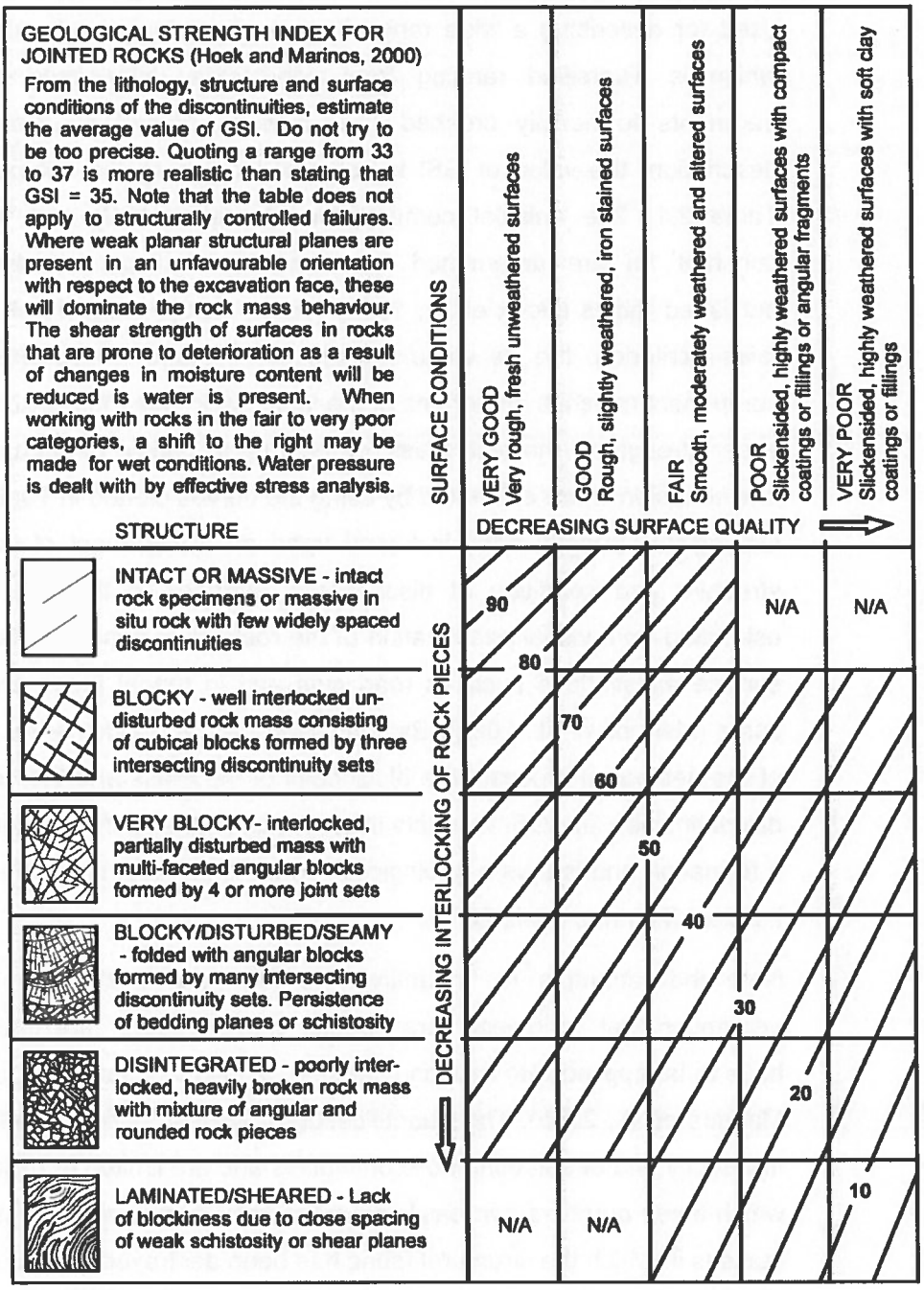

Tabel 2.2. Field estimation of uniaxial compressive strength (UCS) (Hoek, 2007).

Grade*	Term	Uniaxial Compressive Strength (MPa)	Point Load Index (MPa)	Field Estimate of strength	Examples
R6	Extremely strong	>250	>10	Specimen can only be chipped with a geological hammer	Fresh basal, chert, diabase, gneiss, granite, quartzite
R5	Very strong	100 - 250	4 - 10	Specimen requires many blows of geological hammer to fracture it	Amphibolite, sandstone, basalt, gabbro, gneiss, granodiorite, limestone, marble, rhyolite, tuff
R4	Strong	50 - 100	2 – 4	Specimen requires more than one blow of a geological hammer to fracture it	Limestone, marble, phyllite, sandstone, schist, shale
R3	Medium	25 - 50	1 – 2	Can not be scraped or peeled with a pocket knife, specimen can be fractured with a single blow from a geological hammer	Claystone, coal, concrete, schist, shale, siltstone
R2	Weak	5 – 25	**	Can be peeled with a pocket knife, with difficulty, shallow indentation made by firm blow with point of a geological hammer	Chalk, rocksalt, potash
R1	Very weak	1 – 5	**	Crumbles under firm blows with point of a geological hammer, can be peeled by a pocket knife	Highly weathered or altered rock
R0	Extremely weak	0.25 - 1	**	Indented by thumbnail	Stiff fault gouge

*Grade according to Brown (1981).
**Point load test on rocks with a uniaxial compressive strength below 25 MPa are likely to yield highly ambiguous results.

The Hoek–Brown criterion (and other similar criteria) requires that the rock mass behave isotropically and that failure does not follow a preferential direction imposed by the orientation of a specific discontinuity or a combination of two or three discontinuities (Marinos et al., 2005). The use of GSI is meaningless as the failure is governed by the shear strength of these discontinuities or in an anisotropic condition and not by the rock mass (Marinos et al., 2005).

The most common sources of information for the estimation of a rock mass GSI value are outcrops, excavated slopes tunnel faces and the cores of borehole (Marinos et al., 2005). Outcrops are an extremely valuable source of data in the initial stages of a project but outcrops suffer the disadvantage where surface relaxation, weathering and/or alteration may have significantly influenced the appearance of the rock mass components (Marinos et al., 2005). Judgement is therefore required in order to allow for these weathering and alteration effects in assessing the most probable GSI value at the depth of the proposed excavation (Marinos et al., 2005).

The evaluation for a slope stability analysis is based on the rock mass through that it is anticipated that a potential failure plane could pass (Marinos et al., 2005). In these cases the estimation of GSI values requires considerable judgment, when the failure plane can pass particularly through several different quality zones. Therefore, in this case, mean values may not be appropriate (Marinos et al., 2005).

Sometimes, in a numerical analysis that is involving a single well-defined discontinuity for example a shear zone or fault is appropriate to apply the Hoek–Brown criterion to the overall rock mass and to superimpose the discontinuity as a significantly weaker element (Marinos et al., 2005). In that case, the single major discontinuity should be ignored in assigning the GSI value of rock mass. The discontinuity properties may fit the lower portion of the GSI chart or they may require a different approach such as laboratory shear testing of soft clay fillings (Marinos et al., 2005).

Although GSI system may work with the better quality rock masses, it is meaningless in weak (e.g. GSI<35), very weak range and heterogeneous rock masses where these correlations are not recommended but for engineering geologists, this "qualitative" GSI system works well when they are consistent with their experience in describing rocks and rock masses during logging and mapping (Marinos et al., 2005).

Tabel 2.3. Values of the constant *mi* for intact rock, by rock group. Note that values in parenthesis are estimates (Hoek, 2007).

Rock Type	Class	Group	Texture			
			Coarse	Medium	Fine	Very Fine
SEDIMENTARY	Clastic		Conglomerates* (21±3) Breccias (19±5)	Sandstones (17±4)	Siltstones (7±2) Graywackes (18±3)	Claystones (4±2) Shales (6±2) Marls (7±2)
	Non-clastic	Carbonates	Crystalline limestones (12±3)	Sparitic limestones (10±2)	Micritic limestones (9±2)	Dolomites (9±3)
		Evaporites		Gypsum (8±2)	Anhydrite (12±2)	
		Organic				Chalk (7±2)
METAMORPHIC	Non foliated		Marbles (9±3)	Hornfels (19±4) Metasandstone (19±3)	Quartzites (20±3)	
	Slightly foliated		Migmatites (29±3)	Amphibolites (26±6)		
	Foliated**		Gneiss (28±5)	Schists (12±3)	Phyllites (7±3)	Slates (7±4)
IGNEOUS	Plutonic	Light	Granite (32±3) Granodiorite (29±3)	Diorite (25±5)		
		Dark	Gabbro (27±3) Norite (20±5)	Dolerite (16±5)		
	Hypabyssal		Porphyries (20±5)		Diabase (15±5)	Peridotite (25±5)
	Volcanic	Lava		Rhyolite (25±5) Andesite (25±5)	Dacite (25±3) Basalt (25±5)	Obsidian (19±3)
		Pyroclastic	Agglomerate (19±3)	Breccia (19±5)	Tuff (13±5)	

*Conglomerates and breccias may present a wide range of *mi* values depending on the nature of the cementing material and the degree of cementation, so they may range from values similar to sandstone to values used for fine grained sediments.
**This values are for intact rock specimens tested normal to bedding or foliation. The value of *mi* will be significantly different if failure occurs along a weakness plane.

Table 2.4. Relationship between cohesive strength and Geological Strength Index (*GSI*); (left) and relationship between friction angle and GSI (right) (Hoek et al, 1998).

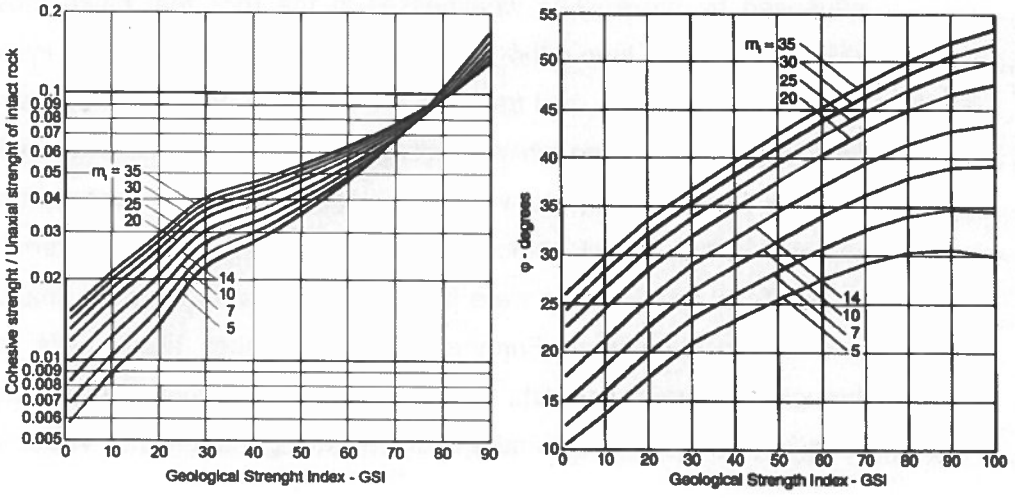

2.3. Landslide

2.3.1. Definition

Mass movement is defined as the outward or downward gravitational movement of earth material without the aid of running water as a transporting agent (Crozier, 1986; Van Westen, 1993). Mass movement is synonymous to landslide, slope movement and slope failure (Van Westen, 1993).

Mass wasting is defined as the downslope movement of products of weathering, and there is a continuum between the processes of weathering, erosion, and mass wasting (Kusky, 2008). Other definition, mass wasting is the movement of soil, regolith, or rock downhill without the direct aid of water. The main driving force behind mass wasting processes is gravity, as it is constantly pulling on mass and attempting to force it downhill (Kusky, 2008). Gravity on a slope can be resolved into two components that are one perpendicular to the slope and one parallel to the slope, the steeper the angle of the slope, the greater the influence of gravity (Kusky, 2008).

2.3.2. Physical condition that control landslide

Mass wasting is controlled by many factors which include characteristics of the regolith and bedrock, the presence or absence of water, overburden, angle of the slope, and the way the particles are packed together (Kusky, 2008).

According to Kusky (2008), in solid bedrock terrain, mass wasting is strongly influenced by pre-existing weaknesses in the rock that make movement along them easier than if the weaknesses were not present. For instance, if bedding planes, joints, and fractures are favorably oriented, they may act as weakness planes along which giant slabs of rock may slide downslope. If the rock or regolith has many pores, or open spaces between grains, it will be weaker than a rock without pores because there is no material in the pores. If the open spaces were filled, the material in the pore space could hold the rock together. Furthermore, pore spaces allow fluids to pass through the rock or regolith, and the fluids may further dissolve the rock, creating more pore space and further weakening the material. Water in open

pore spaces may also exert pressure on the surrounding rocks, pushing individual grains apart and making the rock weaker.

According to Kusky (2008), water typically acts to reduce the adhesion between grains, promoting downslope movements. When the water filled the pore spaces, it acts as a lubricant and may actually exert forces that push individual grains apart. In pore spaces, the water weight also exerts additional pressure on underlying rocks and soils, and this is known as loading. In many cases, the loading from water in pore spaces is enough so that the underlying rocks and soil strength is exceeded and the slope fails, resulting a downslope movement. The way that the particles are arranged or packed in the slope is also a factor, and the denser the packing, the more stable the slope (Kusky, 2008).

2.3.3. Types of landslide

Mass movements are of three basic types, distinguished by the way the rock, soil, and debris move down the slope (Kusky, 2008). Slides move over and in contact with the underlying surface. Flows include movements of regolith, rock, water, and air in which the moving mass breaks into many pieces that flow in a chaotic movement. Falls move freely through the air and land at the base of the slope or escarpment.

Classification of mass wasting are creep, debris flow, slump, rockslide, rock fall and subaqueous flow (Kusky, 2008) (Figure 2.4).

2.3.3.1. Creep

Creep is the imperceptible slow downslope flowing movement of regolith (Kusky, 2008). The process involved is the very slow plastic deformation of the regolith, and also the repetition of bedrock microfracturing at rates which is nearly imperceptible. Creep occurs along the upper parts of the regolith at which there is no single surface along which slip has occurred. Creep rates range from a fraction of an inch to about 2 inches per year on steep slopes. Creep accounts for leaning telephone poles, fences, and many of the cracks in sidewalks and roads. Although creep is slow and not very spectacular, it is one of the most important mechanisms of mass wasting and accounts for the greatest total volume of material moved downhill in any given year.

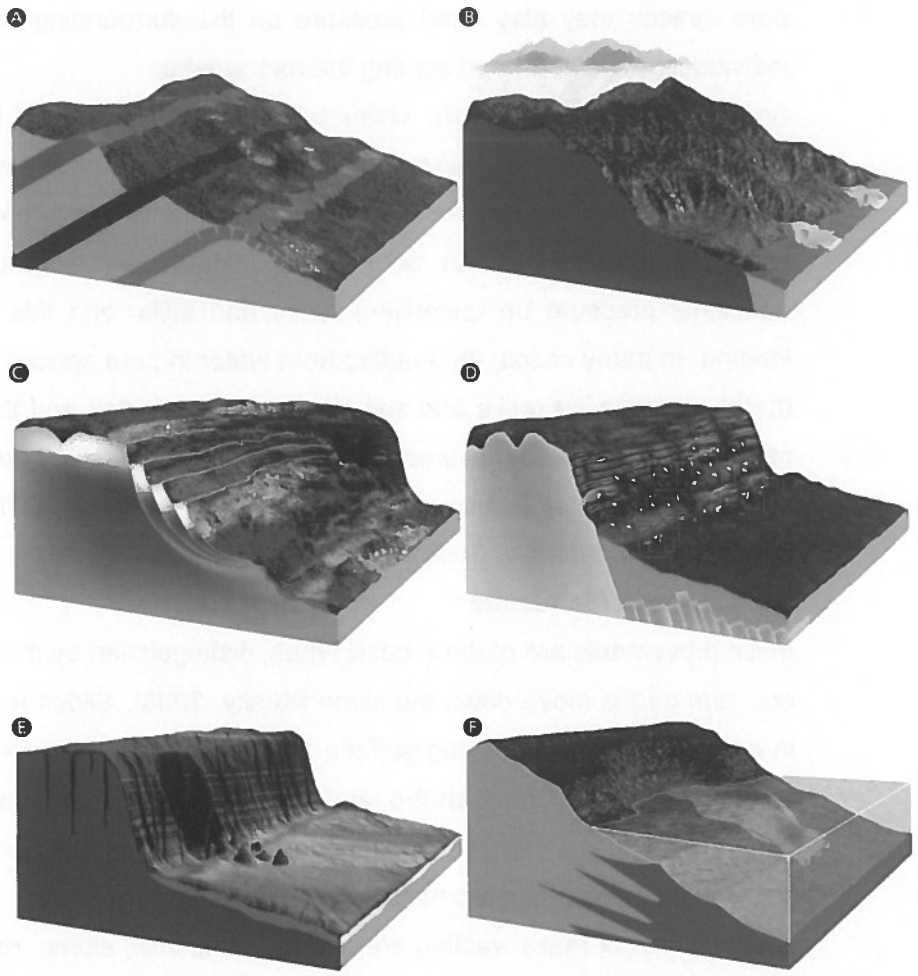

Figure 2.4. Types of mass wasting (Kusky, 2008). Classification is based on the material that is moving, water content, and speed. **A** shows creep, the slow downslope movement of regolith; **B** shows a debris flow, the rapid downslope movement of rock and soil with water; **C** illustrates a slump, the downslope movement of coherent blocks of rocks or soil on curved fault surfaces; **D** illustrates a rockslide, the rapid downslope movement of rocks sliding along a rock surface such as a joint or bedding surface; **E** shows a rockfall, the free fall of rock or debris; and **F** is a subaqueous flow of sand or silt, typically becoming a turbidity current.

2.3.3.2. Slumps

A slump is a type of sliding slope failure in which a downward and outward rotational movement of rock or regolith occurs along a concave up slip surface (Kusky, 2008). This produces either a singular or a series of rotated blocks, each with the original ground surface tilted in the same direction. The geometry of a slump is illustrated in Figure 2.5. Slumps are especially common after heavy rainfalls and earthquakes, and they can often be seen along roadsides and other slopes that have been artificially steepened to

make room for buildings or other structures. Slump blocks may continue to move after the initial sliding event, and, in some cases, this added slippage is enhanced by rainwater that falls on the back-tilted surfaces and infiltrates along the fault, acting as a lubricant for added fault slippage. A *translational slide* is a variation of a slump in which the sliding mass moves not on a curved surface, but downslope on a pre-existing plane, such as a weak bedding plane or a joint. Translational slides may remain relatively coherent or break into small blocks forming a debris slide.

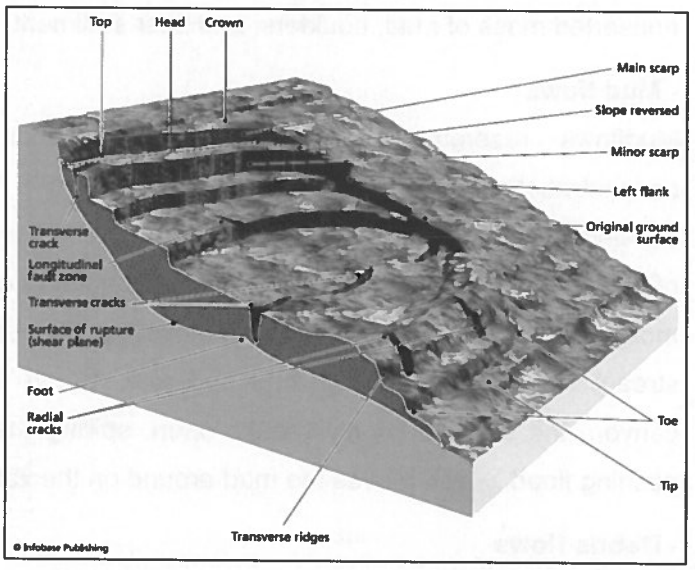

Figure 2.5. Geometry of a slump showing headwall scarp, listric normal fault, and toe (Kusky, 2008).

2.3.3.3. Sediment flows

When mixtures of rock debris, water, begin to move under the force of gravity, they are said to flow (Kusky, 2008). This is a type of deformation that is continuous and irreversible. The way in which this mixture flows depends on the relative amounts of solid, liquid, and air, the grain size distribution of the solid fraction, and the physical and chemical properties of the sediment. Mass wasting flows are transitional with stream-type flows, with changes in the amounts of sediment/water and in velocity. There are many names for the different types of sediment flows, including slurry flows, mudflows, debris flows, debris avalanches, earthflows, and loess flows. Many mass movements begin as one type of flow and evolve into another during the course of the mass wasting event. For instance, it is common for

flows to begin as rockfalls or debris avalanches and evolve into debris avalanches, debris flows, and mudflows along their length as the flows pick up water and debris and flow over different slopes.

- Slurry flows

A slurry flow is a moving mass of sediment saturated in water that is transported with the flowing mass (Kusky, 2008). The mixture, however, is so dense that it can suspend large boulders or roll them along the base. When slurry flows stop moving, the resulting deposit therefore consists of a nonsorted mass of mud, boulders, and finer sediment.

- Mud flows

Mudflows resemble debris flows, except that they have higher concentrations of water (up to 30 percent) that make them more fluid, with a consistency ranging from soup to wet concrete (Kusky, 2008). Mudflows often start as a muddy stream in a dry mountain canyon, which picks up more and more mud and sand as it moves, until eventually the front of the stream is a wall of moving mud and rock. When this comes out of the canyon, the wall commonly breaks open, spilling the water behind it in a gushing flood, which moves the mud around on the valley floor.

- Debris flows

Debris flows involve the downslope movement of unconsolidated regolith, most of which is coarser than sand. Some begin as slumps, but then continue to flow downhill as debris flows (Kusky, 2008). They typically fan out and come to rest when they emerge out of steeply sloping mountain valleys onto flatter plains. Rates of movement in debris flows vary from several feet per year to several hundred miles per hour. Debris flows are commonly shaped like a tongue with numerous ridges and depressions. Many form after heavy rainfalls in mountainous areas, and the number of debris flows is increasing with greater deforestation of mountains and hilly areas.

- Debris avalanche

Debris avalanches are granular flows moving at very high velocity and covering large distances (Kusky, 2008). These are rare but incredibly

destructive and spectacular events. Some have ruined entire towns, killing tens of thousands of people without warning. Some have been known to move as fast as 250 miles per hour (403 km/hr). These avalanches can move so fast that they move down one slope, then thunder right up and over the next slope and into the next valley. One theory of why these avalanches move so fast is that when the rocks fi rst fall, they trap a cushion of air and then travel on top of it like a hovercraft.

-Granular flows and earthflows

Granular flows are unlike slurry flows, since in granular flows the full weight of the flowing sediment is supported by grain-to-grain contact between individual grains (Kusky, 2008). Earthflows are relatively fast granular flows with velocities ranging from three feet (1 m)/day to 1,200 feet (360 m)/hour.

2.3.3.4. Rock falls and debris falls

Rockfalls are the free fall of detached bodies of bedrock from a cliff or steep slope. They are common in areas of very steep slopes, where they may form huge deposits of boulders at the base of cliffs (Kusky, 2008). Rockfalls can involve a single boulder or the entire face of a cliff . Debris falls are similar to rockfalls, but these consist of a mixture of rock and weathered debris and regolith.

2.3.3.5. Rockslides and debris slides

Rockslides is the term given to the sudden downslope movement of newly detached masses of bedrock (or debris slides, if the rocks are mixed with other material or regolith) (Kusky, 2008). These are common in glaciated mountains with steep slopes and also in places where planes of weakness such as bedding planes, or fracture planes, dip in the direction of the slope. Like rockfalls, rockslides may form fields of huge boulders coming off mountain slopes. The movement to this talus slope is by falling, rolling, and sliding, and the steepest angle at which the debris remains stable is known as the angle of repose. The angle of repose is typically 33–37 degrees for most rocks.

2.3.3.6. Subaquaeous flow

Mass wasting is not confined to the land. Submarine mass movements are common and widespread on the continental shelves, slopes, and rises, and also in lakes (Kusky, 2008). Mass movements underwater, however,

typically form turbidity currents, which leave large deposits of graded sand and shale. Under water, these slope failures can begin on very gentle slopes, even of less than one degree. Other submarine slope failures are similar to slope failures on land. Slides and slumps and debris flows are also common in the submarine realm. Submarine deltas, deep-sea trenches, and continental slopes are common sites of submarine slumps, slides, and debris flows. Some of these are huge, covering hundreds of square miles. Many of the mass wasting events that produced these deposits must have produced large tsunamis. The continental slopes are cut by many canyons, produced by submarine mass wasting events, which carried material eroded from the continents into the deep ocean basins.

2.3.4. Landslide hazard

Hazard is defined as the probability of occurrence of a potentially damaging phenomenon within a specified period of time and within a given area (Varnes, 1984; Van Westen, 1993).

Varnes (1984); Fell (1994); Leroi (1996); Lee and Jones (2004); Van Westen et al. (2006), reports hazard is a function of the spatial probability (related to static environmental factors such as slope, strength of materials, depth, etc.) and the temporal probability, related indirectly to some static environmental factors like slope and hydraulic conductivity and directly to dynamic factors like rain input and drainage.

Landslide hazard is commonly shown on maps which display the spatial distribution of hazard classes (landslide hazard zonation) (Varnes, 1984; Van Westen, 1993). This zonation refers to the division of the land in homogeneous areas or domains and their ranking according to degrees of actual/potential hazard caused by mass movement.

The term landslide hazard map will refer to a quantitative prediction of the spatial distribution of both landslide deposits and slopes which are likely to be site of failures whose movement or reactivations will take place in a way and within a time period defined from information that is not directly incorporated in the model (Guzzetti et al,1999).

According to Van Westen (2006), GIS-based landslide hazard assessment methods may involve four different approaches as follows:

- Landslide inventory-based probabilistic approach;
- Heuristic approach (direct geomorphological mapping or indirect combination of qualitative maps);
- Statistical approach (bivariate or multivariate statistics); and
- Deterministic approach (Soeters and Van Westen 1996).

Landslide inventory-based probabilistic approach is an attempt to predict when a landslide will occur by establishing the exceedance probability of landslide occurrence during an established period (Guzzetti et al, 2005). The exceedance probability is most commonly obtained from catalogues of historical landslide events, which are lists showing the time (or period) of occurrence of single or multiple slope failures. No single measure of landslide magnitude exists (Guzzetti, 2002; Guzzetti et al, 2005). This information can be used to determine the expected probability of landslide area and magnitude (Guzzetti et al, 2005).

Heuristic approach is considered to be useful for obtaining qualitative landslide hazard maps for large areas in a relatively short time (Abella and Van Westen, 2008). It does not require the collection of geotechnical data but it needs detailed geomorphological mapping that is essential. The heuristic approach may result in more reliable susceptibility maps than using statistical methods, where a considerable amount of generalization always needs to be accepted in the analysis (Abella and Van Westen, 2008).

Several ways in statistical approach are by using bivariate and multivariate statistics to assess landslide susceptibility of an area. The present bivariate approach uses several variables of instability factor where the influence of each of which on the landslide occurrence is evaluated independently and the variables are combined in the form of a unique equation (Agterberg and Cheng, 2002; Thiart et al., 2003; Conoscenti et al., 2008; Nandy and Shakoor, 2009). Among available multivariate approaches above, for the present study, the most suitable approach found is logistic regression where landslide spatial distribution is assessed on the interaction basis of only statistically significant instability factor data and insignificant data are excluded from consideration. Another statistical approach is logostic regression that is free of data distribution issues and can handle a dataset

variety, such as continuous, categorical, and binary, common types of instability factor data used in landslide studies (Dai et al., 2001; Lee and Min, 2001; Suzen and Doyuran, 2004; Lulseged and Hiromitsu, 2004; Lee, 2005; Yesilnacar and Topal, 2005; Lee and Sambath, 2006; Nefeslioglu et al., 2008; Nandy and Shakoor, 2009).

Deterministic analysis is indirect method in which parameter maps are combined in slope stability calculations (Van Westen, 1993). It requires input data on : soil layer thickness, soil strength, depth below the terrain surface of potential sliding surfaces, slope angle, and pore pressure conditions to be expected on the slip surfaces (Van Westen, 1993). It is applicable only at a large scales and over a small areas where at the regional and the medium scale the detail of the input data, especially concerning groundwater levels, soil profile, and geotechnical descriptions is insufficient. The variability of the input data can be used to calculate the probability of failure in connection with the return period of the trigerring events (Van Westen, 1993). The resulting safety factor should never be used as absolute values that are only indicative and can be used to test different scenarios of slip surfaces and groundwater depths (Van Westen, 1993).

According to Jelinek and Wagner (2007), various approaches of deterministic analysis for landslide hazard zonation have been developed. Some of the earliest studies of deterministic method in a GIS environment were carried out by Van Westen (1993); Terlien, et al. (1995), and Van Westen and Terlien (1996). "The use of a GIS environment made it possible to extend the conventional, site specific deterministic model into larger areas, where the spatial distribution of input parameters is taken into account" (Jelinek and Wagner, 2007). Observed by Corominas and Santacana (2003); Jelinek and Wagner (2007), "geotechnical approaches for landslide hazard analysis in a GIS environment have not been checked with traditional methods of analysis, neither have they been validated with results of landslide monitoring".

2.3.5. Validation

The most important and the absolutely essential component in prediction modelling is to carry out a validation of the prediction results (Chung &

Fabbri, 2003). Without some kind of validation, the prediction model and image are totally useless and have hardly any scientific significance. "Validation" is used solely as a technical term-of-art in testing for model goodness-of-fit and thus judging acceptance; no connotation of absolute "truth" in the strictest sense is intended (Sterman et al., 1994; Chung & Fabbri, 2007).

According to Jimenez-Peralvarez, et al. (2009), the degree of fit was used to assess the association between the inventory and the landslide-susceptibility map. The map quality was assessed by using spatial autocorrelation techniques and measuring the degree of fit between a given dataset and the maps (Goodchild, 1986; Jimenez-Peralvarez, et al., 2009). The final aim of validation is to assess the susceptibility map quality as a predictive tool to explain the landslide inventory of a study area and a given landslide susceptibility or hazard map may be considered acceptable as a predictive tool for future landslides, only when a given level of quality is attained (Jimenez-Peralvarez, et al., 2009).

2.4. Slope Stability

The main driving force behind mass wasting processes is gravity, as it is constantly pulling on mass and attempting to force it downhill (Kusky, 2008). The tangential component of gravity tends to pull material downhill and results in mass wasting (Kusky, 2008). The boulder falls downhill, resulting in a mass wasting event when the tangential component of gravity (gt on figure 2.6) is great enough to overcome the force of friction at the base of the boulder. The friction is really a measure of the resistance to gravity so that the greater the friction, the greater the resistance to gravity's pull (Figure 2.6).

Lubrication of surfaces in contact can greatly reduce the friction, allowing the two materials to slide past one another more easily (Kusky, 2008). Mass wasting events tend to occur more frequently during times of heavy or prolonged rain when water that is a common lubricating agent presents. For a mass wasting event or a mass movement to occur, the forces of lubrication must be strong enough in overcoming the resisting forces that tend to hold the boulder in place against the gravitational force. Lubricating

forces include the cohesion between similar particles (like one clay molecule to another) and the adhesion between different or unlike particles (like the boulder to the clay beneath it). When the resisting forces are greater than the driving force (tangential component of gravity), the slope is steady and the boulder stays in place and when lubricating components reduce the resisting forces so much that the driving forces are greater than the resisting forces, slope failure occurs (Kusky, 2008).

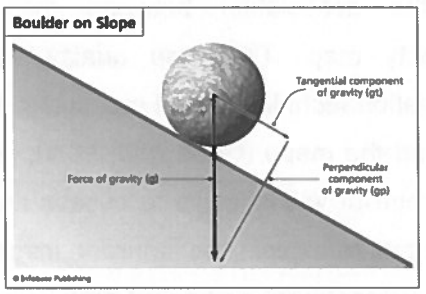

Figure 2.6. Force diagram for mass wasting (Kusky, 2008). Gravity acting on a boulder on a slope can be broken into two components, one parallel to the slope (gt) and one perpendicular to the slope (gp).

The movement process of regolith downslope (or underwater) may occur rapidly or it may proceed slowly (Kusky, 2008). Slopes on mountainsides in any case typically evolve toward steady state angles known as the repose angle balanced by material moving in from upslope and out from downslope. This repose angle is also a function of the regolith grain size.

Driving forces for mass wasting can also be increased by human activity (Kusky, 2008). It includes excavation for buildings, roads, or other features along the lower portions of slopes that may actually remove the slope parts, causing them to become steeper than they were before construction and to exceed the repose angle that will cause the slopes to become unstable or metastable and susceptible to collapse. Building structures on the tops of slopes will also make them unstable, it becomes extra weight of the building that adds extra stresses to the slope that may be enough to initiate slope to collapse.

Jelinek and Wagner (2007) revealed that slope stability analysis requires a suitable geotechnical model. In a GIS environment, the simple infinite slope model is used generally where the material is assumed to be slidden on a slip surface that is plane and parallel to the ground surface. The slope is

assumed to be infinite in extent at a certain inclination to the horizontal (Nash, 1987; Jelinek and Wagner, 2007).

Landslide hazard as the product of slope stability analysis is expressed by the concept of a safety factor. it is the ratio of resisting forces to driving forces. Failure is possible when a safety factor Sf less than 1.0 (Jelinek and Wagner, 2007).

Safety factor formula used in calculation uses Nash's formula (1987); Jelinek and Wagner (2007). In this equation, the conditions of groundwater are accounted from pore water pressure calculation (u), and c′ and φ′ are the effective strength parameters of cohesion and the internal friction angle, respectively; γ is the unit weight of soil; γ_w is the unit weight of water, β is the slope angle, z is the thickness of soil above the slip surface; and h_w is the height of groundwater level above the slip surface (Figure 2.7).

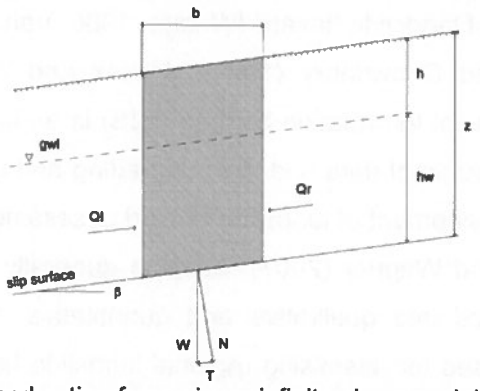

Figure 2.7. Slope slice and acting forces in an infinite slope model based on Nash (1987); Jelinek and Wagner (2007). β is the slope angle, z is the thickness of soil above the slip surface, h is the depth of groundwater table, hw is the height of groundwater level above the slip surface, b is the slice width, W is the weight, N is the normal force, T is the shear force, Ql and Qr are the side forces applied to soil column.

2.5. GIS Application

A geographic information system (GIS) is defined as "a powerful set of tools for collecting, storing, retrieving at will, transforming and displaying spatial data from the real world for a particular set of purposes" (Burrough, 1986; Van Westen, 1993).

Van Westen (1993) revealed that "the applicability of techniques for landslide hazard assessment has been greatly increased by the development of GIS". The first applications of simple, self-programmed, prototype GIS in the analysis of landslide hazard zonation date from the late

1970's until the recent examples of multivariate statistical analysis using GIS have been presented mainly by Carrara and his team (Van Westen, 1993).
Using GIS, deterministic modelling of landslide hazard has become rather popular (Brass et al., 1989; Murphy and Vita-Fincy, 1991; Van Westen, 1993). Most examples of it deal with infinite slope models where they are simple to use separately for each pixel.
In the use of GIS, the application of neighbourhood analysis is a relatively new development for slope instability assessment (Van Westen, 1993). Neighbourhood operations allow as well the neighbouring pixel evaluation around a central pixel, and can be used in the automatic extraction from angle, slope aspect, downslope and cross-slope convexity, ridge and valley lines, catchment area, stream ordering, and the contributing area for each pixel (Van Westen, 1993). This analysis has proved to be very useful in analysis of landslide hazard (Wadge, 1988; Van Westen, 1993).
Aleotti and Chowdhury (1999); Jelinek and Wagner (2007) revealed as Geographical Information System (GIS) is an ideal tool capable of handling large amounts of data and their upgrading and analysis, its expansion led to rapid development of landslide hazard assessment methods.
Jelinek and Wagner (2007) revealed generally hazard evaluation methods are divided into qualitative and quantitative. While statistical analysis is usually used for assessing regional landslide hazard, a physically based or deterministic approach is more frequently used for site-specific areas. The focus of their study was on a deterministic approach of hazard zonation based on a single landslide slope stability analysis. For successful analysis, a basic requirement needed is a thorough knowledge of the geological, geotechnical, and hydrogeological conditions. It needs the extensive background data, which are determined in the field or laboratory. Many limitations of this method because of input data uncertainties are sampling error, spatial variability of land characteristics, or material properties. In general, it can be applied on a large scale over small areas, where it geological and geomorphological conditions are considered as homogeneous.

CHAPTER 3. METHODOLOGY

Methodology of the research generally was separated into 3 phases : pre-fieldwork, fieldwork and post-fieldwork. Pre-fieldwork phase was the preparation activities that could be done before fieldwork activities. Fieldwork phase was the activities in the field to collect data. Post-fieldwork was the activities in analysing field data to achieve the research objectives.

3.1. Materials, Tools and Softwares

For this research, the basic data that were used for deriving parameter maps and for generating and validating the landslide hazard maps are shown in Table 3.1.

The Geological map at scale 1:100,000 from Geological Research and Development Centre was used for creating field guidance map and grouping regolith bulk density of geological formations. The digital topographic map at scale 1:25,000 from Bakosurtanal was used for defining area location, field guidance map, the location of observation sites and landslide locations.

Table 3.1. Materials and sources.

No	Materials	Sources
1	Geological map (1:100,000)	Geological Research and Development Centre
2	Topographic (RBI) map (1:25,000)	Bakosurtanal
3	Digital Elevation Model (DEM) map (10 m)	www.gdem.aster.ersdac.or.jp
4	Actual landslide map	Hadmoko et al. (2008)
5	Cohesion map	Field observation
6	Friction angle map	Field observation
7	Slope map	Generation from DEM map
8	Regolith thickness map	Field observation
9	Regolith bulk density map	Field and laboratory observation
10	Water saturation	Scenarios defined
11	Wetness Index (WI) map	Generation from DEM map

Digital Elevation Model (DEM) map was used for catchment extraction, creating slope map and wetness index (WI) map. The DEM was ASTER GDEM that is Advanced Spaceborne Thermal Emission and Reflection Radiometer (ASTER) Global Digital Elevation Model (GDEM) downloaded from URL: www.gdem.aster.ersdac.or.jp. It has pixel size 30 m and has

been resampled to be 10 m. In catchment extraction, catchment boundary was used for creating field guidance map. Slope map was used to derive sine, cosine, cosine squared maps that were used in safety factor calculation.

Actual landslide map from previous researcher (Hadmoko et al., 2008) provided landslide information including it locations and time of landslide. This map was updated by adding new information of landslide found in the field in 2010. This map was used for validation of landslide hazard maps resulted from analysis.

Other data such as cohesion, friction angle, regolith thickness, and regolith bulk density maps were obtained from field and laboratory investigation. Water saturation was defined from scenarios of saturation.

For this research, several tools as field and laboratorical tools were used that are listed in the following Table 3.2.

Table 3.2. Field and laboratory tools used in the research.

No	Tools	Use	Pictures
1	Global Positioning System (GPS)	Determining geographic position	
2	Geological Hammer	Measuring Uniaxial Compressive Strength (UCS), fracturing stone, blowing iron pipe in rockmass sampling	
3	Geological Compass	Measuring the azimuth/direction	
4	Pocket knife	Measuring UCS	
5	Meter	Measuring regolith thickness	
6	Iron pipe	Sampling rockmass	
7	Plastic bag for samples	Collecting rockmass samples	
8	Oven	Drying rockmass samples	
9	Weight scale	Measuring the weight of samples	
10	Camera	Taking pictures of research activities	

Several softwares were used in this research which consist of GIS software, word processing, spreadsheet data processing, and presentation preparation. Those softwares are listed as follows:

- Ilwis 3.7;
- MS Excel 2003;
- MS Word 2003;
- MS Power Point 2003.

Ilwis 3.7 was used for importing some image files based on it, performing data analysis, laying out and presenting the results.

MS Excel 2003 was the software for spreadsheet data processing such as tabulating field data, calculating cohesion and friction angle, and calculating regolith bulk density.

MS Word 2003 was the software for creating and presenting the report as the result of all research activities.

MS Power Point 2003 was the software for preparating and presenting the result of research in presentation.

3.2. Methods Applied

3.2.1. General method

General method used in this research for assessing landslide hazard zones was deterministic method using outcrop-based Geological Strength Index (GSI) system. In pre-fieldwork phase, it included collecting basic data (geological, topographic, DEM and actual landslide maps), creating field gudance map and preparing tools for fieldwork. In fieldwork phase, itincluded collecting outcrop GSI data (GSI, UCS and *mi* values), outcrop regolith thickness, outcrop regolith samples for bulk density and new landslide data. In post-fieldwork phase included creating parameter maps of slope stability calculation, calculating slope stability, creating landslide hazard zones, updating the actual landslide map, and validating landslide hazard zones. Creating parameter maps included creating cohesion and friction angle maps, regolith thickness map, regolith bulk density map, and water saturation scenarios. Calculating slope stability was by using infinite slope formula that used parameter maps as the input. Creating landslide hazard zones was using the result of slope stability calculation in the term

of hazard in landslide. Updating the actual landslide map was by adding new landslide data to be actual landslide updated map. Validating landslide hazard zones was by using degree of fit method that could be used to examine the reliability of the method.

The methods are represented in a conceptual framework as shown in the following figure.

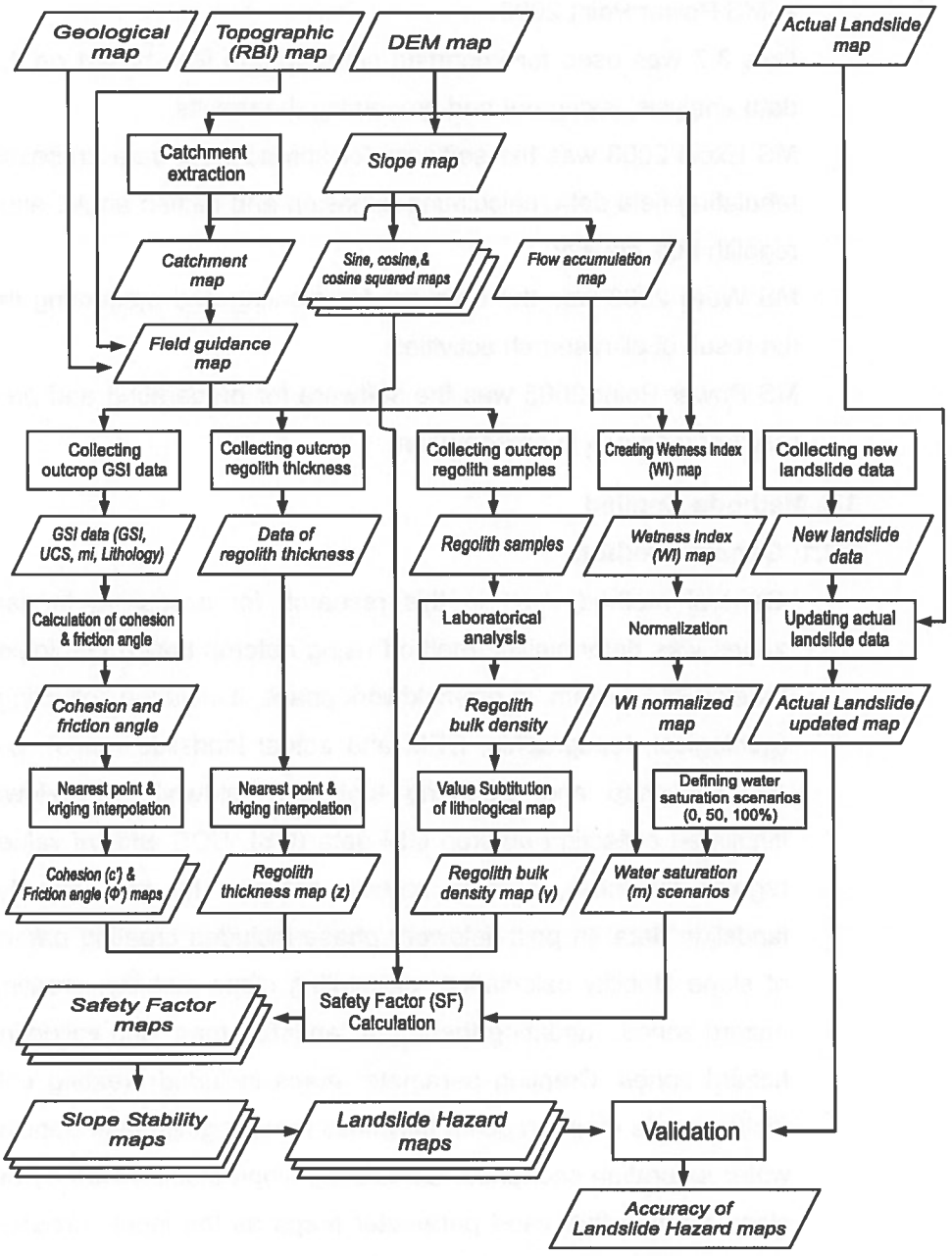

Figure 3.1. Conceptual framework of research.

3.2.2. Data collection

Data collection was performed to obtain some field (outcrop-based) GSI data and other parameter data such as regolith thickness and regolith bulk density. GSI data is the data that is taken into account in GSI system that can be collected from outcrops, surface excavations and borehole cores. In this research GSI data was collected from outcrops that are GSI value, uniaxial compressive strength (UCS), and *mi* (contant of intact rockmass) defined from lithology.

3.2.2.1. Collecting field GSI data

Method used to obtain field GSI data is visual inspection by estimating the reduction in rock mass strength for different geological conditions in term of blockiness, and the discontinuities indicated by joint roughness and alteration.

The steps for obtaining GSI data in the field were :

- Finding outcrop for investigation;
- Identifying the structure of regolith found;
- Identifying the structure of rock mass (at saprolith portion) that is ranging from intact to laminated/sheared;
- Identifying surface condition (roughness and weathering condition) that is ranging from very good to very poor;
- Defining ranging GSI value by using the GSI table (Hoek, 2007).

Uniaxial Compressive Strength (UCS) was also measured. In the field, the steps for obtaining UCS were :

- Using the tools such as geological hammer, pocket knife and thumbnail to chip, scrape or peel, and indent rock mass (saprolith);
- Grading the result of strongness ranging from R0 to R6 and define the UCS in the other column of field estimates of uniaxial compressive strength table (Hoek, 2007).

The constant of rock mass (saprolith) and lithology were defined from the following steps :

- Defining the rock type of lithology (saprolith);
- Defining the name of rock mass (saprolith);
- Defining the *mi* value of rock mass (saprolith) by using table of values of the constant *mi* for intact rock, by rock group (Hoek, 2007).

3.2.2.2. Collecting regolith thickness data

Method used to obtain regolith thickness was field measurement using height meter and estimation by using height scale. For thin regolith, it was measured a height meter and if the regolith outcrop was thick, estimation was done by using scale from height meter (Figure 3.2). Due to the variation of field condition, some sites were found to have complete regolith called true regolith thickness and some sites were found not to have complete regolith that were called minimum regolith.

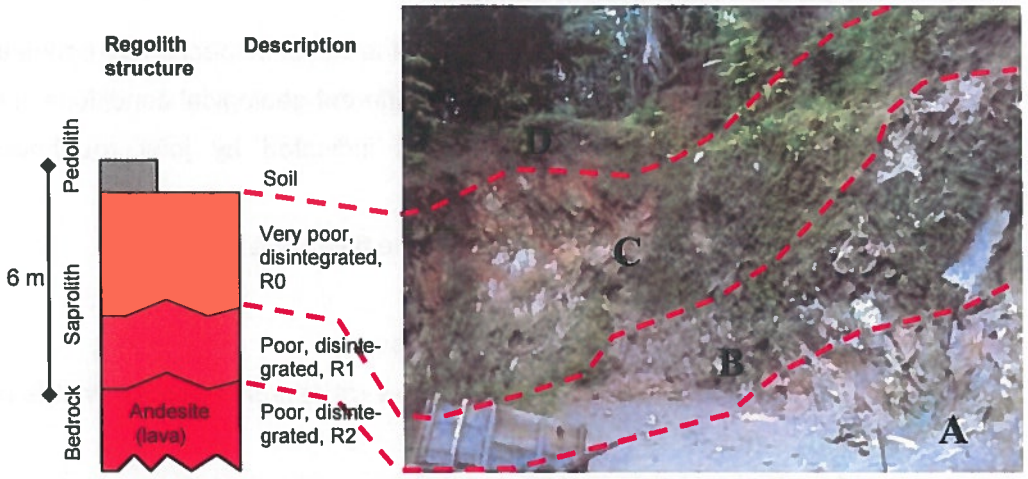

Figure 3.2. Field investigation at site 113 as an ilustration of field data collection where A = bedrock (andesite lava), B,C = saprolith and D = soil. B portion was the place for collecting GSI data of this site. Regolith thickness was estimated from boundary between A-B to soil surface (D).

3.2.2.3. Collecting regolith bulk density data

Method used to obtain regolith bulk density data in the field was taking samples from each geological formation in research area. Samples were taken from saprolith portion of regolith (Figure 3.2) by using iron pipe blowed by geological hammer (Figure 3.3) and taking handspecimen if the lithology was compact enough.

The samples were kept in plastic bags and numbered with it sites (Figure 3.3). Samples were prepared (Figure 3.4) by measuring its volume and they were dried using oven and measured the weight using a scale. Bulk density was calculated using bulk density formula that is bulk density = mass/volume = sample weight (in dry condition)/volume.

Figure 3.3. Rock mass sampling using iron pipe blowed by geological hammer at saprolith portion of regolith.

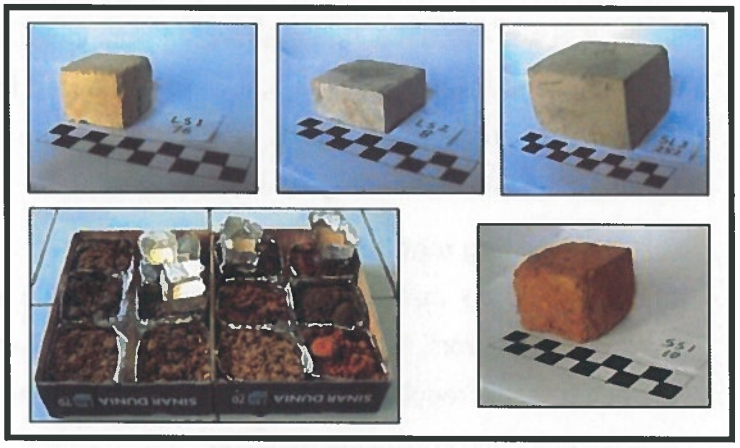

Figure 3.4. Rock mass samples after measuring their volumes were ready to be oven dried.

3.2.3. Data analysis

Data analysis was performed to derive parameter maps to assess landslide hazard.

3.2.3.1. Catchment extraction

Catchment extraction was generated by using DEM from aster GDEM in Ilwis 3.7. Catchments were calculated for each stream found in the output map of the Drainage network ordering operation. The operation uses a Flow direction map to determine the flow path of each stream. Catchment can be merged afterwards with the Catchment merge operation.

3.2.3.2. Creating slope maps and wetness index (WI) map

Method used to create slope maps is deriving those maps from DEM map. Slope maps (sine, cosine, cosine squared) were also created in Ilwis 3.7. The WI map was processed in Compound Index Calculation by putting DEM map and Flow Accumulation Map.

3.2.3.3. Creating cohesion and internal friction angle maps

Method used to create cohesion and friction angle maps is interpolating cohesion and friction angle data processed from field GSI data. In order to obtain the better result, interpolation methods used were nearest point and kriging that involved field data from 259 sites of observation. Cohesion and friction angle values were obtained from Hoek et al. (1998) (Table 2.4).

GSI system was made to assess the rock mass qualitatively that produces GSI, UCS and *mi* values that are ranging from lower to higher value (Table 2.1-3). Due to this ranging value, it were processed in lower, mean, higher range. This process, of course, resulted cohesion and friction angle in lower, mean and higher range (Appendix 3).

3.2.3.4. Creating regolith thickness map

Method used to make regolith thickness map is interpolating regolith thickness data from field outcrop-based measurement. In order to obtain the better result, regolith thickness maps were created in Ilwis 3.7. by using nearest point and kriging interpolation.

3.2.3.5. Creating regolith bulk density map

Method used to make regolith bulk density map was subtituting geological formations in geological map with bulk density values derived from laboratory analysis of samples (Appendix 4).

3.2.3.6. Defining water saturation scenarios

Method used to define water saturation scenarios were by imposing water saturation scenarios in 0, 50, and 100% saturation and Wetness Index based water saturation (Wetness Index normalized).

3.2.3.7. Calculating safety factor

Method used to calculate safety factor was the infinite slope formula of Nash (1987); Jelinek and Wagner (2007) that expresses the safety factor as follows :

$$Sf = \frac{c' + (\gamma.z\cos^2\beta - u)\tan\varphi'}{\gamma.z\sin\beta\cos\beta}$$

Groundwater conditions in the above equation are accounted for by calculating pore water pressure u described as:

$$u = \gamma_w h_w \cos^2\beta$$

Those two formulas above can be expressed as follows :

$$SF = \frac{c' + (\gamma - m\gamma_w)z\cos^2\beta\tan\varphi')}{\gamma z\sin\beta\cos\beta}$$

where c' and φ' are the effective strength parameters of cohesion and the angle of internal friction, respectively; γ is the bulk density of regolith; γ_w is the density of water, β is the slope angle, z is the thickness of regolith above the slip surface; and h_w is the height of groundwater level above the slip surface.

For calculating the safety factor, the cohesion values were calculated from cohesion map, friction angle was generated from GSI data, regolith bulk density was generated from subtitution of geological formations with regolith bulk density data, sin β, cos β, cos^2 β were generated from radian map generated from slope map and m is water saturation scenarios in 0, 50, and 100%.

3.2.3.8. Defining slope stability

Method used to create slope stability map was by slicing the safety factor values of area. Slope stability is considered unstable if the safety factor is less than 1, critical if it is between 1 and 1.5, and unstable if it is more than 1.5.

3.2.3.9. Defining landslide hazard zones

Method used to create landslide hazard map was also created using slope stability values. High hazard is considered if the safety factor is less than 1, moderate if it is between 1 and 1.5 and low if it is more than 1.5. In other word, landslide hazard zones and slope stability map are the same thing but have different term.

3.2.3.10. Validating landslide hazard zones

Method used to validate landslide hazard map was the degree of fit (DF). It assesses the association between the landslide inventory map and the generated landslide hazard map by using the following formula (Goodchild, 1986; Jimenez-Peralvarez, et al., 2009):

$$DFi = \frac{mi / ti}{\sum mi / ti}$$

where *mi* is the area occupied by the source areas of the landslides at each susceptibility level *i*, and *ti* is the total area covered by that susceptibility level. The degree of fit for each susceptibility level represents the percentage of mobilized area located in each susceptibility class. The lower the degree of fit (less than 7%) in the low and very low susceptibility classes (relative error), and the higher the degree of fit in the high or very high susceptibility classes (relative accuracy), the higher the quality of the susceptibility map will be (Ferna´ndez et al. 2003; Irigaray et al. 2007; Jimenez-Peralvarez, et al. 2009).

CHAPTER 4. RESEARCH AREA

4.1. Area Profile of Kulon Progo Regency

The information from URL: http://www.kulonprogokab.go.id/, Kulon Progo is a regency of five regency in Yogyakarta Province, Indonesia that is located at west side. Kulon Progo is bordered by Bantul and Sleman Regency at east, Purworejo Regency, Central Java Province at west, Magelang Regency, Central Java Province at north, and Hindia Ocean at south side. Kulon Progo varies in topographic condition with the elevation between 0-1000 meters above sea level, that is distinguihed into three area as follows :

- North Area

North area is Menoreh mountains with elevation between 500-1000 meters abobe sea level. This region includes Girimulyo, Kokap, Kalibawang and Samigaluh districts. The usage of this area are conservation area and as the area that is susceptible to landslide disaster.

- Central Area

Central area is a hilly area that has elevation between 500-1000 meters above sea level. It includes Nanggulan, Sentolo, Pengasih, and a part of Lendah districts that has slope between 2-15% (undulating area) as the area between flat area to mountainous area.

- South Area

South area is a low flat area with elevation between 0-100 meters above sea level. It includes Temon, Wates, Panjatan, Galur and a part of Lendah districts. This area is coastal plain area that has slope between 0-2% and in rainy season it becomes an area that is susceptible to flood disaster.

The extent of Kulon Progo Regency is about 58,627.54 hectars, administratively distinguished into 12 district that includes 88 villages and 930 subvillages. Its landuse are paddy field 10,732.04 Ha (18.30%), dry field 7,145.42 Ha (12.19%), mixed plantation 31,131.81 Ha (53.20%), residential area 3,337.73 Ha (5.69%), forest 1,025 Ha (1.75%), farmer's plantation 486 Ha (0.80%), bareland 1,225 Ha (2.09%), dam 197 Ha (0.34%), fishpond 50 Ha (0.09%), and other usage 3,315 Ha (5.65%).

Kulon Progo Regency is crossed by two traffic lane that are national traffic in Java Island. Those are National road along 28.57 km and train rail about 25 km. Almost all of Kulon Progo area can be reached by land transportation.

The average rainfall/year is up to 2,150 mm, and average of rainy days is 106 days/year or 9 days/month with the highest rainfall value on January and the lowest on August. The lowest temperature is about 24.2°C on July and the highest 25.4°C on April, the lowest humidity 78.6% on August, and the highest 85.9% on Januari. Monthly intensity average of sun shining is about 45.5%, the lowest 37.5% on March and the highest 52.5% on July.

Location of research is Kayangan catchment located at the north part of Kulonprogo Regency, Yogyakarta Province, Indonesia. This location is approximaly 40 km at the west of Yogyakarta city (Figure 4.1). It includes Samigaluh district at north side, Giripurwo district at south side, Nanggulan districts at east side of Kulon Progo Regency, Yogyakarta Province and small part of Kaligesing district of Purworejo Regency at west side, Central Java Province.

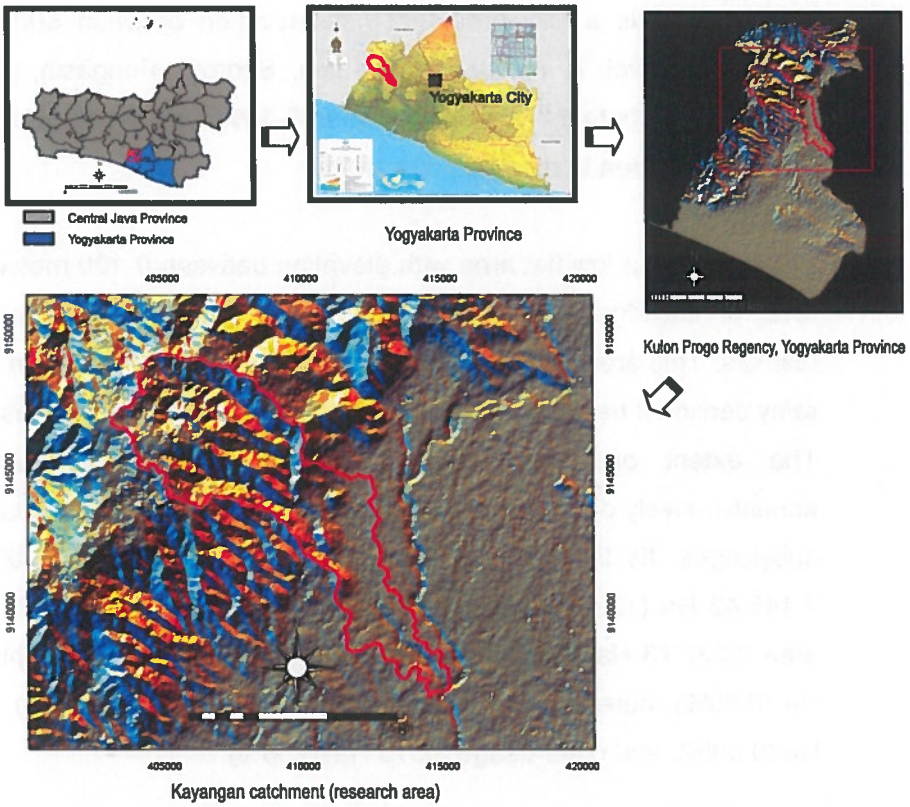

Figure 4.1. Administrative map of Central Java and Yogyakarta Province, Kulon Progo Regency and the Research Area.

4.2. Geology of Kulon Progo Area

4.2.1. Regional Geomorphology

According to Bemmelen (1949); Haryono (2001), physiographically Java and Madura are distinguished into four regional physiography : a) West Java (west of Cirebon), b) Central Java (between Cirebon and Semarang), c) East Java (between Semarang and Surabaya), d) Corner of East Java narrows and Madura Island. Central Java physiography are distinguished into four : a) North Coastal Plain, b) North Serayu Mountains, c) South Serayu Mountains, d) South Coastal Plain. From this distinguishing, Kulon Progo area is included into South Serayu Mountains. This physigraphy is bordered by Purworejo area at west, Magelang plain at north, Progo river at east, and south coastal plain at south.

4.2.2. Stratigraphy

According to Rahardjo, et al. (1995), stratigraphic sequence of Kulon Progo mountains from the oldest to youngest are as follows :

4.2.2.1. Nanggulan Formation

Nanggulan Formation consists of sandstone with intercalation of lignite, sandy marl, claystone with limonite concretion, intercalations of marl and limestone, sandstone, and tuff that is rich of foraminifers and molluscs (Figure 4.2). This formation is estimated 300 meters in thickness (Rahardjo, et al. 1995). Based on planktonic foraminifer study, this formation has the range of age between Middle Eocene – Upper Oligocene (Hartono, 1969; Rahardjo, et al., 1995).

Figure 4.2. Site 221 showed intercalation of marl and siltone of Nanggulan Formation (left), site 224 showed andesitic breccia of Kebobutak Formation (middle), site 108 showed andesite (lava) of Kebobutak Formation (right).

4.2.2.2. Kebobutak Formation

Kebobutak Formation consists of andesitic breccia, tuff, lapilli tuff, agglomerate and intercalations of andesitic lava flows (Figure 4.2). It is estimated about 600 meters in thickness and has the range of age between Upper Oligocene-Lower Miocene (Rahardjo, et al. 1995).

4.2.2.3. Jonggrangan Formation

Jonggrangan formation consists of conglomerate, tuffaceous marl and calcareous sandstone with intercalations of lignite seams, limestone and coralline limestone (Figure 4.3). Rock sequence to the top becomes bedded limestone and coralline limestone with 250 meters in thikness (Rahardjo, et al. 1995).

According to Haryono (2001), the lower part of this formation consists of intercalation of conglomerate, sandstone, siltstone, and claystone and also some lignite seams (Figure 4.3). The source rocks of this part are Old Andesite (Kebobutak) and Nanggulan Formations. This part was sedimented in deltaic environment controlled by transgression relative sea level change with 82 m in thickness. From palynomorph analysis by Hassan (1999); Haryono (2001), its age is Early Miocene (N6-N7).

Figure 4.3. Site 8 showed limestone of upper portion of Jonggrangan Formation (left), site 1 showed conglomerate and sandstone of lower portion of Jonggrangan Formation (right).

4.2.2.4. Sentolo Formation

Sentolo formation consists of limestone and marly sandstone (Figure 4.4). Rock sequence to the top gradually changes to be bedded limestone that is rich of foraminifers. The thickness is about 950 meters (Rahardjo, et al. 1995).

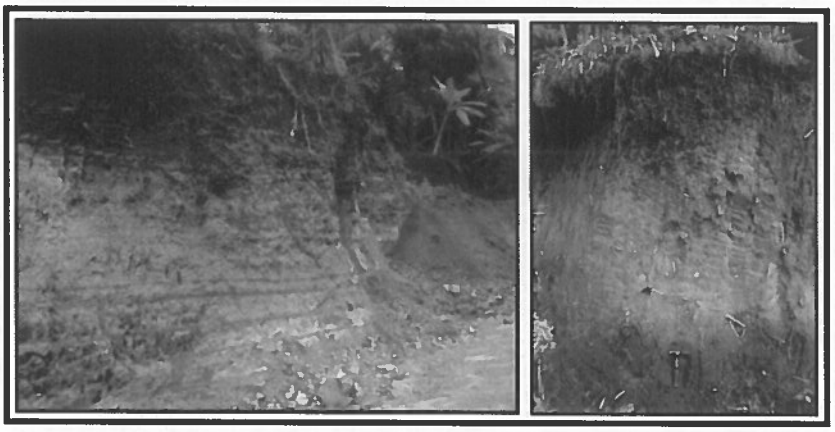

Figure 4.4. Site 197 showed intercalation of siltstone-sandstone of Sentolo Formation (left), site 253 showed sand deposit of Young Volcanic Deposits of Merapi Volcano.

4.2.2.5. Young Volcanic Deposits of Merapi Volcano

Young volcanic Deposits of Merapi Volcano consists of undifferenciated tuff, ash, breccia, agglomerate and lava flows (Rahardjo, et al. 1995) (Figure 4.4).

4.2.2.6. Colluvium

Colluvium consists of unsorted debris from the Kebobutak Formation (Rahardjo, et al. 1995).

4.2.2.7. Alluvium

Alluvium consists of gravel, sand, silt and clay along larger streams and coastal plain (Rahardjo, et al. 1995).

4.2.3. Geological Structure

According to Bemmelen (1949); Haryono (2001), Kulon Progo mountains is an oblong dome long shaped, diameter NNE-SSW is about 32 km and diameter WNW-ESE is about 15-20 km. After subsidence occured in Eocene period, Kulon Progo basin was uplifted and domed by uptrusion activities of Menoreh Mountains with the tendency of axe is WNW-ESE. In lower Burdigalian subsidence occured at Kulon Progo mountains complex untill below of sea level surface that caused synclinal structures at the south foot of Menoreh Mountains and faults with direction east-west (E-W) or flexure that seperated Menoreh Mountains from Gadjah Volcan. At the Upper Miocene Kulon Progo area becomed low plain and at peak of Menoreh was formed the remaining hills with the elevation about 400 meters. At last the overall Kulon Progo Mountains complex was domed in Pleistocene that caused radial fault

that cut breccia of Idjo Mountain and Sentolo Formation, also faults that cut Jonggrangan limestone and low graben was formed at south-east of the dome.

4.3. Kayangan Catchment

The extent of Kayangan cathment extracted from catchment extraction process in Ilwis 3.7 is 44,6 km^2 and its perimeter is 49.5 km. It has altitude between 33 – 811 m above sea level. The lower altitude (33 – 360 m) is located at east side and the higher altitude (360-811 m) at west side (Figure 4.5).

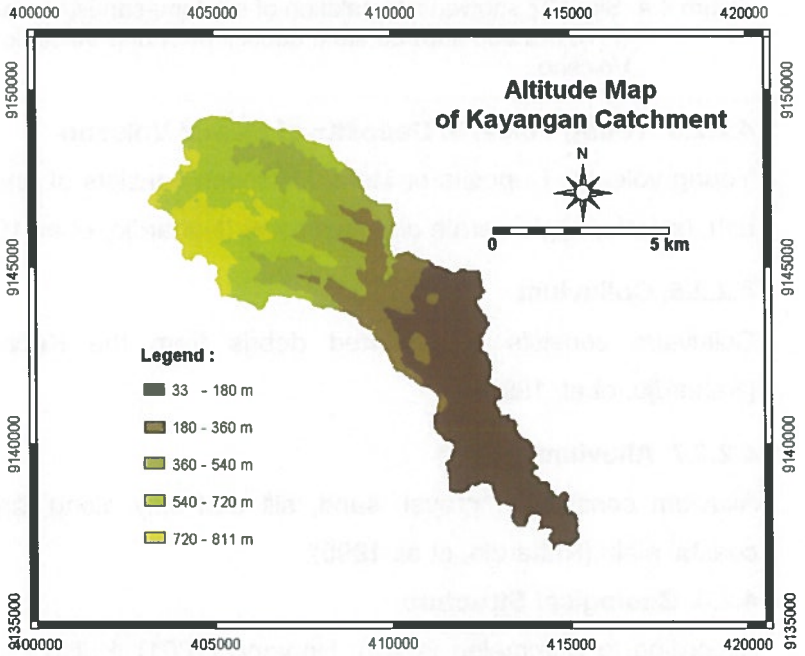

Figure 4.5. Altitude map of Kayangan cathment.

Relief class of this catchment according to Zuidam, van, R.A.; Zuidam-Cencelado van, F.I.; (1979); Colombo et al. (2001), varies from flat (0-2%) to extremely steep (>40%). West side is dominated by steep-extremely steep relief and east side is dominated by flat-moderately steep relief (Figure 4.6).

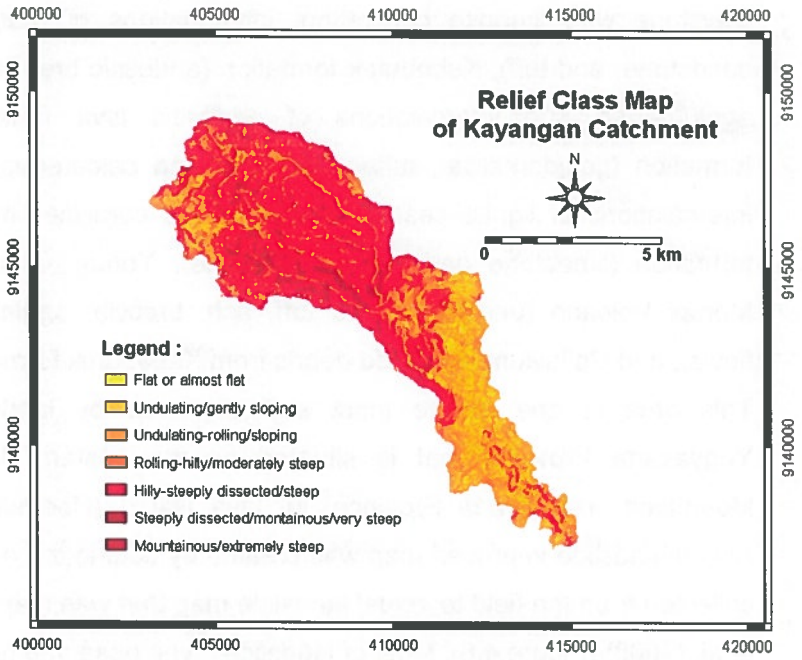

Figure 4.6. Relief class map of Kayangan Cathment.

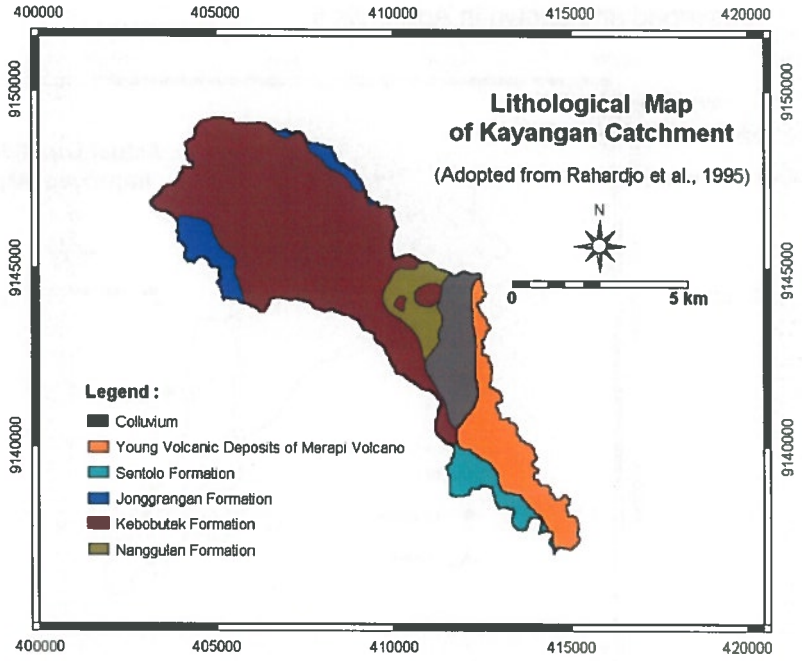

Figure 4.7. Lithological map of Kayangan Catchment adopted from Rahadjo et al. (1995).

Adopted from Rahardjo et al. (1995), Kayangan catchment consist of 6 geological formations (Figure 4.7). Those from lower to uppper are as follow: Nanggulan formation (sandstone with intercalated of lignite, sandy marl,

claystone with limonite concretion, intercalations of marl and limestone, sandstone, and tuff), Kebobutak formation (andesitic breccias, tuff, lapilli tuff, agglomerate and intercalations of andesitic lava flows), Jonggrangan formation (conglomerate, tuffaceous marl and calcareous sandstone, with intercalations of lignite seams, limestone and coralline limestone), Sentolo formation (limestone and marly sandstone), Young Volcanic Deposits of Merapi Volcano (undifferentiated tuff, ash, breccia, agglomerate and lava flows), and Colluvium (unsorted debris from Kebobutak formation).

This area is one of the most suffering area by landslide disaster in Yogyakarta Province that is situated on the eastern flank of Menoreh Mountains, Yogyakarta Province, in Java Island (Hadmoko et al., 2008). Actual landslide improved map was created by adding the new landslide data collected from the field to actual landslide map that was mapped by Hadmoko et al. (2008) (Figure 4.8). Most of landslides type observed from the field were debris flow that occured in high rainfall event. Those landslides were described and shown in Appendix 5.

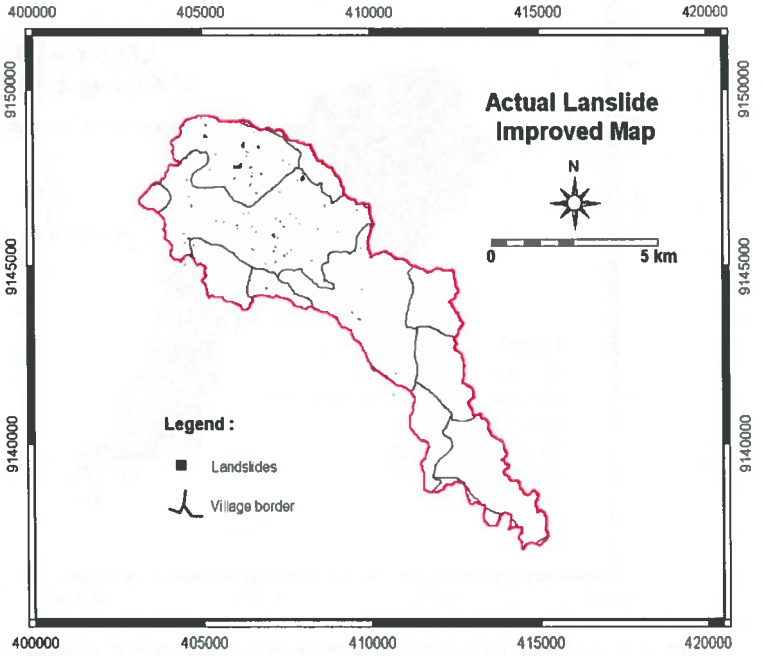

Figure 4.8. Actual landlide map of Kayangan Catchment that was improved by adding new landslide data (modified from Hadmoko et al. (2008)).

CHAPTER 5. DATA ANALYSIS

In order to obtain the results of research, several data analysis had to be done. Those were analysis for obtaining catchment boundary (catchment extraction), obtaining parameter maps (cohesion, friction angle, slope, wetness index, regolith thickness, regolith bulk density maps), defining landslide hazard zones (calculating safety factor and slope stability), updating actual landslide map and validating landslide hazard zones. The basic data of those analysis were secondary data (DEM, topographic, geological maps and actual landslide data) and primary data (GSI, regolith thickness, regollith bulk density and new landslide data). Analysis were performed by using software Ilwis 3.7 for GIS analysis and MS Excel for spreadsheet analysis.

5.1. Catchment Extraction

Kayangan catchment was extracted by using DEM as the basic data (Figure 5.1). This boundary catchment extracted was used to limit the area processed in all processes of landslide hazard zonation.

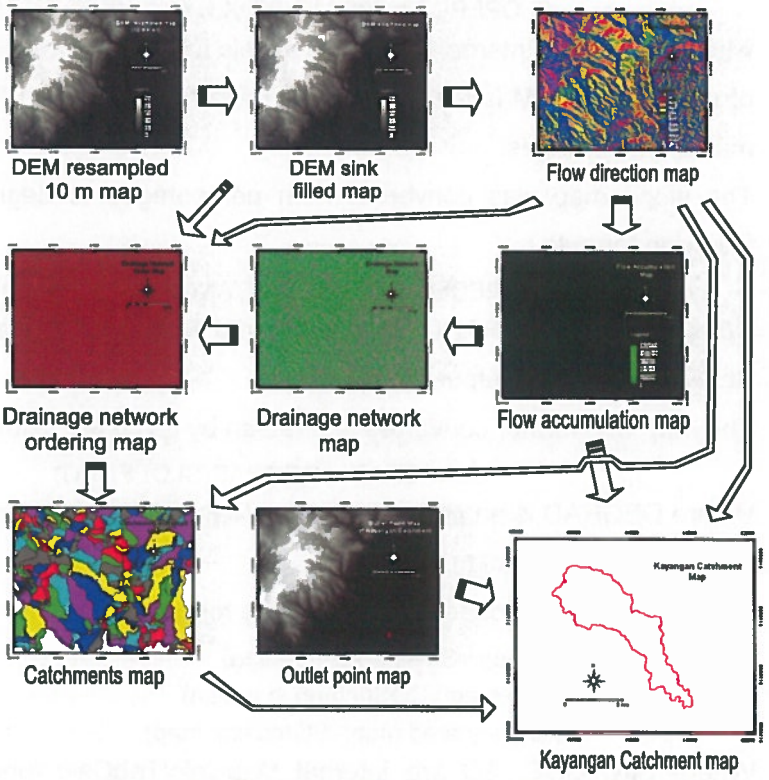

Figure 5.1. Kayangan catchment extraction process.

The detail extraction processes are enlightened as follows (Figure 5.1): DEM original image (tiff format) was imported to Ilwis format and resampled in 10 meter pixel size. The new resampled DEM was processed using fill sinks and then flow direction operations. In creating flow direction map, parallel drainage correction algorithm and steepest slope method was followed. Drainage network was extracted using flow accumulation map and stream threshold of 9 pixels and the streams were ordered using minimum drainage length of 1000 m. Catchments map was created using drainage network order and flow direction map. Outlet point was defined using flow accumulation map at coordinate (414992, 9137086).

5.2. Creating Slope maps and Wetness Index (WI) map

Derivatives of the slope map (sine, cosine, cosine squared) were created. The detail processes are enlightened as follow (Figure 5.2) :

First of all height differences in x and y axis directions were created using filter operations (linear DFDX and linear DFDY). Then the slope map in percentages was calculated using the following formula :

SLOPEPCT = 100 * HYP(DX,DY)/ PIXSIZE(DEM)

where HYP is an internal Mapcalc/Tabcalc function, PIXSIZE is the pixel size of DEM map, DEM is the DEM map file name and SLOPEPCT is the output map in percentages.

The slope map was converted from percentages to degree by using the following formula :

SLOPEDEG = RADDEG(ATAN(SLOPEPCT/100))

Where ATAN and RADDEG are internal MapCalc/TabCalc functions and SLOPEDEG is the output map in degree.

The map was further converted into radian by using the following formula :

SLOPERAD = DEGRAD(SLOPEDEG)

Where DEGRAD is an internal MapCalc/TabCalc function and SLOPERAD is the output map in radian.

Slope maps were processed by using the following formula :

Sine map:=SIN(inmap in radian)
Cosine map:=COS(inmap in radian)
Cosine squared map:=SQ(cosine map)

Where SIN, COS, SQ are internal MapCalc/TabCalc functions and Sine, Cosine and Cosine squared are the outmaps of slope map (Figure 5.2).

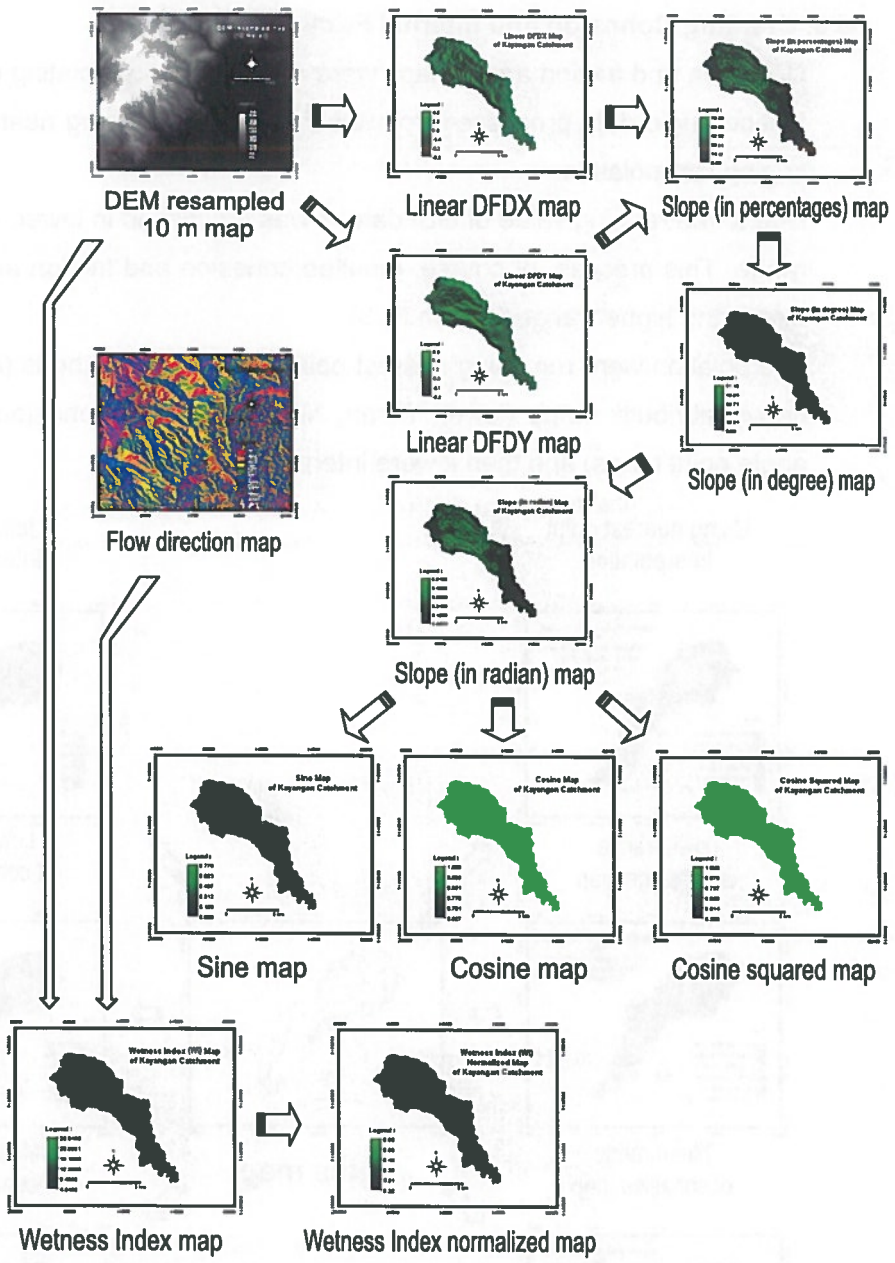

Figure 5.2. Processes in creating sine, cosine, and cosine squared of slope maps, wetness index, and wetness index normalized maps of Kayangan Catchment.

Wetness index (WI) map was processed in Compound Index Calculation by putting DEM map and Flow Accumulation Map into calculation. It then was normalized (Figure 5.2) using following equation :

WI normalized map := WI map/(maximum value of WI).

Where WI map is Wetness Index map, maximum value of WI is 23.9459, and WI normalized map is the output map of normalization of WI map.

5.3. Creating Cohesion and Internal Friction Angle Maps

Cohesion and friction angle maps were created by interpolating cohesion and friction angle data processed from the field GSI data using nearest point and kriging interpolation.

Due to the ranging value of GSI data, it was processed in lower, mean, higher range. This process, of course, resulted cohesion and friction angle in lower, mean and higher range (Appendix 3).

Interpolation were run using nearest point and kriging methods (Figure 5.3) to derive attribute maps (lower, mean, higher value of cohesion and friction angle point maps) and then it were interpolated.

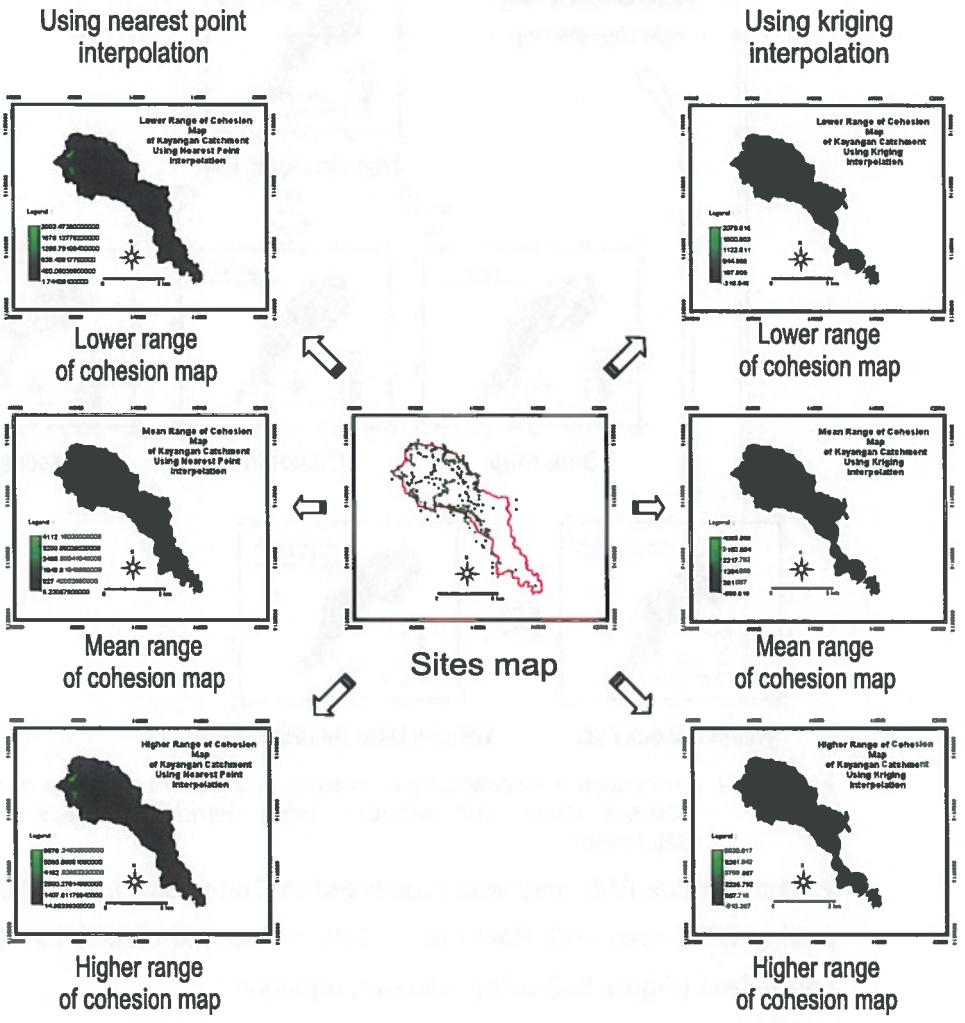

Figure 5.3. Processes in creating cohesion maps using nearest point and kriging interpolation.

The friction angle map in tangent was created by using the following formula (Figure 5.4):

OutMap = TAN(InMap)

Where TAN is an internal MapCalc/TabCalc function, InMap is friction angle map and OutMap is tangent of friction angle map.

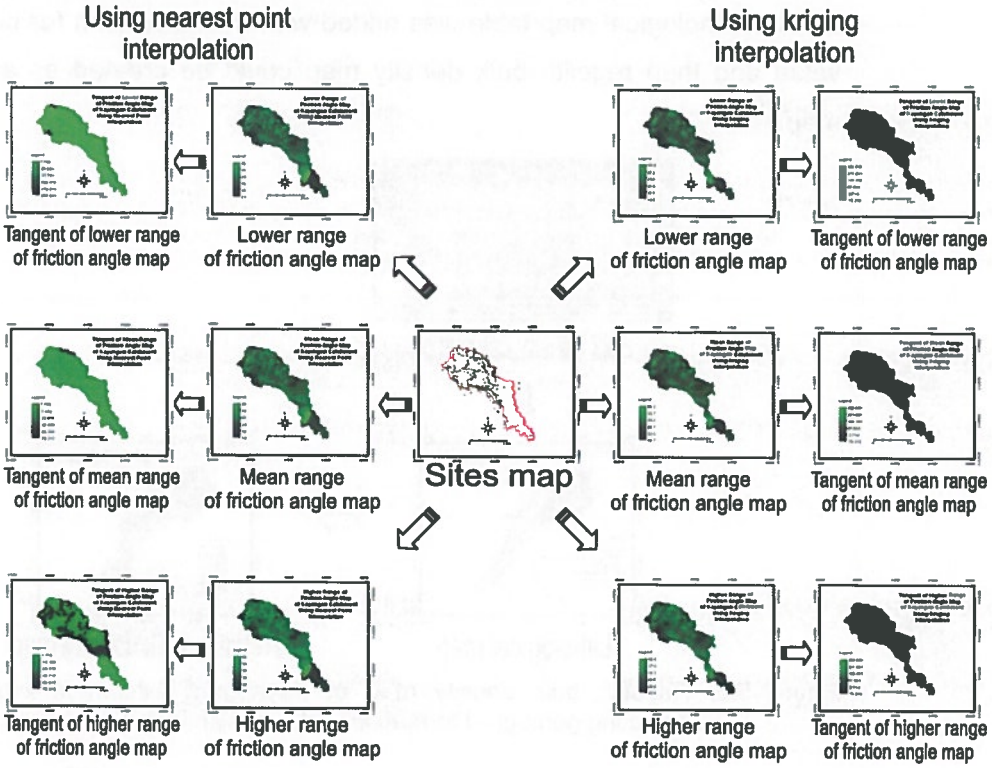

Figure 5.4. Processes in creating friction angle maps using nearest point and kriging interpolation.

5.4. Creating Regolith Thickness Map

Regolith thickness map was created from regolith outcrop estimation of 259 observation sites Figure 5.5).

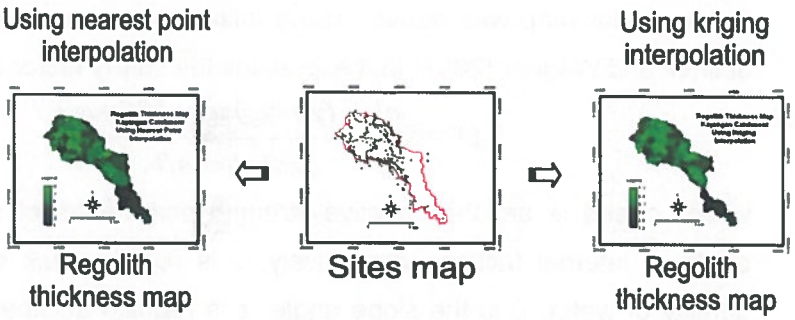

Figure 5.5. Regolith thickness map of Kayangan Catchment processed using nearest point and kriging interpolation.

5.5. Creating Regolith Bulk Density Map

Regolith bulk density map was created by subtituting geological formations in geological (lithological) map with bulk density values analized from laboratory. Bulk density value of each formation was the average of its bulk densities (Appendix 4).

In Ilwis, lithological map table was added with a new column for bulk density value and then regolith bulk density map could be created as an attribute map.

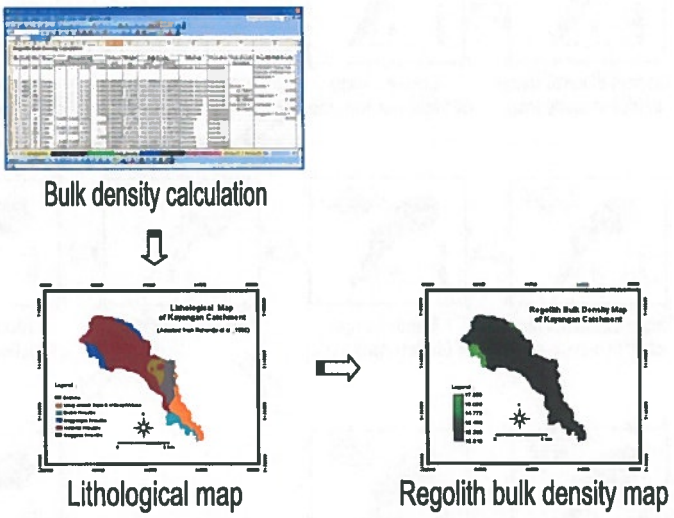

Figure 5.6. Regolith bulk density map of Kayangan Catchment processed by subtituting geological formations with regolith bulk density values.

5.6. Calculating Safety Factor

Safety factor calculation was performed in 24 scenarios (Table 5.1) due to the ranging GSI value (lower, mean, higher), interpolation methods (nearest point, kriging) and water saturation scenarios (0, 50, 100%, wetness index (WI) -based).

Safety factor map was derived using infinite slope formula of Nash (1987); Jelinek and Wagner (2007) that expresses the safety factor as follows :

$$SF = \frac{c' + (\gamma - m\gamma_w) z \cos^2 \beta \tan \varphi')}{\gamma z \sin \beta \cos \beta}$$

where c' and φ' are the effective strength parameters of cohesion and the angle of internal friction, respectively; γ is regolith bulk density; γ_w is the density of water, β is the slope angle, z is regolith thickness above the slip surface; and h_w is the height of groundwater level above the slip surface.

Table 5.1. Safety factor calculation scenarios.

No	Safety Factor Calculation									Scenario
	Ranging GSI value			Interpolation method		Water saturation (%)				
	Lower	Mean	Higher	Nearest point	Kriging	0	50	100	WI-based	
1	X			X		X				1
2	X			X			X			2
3	X			X				X		3
4	X			X					X	4
5	X				X	X				5
6	X				X		X			6
7	X				X			X		7
8	X				X				X	8
9		X		X		X				9
10		X		X			X			10
11		X		X				X		11
12		X		X					X	12
13		X			X	X				13
14		X			X		X			14
15		X			X			X		15
16		X			X				X	16
17			X	X		X				17
18			X	X			X			18
19			X	X				X		19
20			X	X					X	20
21			X		X	X				21
22			X		X		X			22
23			X		X			X		23
24			x		X				X	24

The formula above was created as a function in Ilwis. Safety factor function for water saturation in percentages is as follows :

```
Function Safety Factor(Value M) : Value
Begin
Return (cohesion map+(regolith bulk density map-M*10.000)*regolith thickness map*cosine squared map*tangent of friction angle map)/(regolith bulk density map*regolith thickness map*sine map*cosine map)
;
End;
```

where M is water saturation scenario in percentages and 10.000 is the density value of water (KN/m^3).

Safety factor function for wetness index (WI) based water saturation is as follows :

```
Function L_D_SF_lower_nearest_WI () : Value
Begin
Return (cohesion map+(regolith bulk density map-wetness index normalized map*10.000)*regolith thickness map*cosine squared map*tangent of friction angle map)/(regolith bulk density map*regolith thickness map*sine map*cosine map)
;
End;
```

To run the function, another formula in Ilwis command line for water saturation scenario in percentages must be created as follows :

OutMap:=Function(M)

where M is percentages value of water saturation scenario.

For WI-based water saturation scenario, the formula used is as follows :

OutMap:=Function().

The processes run basically are the processes of paramater maps as input data, safety factor calculation using functions, and safety factor maps as the output (Figure 5.7).

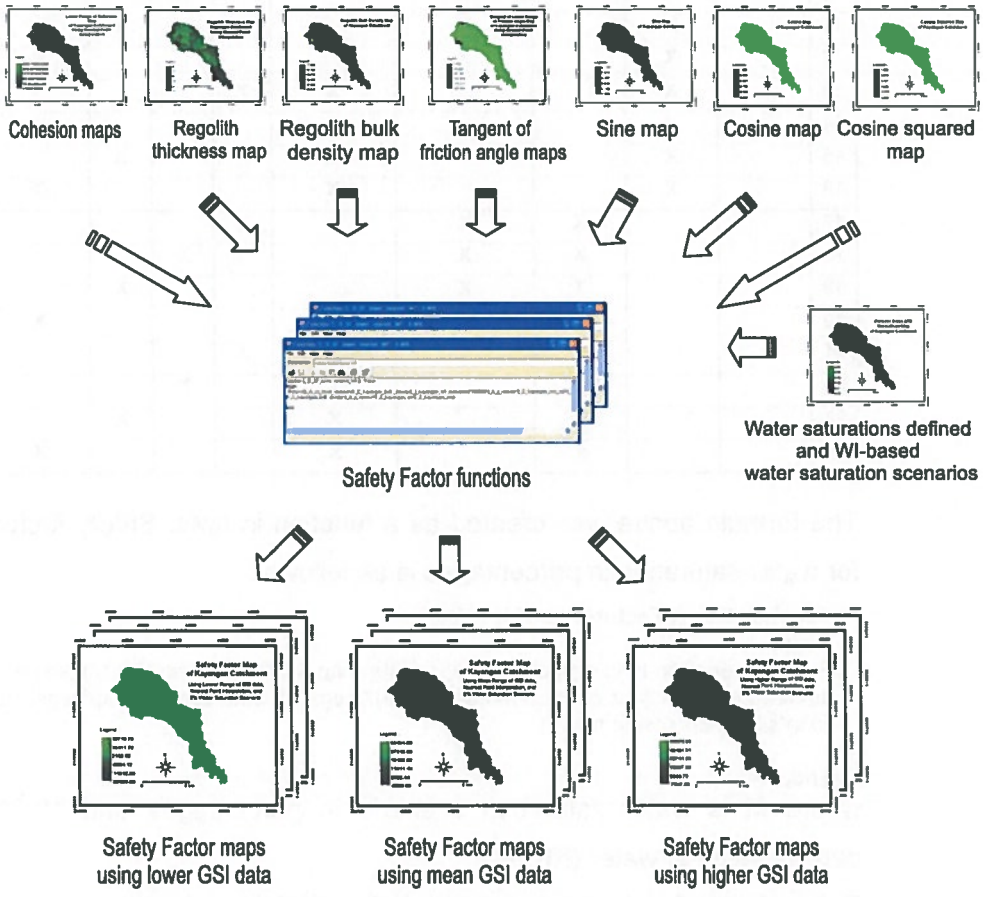

Figure 5.7. Safety factor calculations using lower, mean, and higher range of GSI data and using 0, 50, 100% and Wetness Index based water saturation scenarios. GSI data were processed in nearest point and kriging interpolation.

5.7. Defining Slope Stability

Creating slope stability map was processed by slicing the safety factor value of area by using slope stability domain (Figure 5.8). Slope stability domain was based on the condition that safety factor <1 is unstable, 1-1.5 is critical and >1.5 is stable.

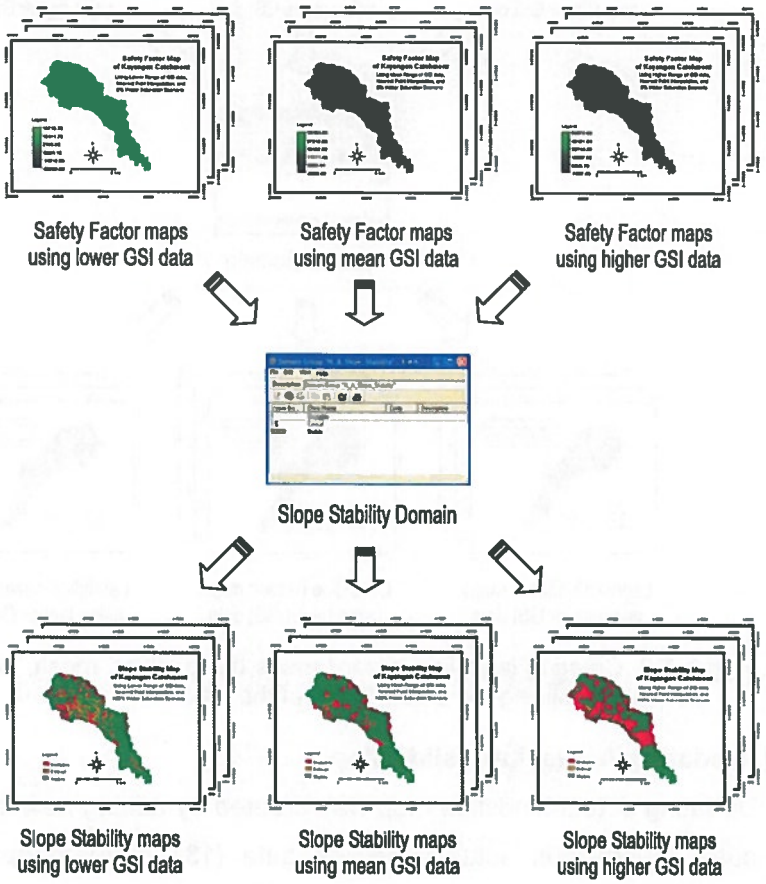

Figure 5.8. Creating slope stability maps using lower, mean, and higher range of GSI data by slicing the safety factor value of area.

5.8. Defining Landslide Hazard Zones

Creating landslide hazard map was created in the same as that of creating slope stability map. It was done by slicing the safety factor value of area by using hazard domain (Figure 5.9). Hazard domain was based on the condition that safety factor <1 is high, 1-1.5 is moderate and >1.5 is low. In other word, landslide hazard zones and slope stability map are the same thing but have different term.

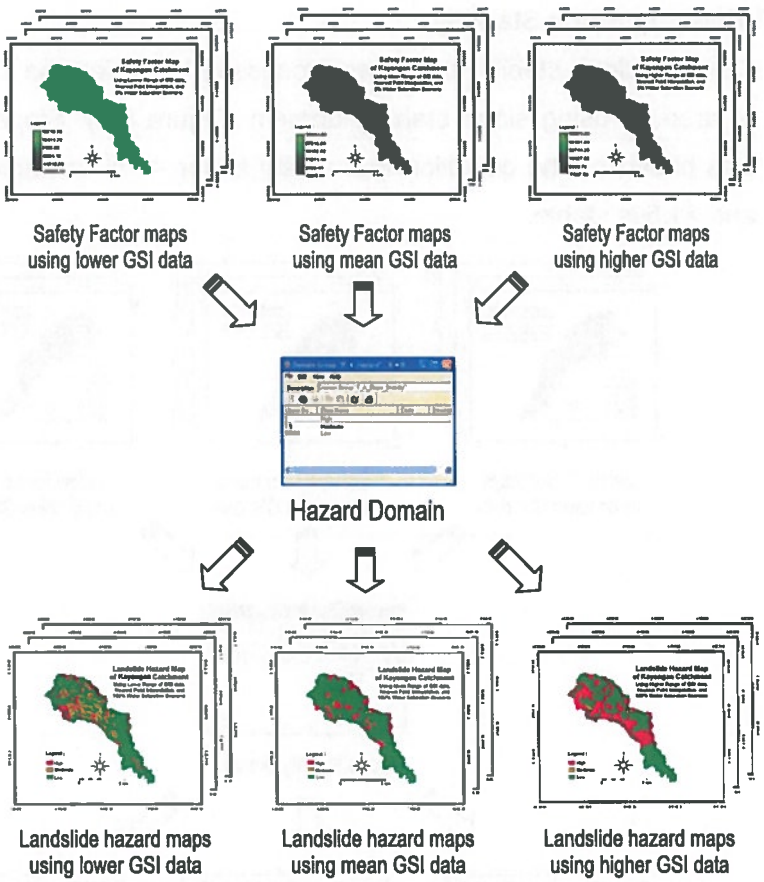

Figure 5.9. Creating landslide hazard maps using lower, mean, and higher range of GSI data by slicing the safety factor of the area.

5.9. Updating Actual Landslide Map

Updating actual landslide map was created by adding new landslide data (42 data) to previous actual landslide data (131 data) mapped by Hadmoko (2008) (Figure 5.10).

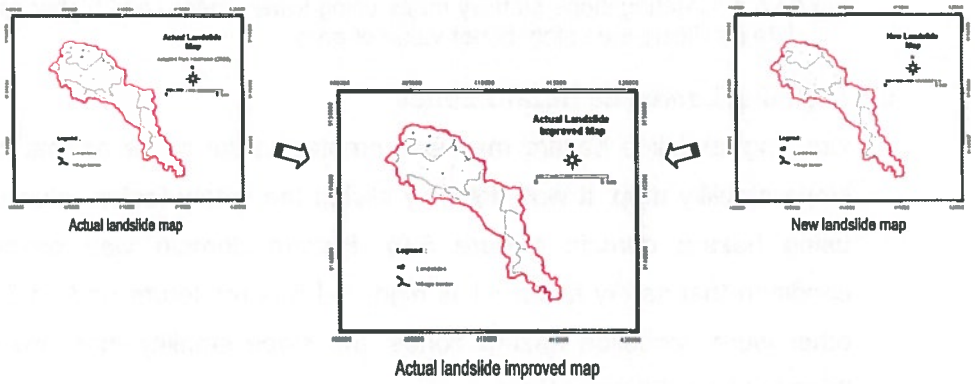

Figure 5.10. Updating actual landslide map by adding new landslide data to actual landslide map.

5.10. Validating Landslide Hazard Maps

Validating landslide hazard map was using degree of fit (DF) (Appendix 4). It assesses the association between the landslide inventory map and the landslide hazard map by using the following formula (Goodchild, 1986; Jimenez-Peralvarez, et al., 2009):

$$DFi = \frac{mi / ti}{\sum mi / ti}$$

where *mi* is the area occupied by the source areas of the landslides at each susceptibility level *i*, and *ti* is the total area covered by that susceptibility level. All landslide hazard maps were crossed with actual landslide inventory map that resulted crossed tables containing landslide and hazard level area. It was processed to obtain landslide area (*mi*) and hazard level area (*ti*) of each hazard level. All *mi* and *ti* were put in excel spreadsheet and processed to obtain the degree of fit (DF). From DF values, the accuracy were defined in perpective of Ferna´ndez et al. (2003); Irigaray et al. (2007); Jimenez-Peralvarez, et al. (2009).

CHAPTER 6. RESULT AND DISCUSSION

6.1. Applying outcrop-based GSI system in collecting data in the field

The result of applying outcrop-based GSI system is a group of GSI data (GSI, UCS, and *mi*). It was collected from 259 observation sites shown completely in Appendix 2. Its statistical data is shown in Table 6.1, Graph 1,2,3.

Table 6.1. GSI statistical data.

Formation	Statistics	GSI data								
		GSI			UCS (Mpa)			*mi*		
		Lower	Mean	Higher	Lower	Mean	Higher	Lower	Mean	Higher
All formations	Min	6	13	20	0.25	0.63	1	2	4	6
	Max	55	67.5	80	50	75	100	20	25	30
	Average	11	17.8	25	3.46	6.89	10.3	14	18	22.6
Nanggulan	Min	6	13	20	1	3	5	5	7	9
	Max	6	13	20	1	3	5	5	7	9
	Average	6	13	20	1	3	5	5	7	9
Kebobutak	Min	6	13	20	0.25	0.63	1	2	4	6
	Max	55	67.5	80	50	75	100	20	25	30
	Average	9.7	16.8	23.9	2.24	5.12	8	15	20	24.5
Jonggrangan	Min	6	13	20	0.25	0.63	1	2	4	6
	Max	45	55	65	50	75	100	18	21	24
	Average	14	21.4	28.9	12.7	20.5	28.3	9.3	12	14.5
Sentolo	Min	14	21	28	1	3	5	2	4	6
	Max	44	55.5	67	1	3	5	5	7	9
	Average	22	29.5	37.4	1	3	5	13	17	21
Young deposit of Merapi Volcano	Min	14	21	28	0.25	0.63	1	6	8.3	10.5
	Max	14	21	28	0.25	0.63	1	13	17	21
	Average	14	21	28	0.25	0.63	1	13	17	21
Colluvium	Min	6	13	20	1	3	5	14	19	24
	Max	6	13	20	1	3	5	14	19	24
	Average	6	13	20	1	3	5	14	19	24

GSI value of all formations is ranging from 6 – 80, Nanggulan from 6 – 20, Kebobutak from 6 – 80, Jonggrangan from 6 – 65, Sentolo from 14 – 67, Young deposits of Merapi Volcano from 14 – 28, and Colluvium from 6 – 20 (Table 6.1 and Figure 6.1).

UCS value of all formations is ranging from 0.25 – 75, Nanggulan from 1 – 5, Kebobutak from 0.25 – 75, Jonggrangan from 0.25 – 75, Sentolo from 1 – 5, Young deposits of Merapi Volcano from 0.25 – 1, and Colluvium from 1 – 5 (Table 6.1 and Figure 6.2).

mi value of all formations is ranging from 2 – 30, Nanggulan from 5 – 9, Kebobutak from 2 – 30, Jonggrangan from 2 – 24, Sentolo from 2 – 9, Young deposits of Merapi Volcano from 6 – 21, and Colluvium from 14 – 24 (Table 6.1 and Figure 6.3).

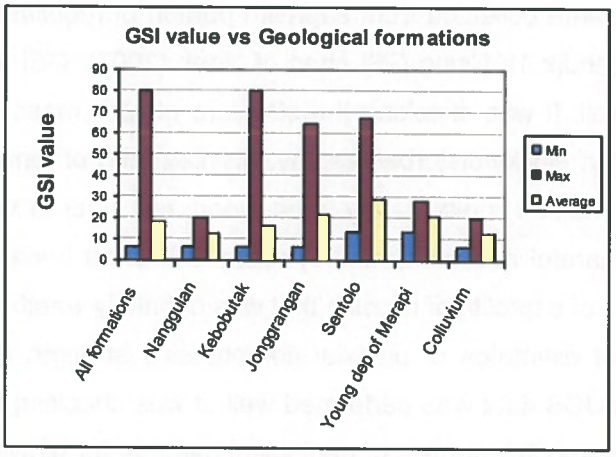

Figure 6.1. GSI value vs geological formations.

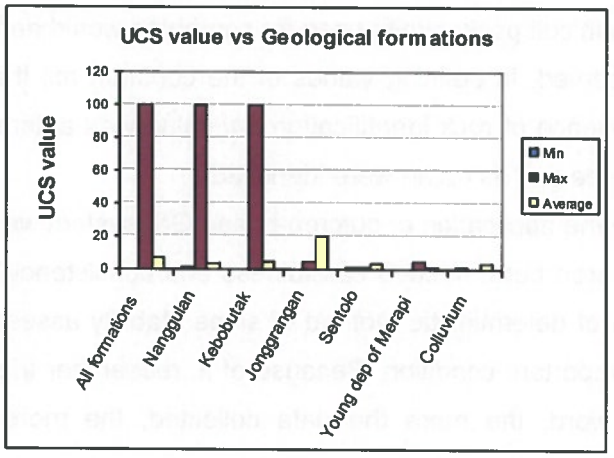

Figure 6.2. UCS value vs geological formations.

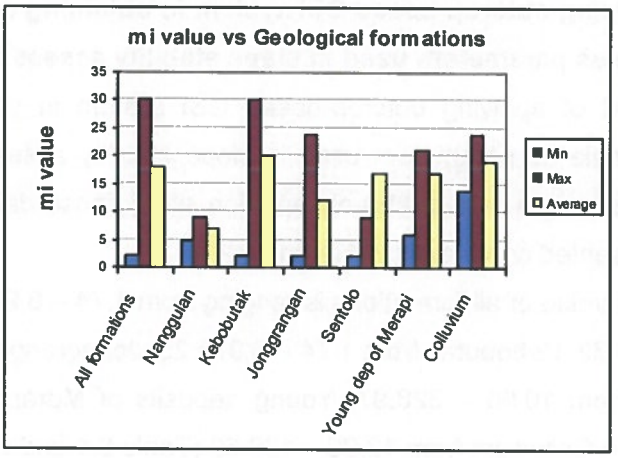

Figure 6.3. *mi* value vs geological formations.

GSI data were collected from saprolith portion of regolith found in outcrop in the field (Appendix 1). Using GSI chart of Hoek (2007), GSI value of each site were defined well. It was checking the structure of rock mass is either intact, blocky, very blocky, blocky/disturbed/seamy, disintegrated or laminated/sheared and the surface condition is either very good, good, fair, poor or very poor. In this part, it must be careful and consistent in using GSI chart because the object was the rock mass of saprolith of regolith that was definitely weathered.

Using field estimates of uniaxial compressive strength (UCS) of Hoek (2007), collecting UCS data was performed well. It was checking the rock mass strength by using some field tools e.g. geological hammer for blowing and pocket knife for scrubbing. How many blows of geological hammer needed to fracture rock mass and how difficult pocket knife used for scrubbing would define the strength of rock mass observed. In defining values of the constant *mi*, it needed the knowledge and experience of rock identification. *mi* value was automatically obtained when the rock type and its name were identified.

Generally the application of outcrop-based GSI system was well performed in this research area but it needed carefulness and consistency in field observation. In the frame of deterministic method of slope stability assessment, data sufficiency was the important condition. Because of it, researcher tried to obtain more data. In other word, the more the data collected, the more sufficient data to be processed.

6.2. Applying outcrop-based GSI system in obtaining cohesion and friction angle as parameters used in slope stability assessment

The result of applying outcrop-based GSI system in obtaining cohesion and friction angle as parameters used in slope stability assessment were cohesion and friction angle data of 259 observation sites. Those data and their calculation were presented completely in Appendix 2.

Cohesion value of all formations is ranging from 1.74 – 6,978.25, Nanggulan from 7.27 – 89.72, Kebobutak from 1.74 – 6,978.25, Jonggrangan from 1.74 – 5781.97, Sentolo from 10.96 – 328.97, Young deposits of Merapi Volcano from 3.73 – 34.89, and Colluvium from 12.95 – 129.59 (Table 6.1 and Figure 6.4).

Table 6.2. Cohesion and friction angle statistical data.

Formation	Statistics	GSI data					
		c' (KN/m^2)			Φ' (...°)		
		Lower	Mean	Higher	Lower	Mean	Higher
All formations	Min	1.74	6.23	14.95	11	14	18
	Max	2,093.47	4,112.18	6,978.25	36	42	46
	Average	75.68	187.76	375.06	21.1	26.1	30.7
Nanggulan	Min	7.28	38.88	89.72	13	17	19
	Max	7.28	38.88	89.72	13	17	19
	Average	7.28	38.88	89.72	13	17	19
Kebobutak	Min	1.74	6.23	14.95	11	14	18
	Max	2,093.47	4,112.18	6,978.25	36	42	46
	Average	48.00	135.63	288.02	21.6	26.5	31.3
Jonggrangan	Min	1.74	6.23	14.95	11	14	18
	Max	1,595.03	3,289.74	5,781.97	24	33	37
	Average	287.17	590.94	1,061.04	18.6	23.9	27.7
Sentolo	Min	10.97	50.84	129.60	15	21	24
	Max	37.88	149.53	328.97	32	38	43
	Average	16.95	74.77	160.13	18.5	24.4	26.9
Young deposit of Merapi Volcano	Min	3.74	14.95	34.89	22	27	33
	Max	3.74	14.95	34.89	22	27	33
	Average	3.74	14.95	34.89	22	27	33
Colluvium	Min	12.96	53.83	129.60	20	25	30
	Max	12.96	53.83	129.60	20	25	30
	Average	12.96	53.83	129.60	20	25	30

Friction angle value of all formations is ranging from 11 – 46, Nanggulan from 13 – 19, Kebobutak from 11 – 46, Jonggrangan from 11 – 37, Sentolo from 15 – 43, Young deposits of Merapi Volcano from 22 – 33, and Colluvium from 20 – 30 (Table 6.2 and Figure 6.5).

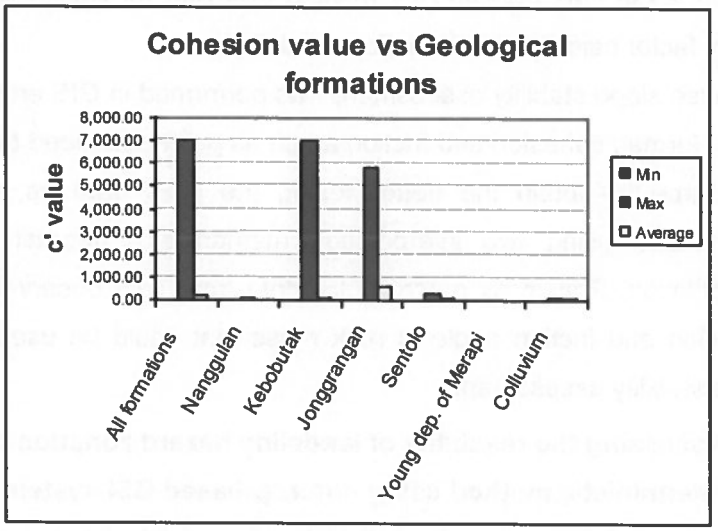

Figure 6.4. Cohesion vs geological formations.

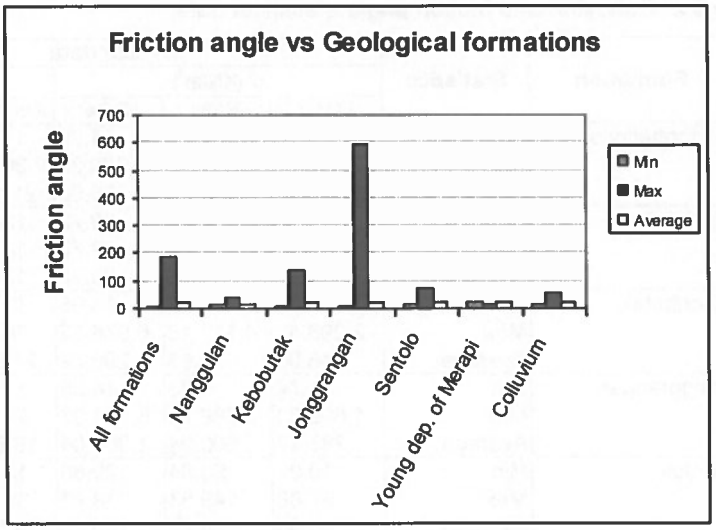

Figure 6.5. Friction angle vs geological formations.

Some parameters as the derivation of GSI field data that were used in slope stability assessment were cohesion and friction angle of rock mass. In this research, those rock mass behaviour could be obtained from estimation using tables published by Hoek et al. (1998) (Table 2.4).

From field observation, each observation site provided geological strength index (GSI), uniaxial compressive strength (UCS), *mi* data. By using published tables of Hoek (1998), cohesion was obtained by relating GSI, *mi* and UCS values and friction angle was obtained by relating GSI and *mi* values which were used in safety factor calculation of the slope stability.

Because slope stability assessment was performed in GIS environment based on raster format, cohesion and friction angle as point data need to be interpolated. In the frame to obtain the better result, the sites data as a point data were interpolated using two interpolation method e.g. nearest point and kriging interpolation. Principally outcrop GSI data from field observation could produce cohesion and friction angle of rock mass that could be used as parameters in slope stability assessment.

6.3. Assessing the reliability of landslide hazard zonation based on deterministic method using outcrop-based GSI system

The result of assessing the reliability of landslide hazard zonation based on deterministic method using outcrop-based GSI system are landslide hazard maps, their acuracy and reliability of the method.

Landslide hazard zonation were performed to result 24 maps of landslide hazard maps (Figure 6.6, 9, 12, 15, 18, 21). It is based on the scenarios in safety factor calculation (Table 5.1). Success rates of those maps are presented in Figure 6.7, 10, 13, 16, 19, 22. The percentages distibutions of hazard level area are presented in Figure 6.8, 11, 14, 17, 20, 23. Performing landslide hazard zonation was done by slicing the safety factor calculated from slope stability formula defined using hazard level domain that were high, moderate, and low.

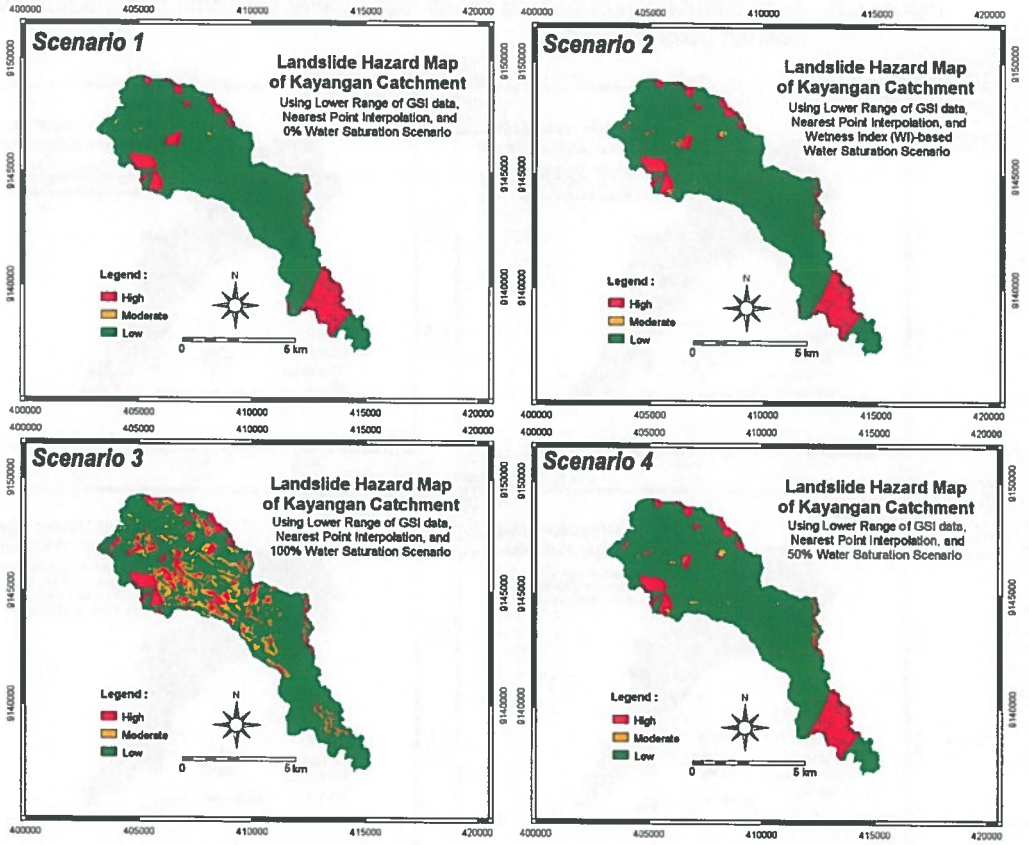

Figure 6.6. Landslide hazard maps using lower GSI data interpolated by using nearest point method.

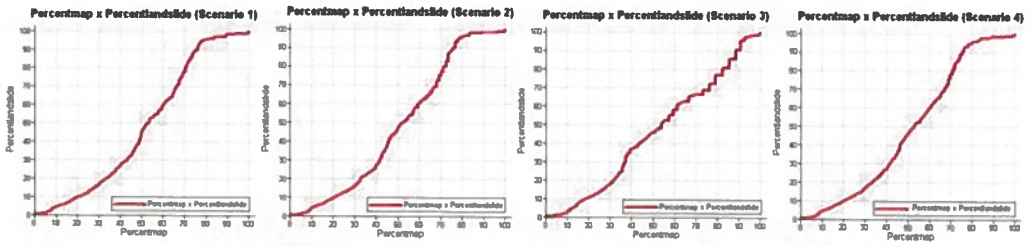

Figure 6.7. Success rate of landslide hazard maps using lower GSI data interpolated by using nearest point method.

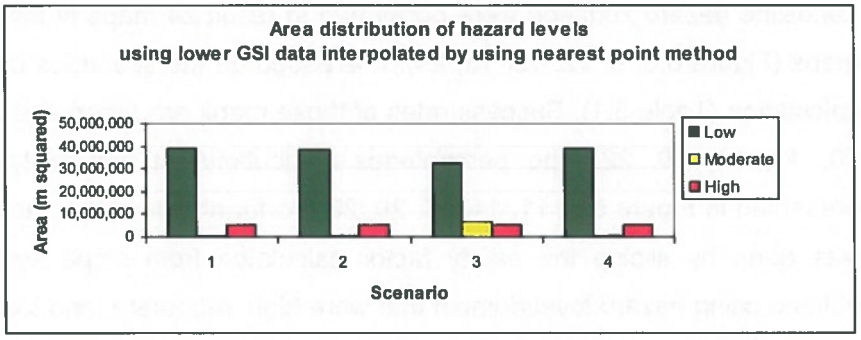

Figure 6.8. Area distribution of hazard levels using lower GSI data interpolated by using nearest point method.

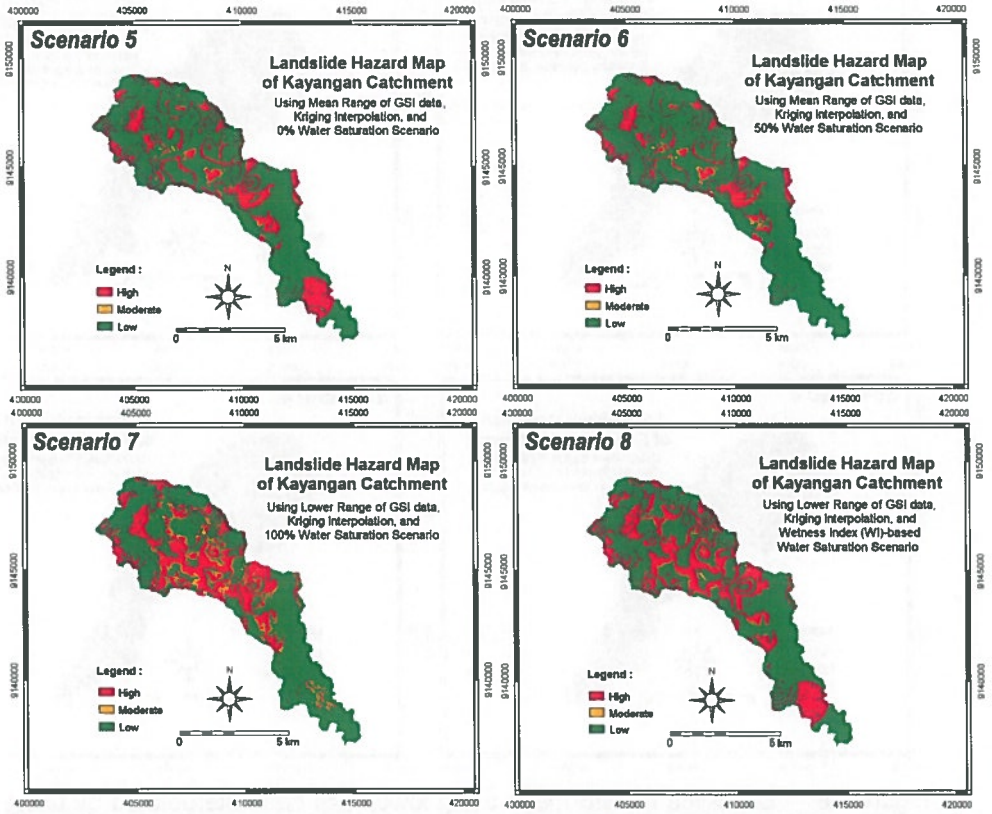

Figure 6.9. Landslide hazard maps using lower GSI data interpolated by using kriging method.

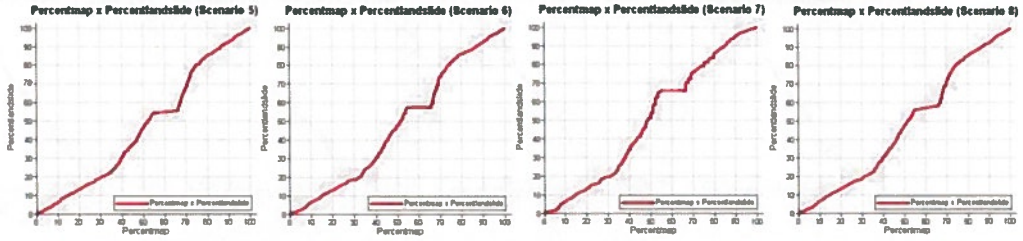

Figure 6.10. Success rate of landslide hazard maps using lower GSI data interpolated by using kriging method.

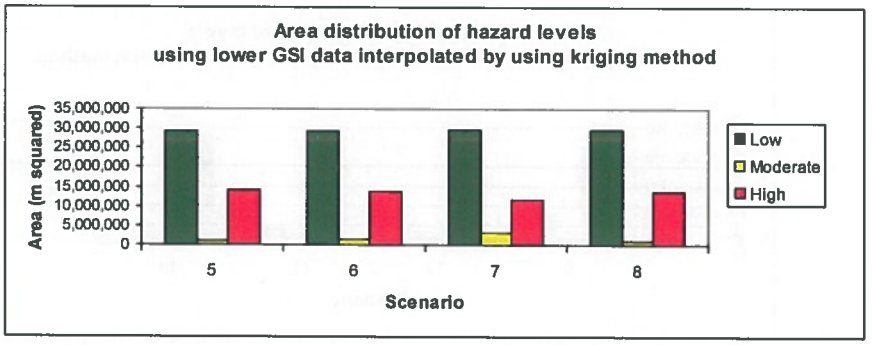

Figure 6.11. Area distribution of hazard levels using lower GSI data interpolated by using kriging method.

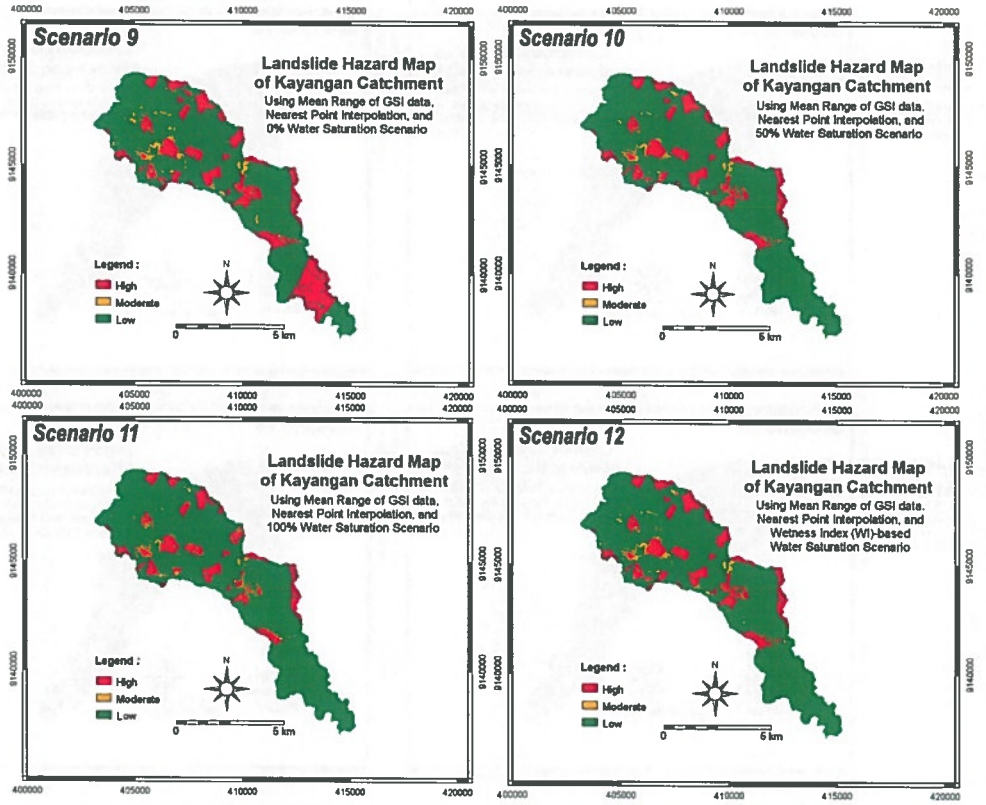

Figure 6.12. Landslide hazard maps using mean GSI data interpolated by using nearest point method.

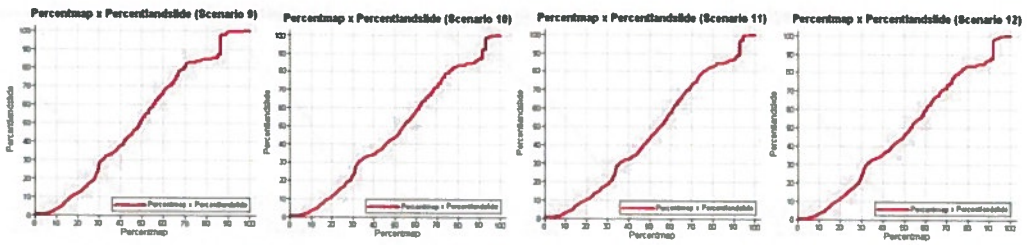

Figure 6.13. Success rate of landslide hazard maps using meanGSI data interpolated by using nearest point method.

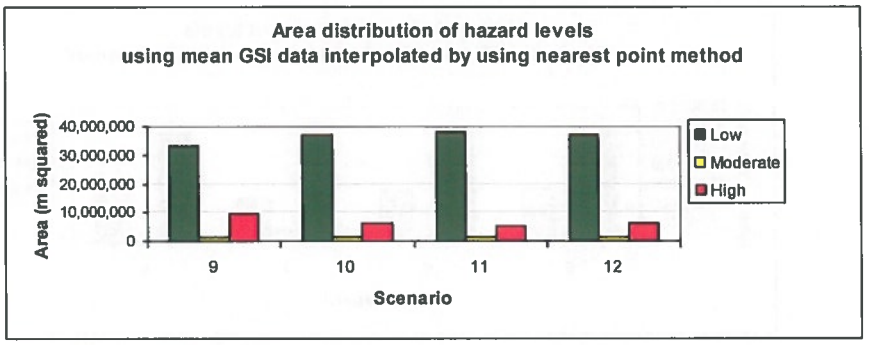

Figure 6.14. Area distribution of hazard levels using mean GSI data interpolated by using nearest point method.

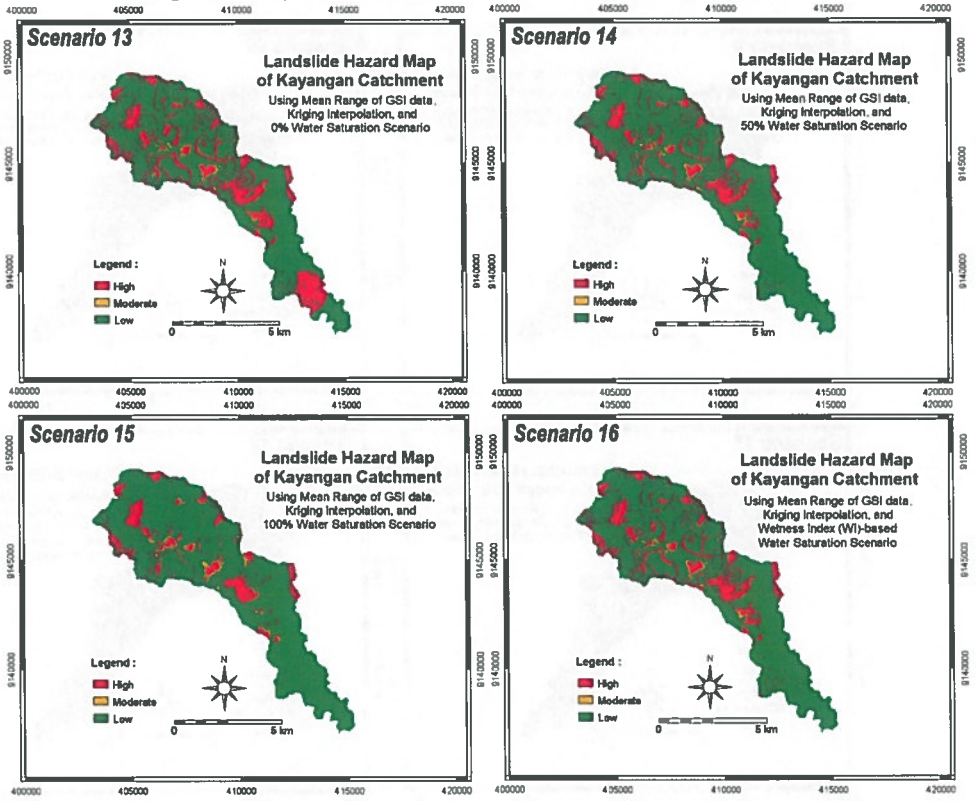

Figure 6.15. Landslide hazard maps using mean GSI data interpolated by using kriging method.

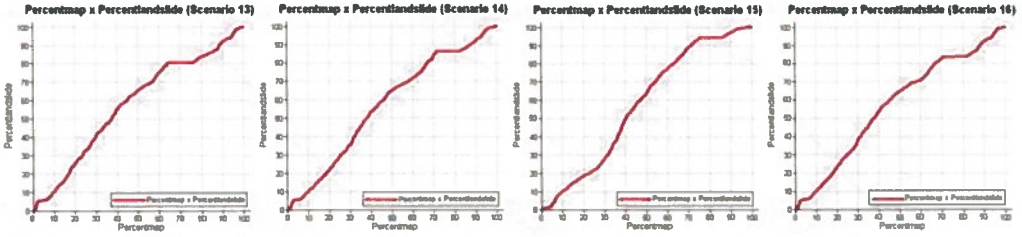

Figure 6.16. Success rate of landslide hazard maps using mean GSI data interpolated by using kriging method.

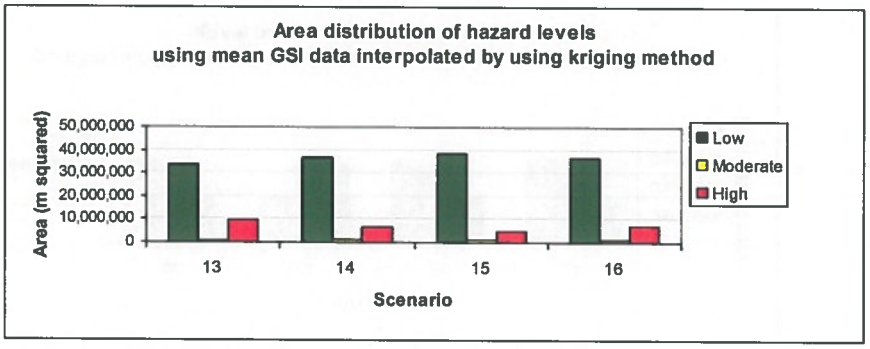

Figure 6.17. Area distribution of hazard levels using mean GSI data interpolated by using kriging method.

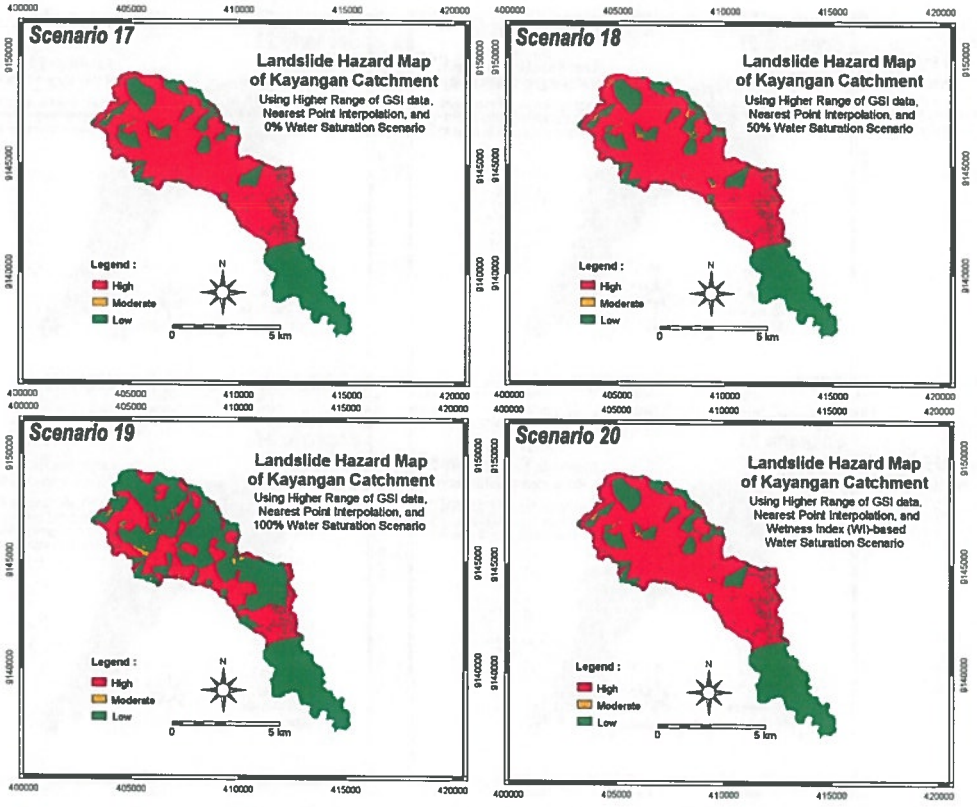

Figure 6.18. Landslide hazard maps using higher GSI data interpolated by using nearest point method.

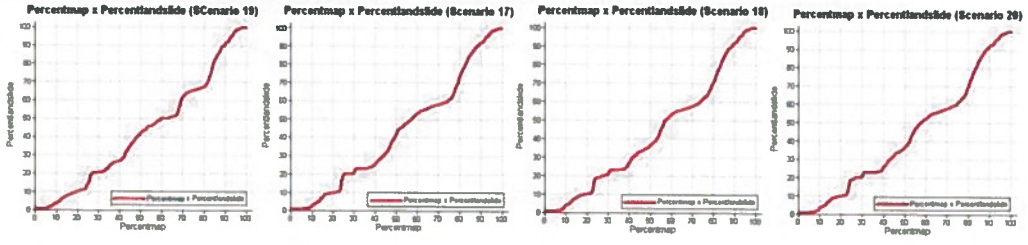

Figure 6.19. Success rate of landslide hazard maps using higher GSI data interpolated by using nearest point method.

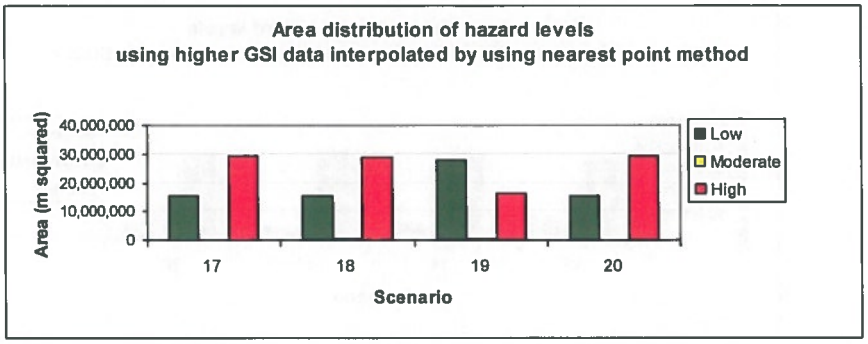

Figure 6.20. Area distribution of hazard levels using higher GSI data interpolated by using nearest point method.

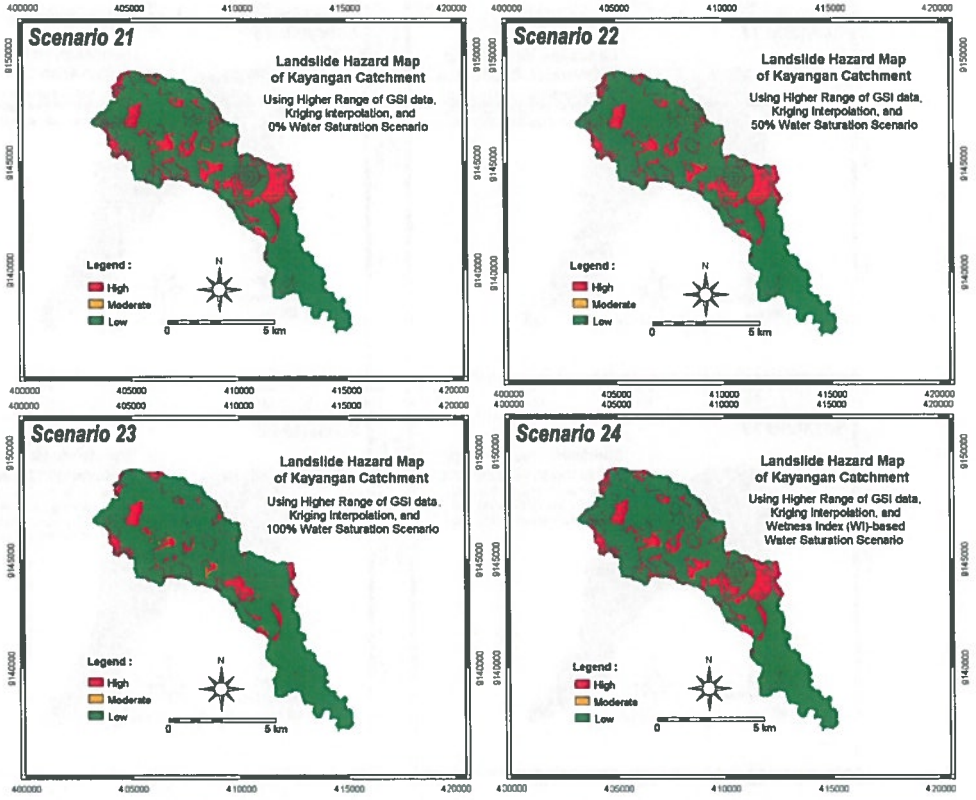

Figure 6.21. Landslide hazard maps using higher GSI data interpolated by using kriging method.

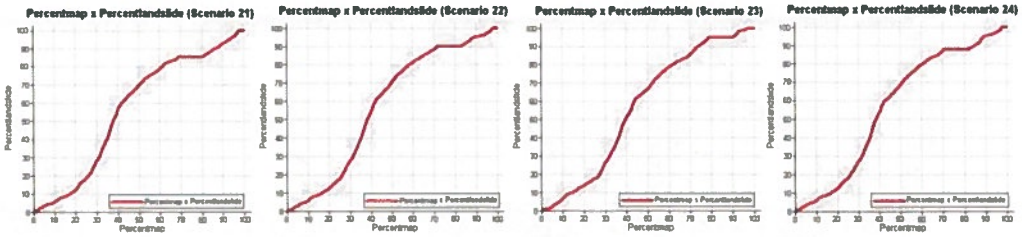

Figure 6.22. Success rate of landslide hazard maps using higher GSI data interpolated by using kriging method.

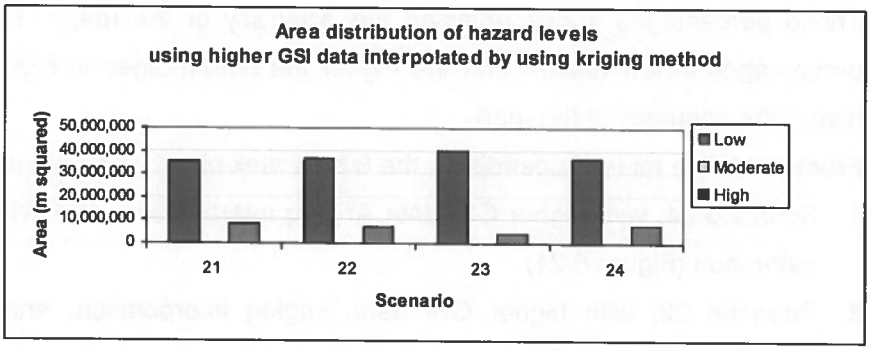

Figure 6.23. Area distribution of hazard levels using higher GSI data interpolated by using kriging method.

Generally performing landslide hazard zonation were easily done but needed more time to prepare the parameter maps that depended on the ranging parameter data and how many scenarios defined.

Validation of the resulted landslide hazard maps was done by using the degree of fit (DF) (Appendix 4) that assesses the association bewtween the inventory and the landslide hazard map. The accuracy assessment was carried out according to Goodchild (1986); Jimenez-Peralvarez, et al., (2009).

The accuracy assessment gave varying results (Appendix 4). Degree of fit (DF) of landslide hazard maps using lower GSI data interpolated by using nearest point in high hazard level (scenario 1-4) is 9.87 – 86.01%, in moderate 0 – 37.00%, and in low is 13.99 – 63.53%. DF of landslide hazard maps using lower GSI data interpolated by using kriging method in high hazard level (scenario 5-8) is 16.98 – 25.20%, in moderate 46.04 – 68.03%, and in low 14.65 – 28.76%. DF of landslide hazard maps using mean GSI data interpolated by using nearest point method in high hazard level (scenario 9-12) is 30.74 – 45.32%, in moderate 14.36 – 21.89%, and in low 37.02 – 47.37%. DF of landslide hazard maps using mean GSI data interpolated by using kriging method in high hazard level (scenario 13-16) is 25.35 – 34.26%, in moderate 22.25 – 73.86%, and in low 0.79 – 43.49%. DF of landslide hazard maps using higher GSI data interpolated by using nearest point method in high hazard level (scenario 17-20) is 49.53 – 63.82%, in moderate 0.00 – 21.61%, and in low 28.87 – 36.18%. DF of landslide hazard maps using higher GSI data interpolated by using kriging method in high hazard level (scenario 21-24) is 32.48 – 54.86%, in moderate 20.43 – 62.37%, and in low 0.70 – 47.08%.

Those percentages above reflected the accuracy of the maps. The lower the percentages in low hazard and the higher the percentages in high hazard, the higher the accuracy of the map.

From validation table (Appendix 4), the 5 best rank of accuracy are as follows :

1. Scenario 24, with higher GSI data, kriging interpolation, and WI-based water saturation (Figure 6.21)
2. Scenario 22, with higher GSI data, kriging interpolation, and 50% water saturation (Figure 6.21)
3. Scenario 23, with higher GSI data, kriging interpolation, and 100% water saturation (Figure 6.21)
4. Scenario 15, with mean GSI data, kriging interpolation, and 100% water saturation (Figure 6.15)
5. Scenario 2, with lower GSI data, nearest point interpolation, and 50% water saturation (Figure 6.6).

The results showed that the highest 5 accuracy were in landslide hazard maps that used higher GSI data and kriging interpolation technique (scenario 24, 22, 23). This was followed by hazard assessments using mean GSI data and kriging interpolation (scenario 15), and lower GSI data, nearest interpolation (scenario 2). It could be concluded that higher GSI data gives better results as compared to that using mean and lower GSI data, and kriging interpolation is better than nearest point interpolation.

Based on the best result of validation on scenario 24, the degree of fit (DF) in high hazard level = 54.86%, in moderate level = 44.28% and in low level = 0.86%, according to degree of fit levels of Ferna´ndez et al. (2003); Irigaray et al. (2007); Jimenez-Peralvarez, et al. (2009), this map was moderately accurate because the DF in low was 0.70% below 7%, and total DF in high (54.86%) was in moderate percentage.

The reliability of landslide hazard zones depends on the accuracy of validation. If the result of validation shows that the map is accurate, it also shows that the method used in processing the map is reliable. The best landslide hazard map from this research showed that it was moderately accurate, therefore it could be concluded that deterministic method using outcrop-based GSI data could be considered as a reliable method in landslide hazard zonation.

Many landslides occured in the research area before 2010 and along the research done in the field. Landslides found in research area and it characteristics were listed in Appendix 2 and described in Appendix 5.

According to Kusky (2008), many factors control the occurrence of landslide and its type. One of those factors was the characteristics of the regolith and bedrock. In this research, data on the characteristics of regolith (GSI, UCS, *mi*, and lithology type) were collected from 259 sites out of which 42 sites had landslides and 217 sites without landslides.

Figure 6.24-28 show the plotting of GSI data in all the sites, some of which have landslides. The graph can be used to make qualitative comparison between the occurrence of landslides and the GSI data.

Figure 6.24 showed that GSI values at sites with landslide tended to be dominated by value in the range 6-20, and some sites without landslide tended to be dominated by value in the range 14-28. It meant that GSI value at sites with landslides tend to be lower than that at sites without landslide.

Figure 6.25 showed that UCS values at sites with landslide tended to be dominated by value range of 1-5, and some sites without landslide had higher UCS values (50 to 100). It meant that UCS value at sites with landslides tend to be lower than that at sites without landslide.

Figure 6.26 showed that *mi* values at sites with landslide were dominated by value in the range of 14-24, and sites without landslide were the same. In these sites the lithology was dominated by andesitic breccia.

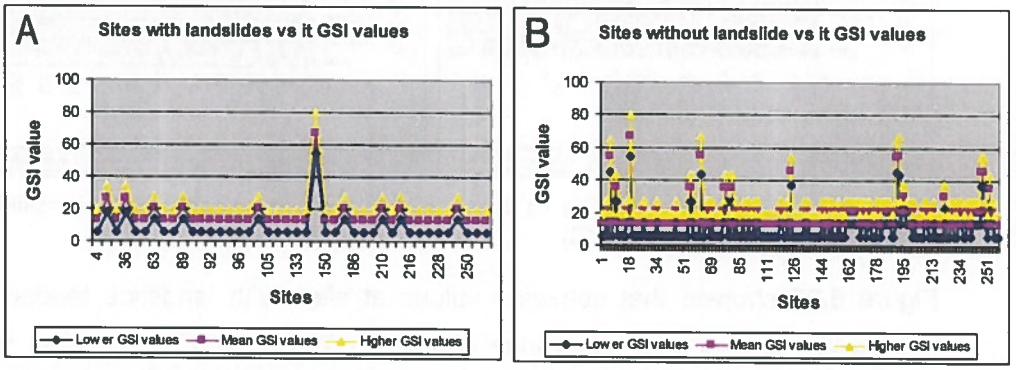

Figure 6.24. Sites with landslide vs it GSI values (A), sites without landslide vs it GSI values (B).

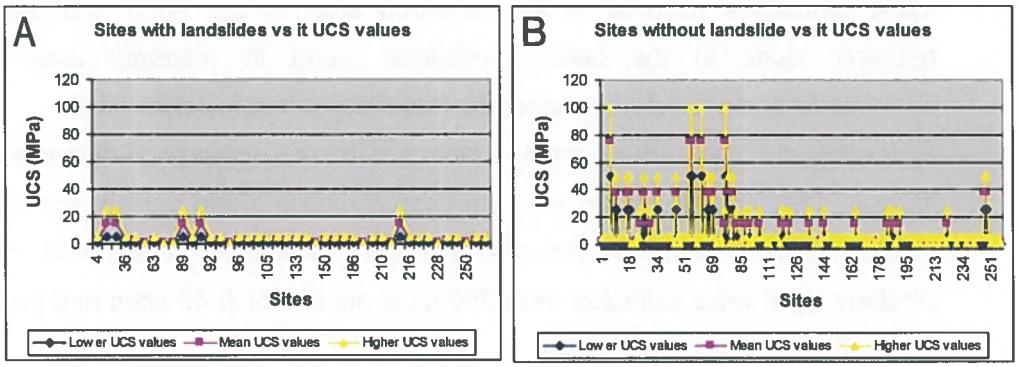

Figure 6.25. Sites with landslide vs it UCS values (A), sites without landslide vs it UCS values (B).

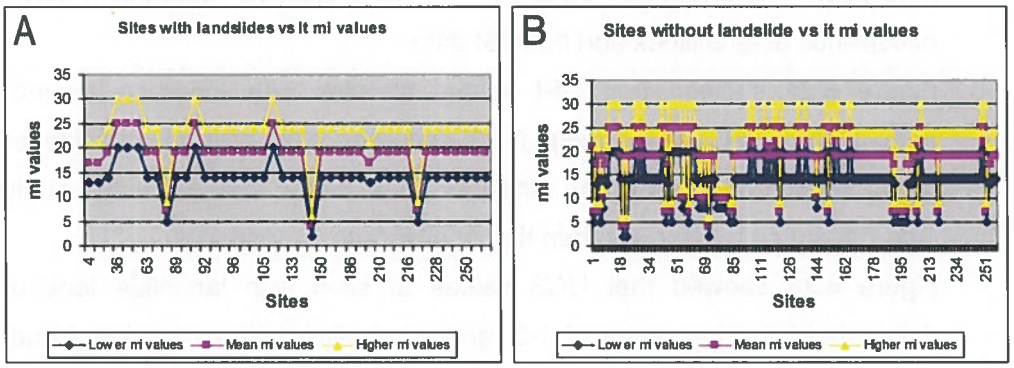

Figure 6.26. Sites with landslide vs it mi values (A), sites without landslide vs it mi values (B).

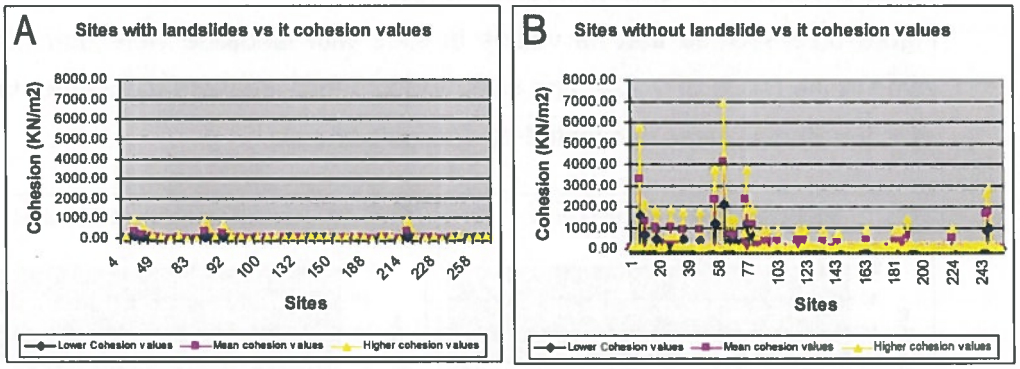

Figure 6.27. Sites with landslide vs it cohesion values (A), sites without landslide vs it cohesion values (B).

Figure 6.27 showed that cohesion values at sites with landslide tended to be dominated by value in the range of 12.96-129.60, and some sites without landslide had value more than 1,000. It means that cohesion value at sites with landslides tend to be lower than tthat at sites without landslide.

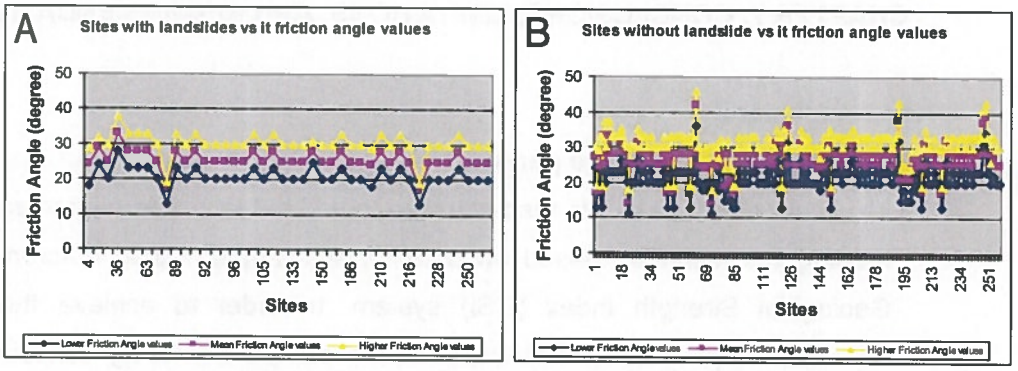

Figure 6.28. Sites with landslide vs it friction angle values (A), sites without landslide vs it friction angle values (B).

Figure 6.28 showed that friction angle values at sites with landslide tended to be dominated by value in the range of 20-30°, and some sites without landslide had value in the range of 23-33°. It means that friction angle value at sites with landslides tend to be lower than the ones with sites without landslide.

From all the comparisons, it can be concluded that the GSI data at sites with landslide tend to be lower than that at sites without landslide. In other word, the sites that have low GSI data tend to have higher possibility of landslide occurence than the sites that have higher GSI data.

CHAPTER 7. CONCLUSIONS, LIMITATIONS, AND RECOMMENDATIONS

7.1. Conclusions

7.1.1. Conclusions from the perspective of research objectives

The main objective of this research was to find out landslide hazard zones of Kayangan Catchment based on deterministic method using outcrop-based Geological Strength Index (GSI) system. In order to achieve the main objective, slope stability assessment was carried out using cohesion and friction angle data.

The application of outcrop-based GSI system showed a good performance but it needed carefulness and consistency in field observation especially in describing regolith portions of weathered rock mass of outcrops. The difficulty was that some outcrop sites did not show the complete regolith structure that did not give true regolith thickness. Because of this reason, it was called minimum regolith thickness.

The maps used for landslide hazard assessment had varrying accuracy level (from low to high) as estimated on the basis of the percent of its degree of fit (DF). From validation, the best 5 accurate maps were dominated by higher range of GSI value and kriging intepolation method. Those maps showed moderate level of accuracy where in high hazard the DF were 36.84, 37.12, and 54.86 % and in low hazard below 1%. Based on the accuracy level of those maps that were moderate, it could be concluded that the method performed could be considered as a reliable method in landslide hazard zonation.

In this research, the characteristics of regolith collected from the field were GSI, UCS, *mi*, and lithology at 259 sites of which 42 sites were with landslides and 217 sites without landslide. The GSI data of sites with and without landslide were compared in graphs that showed that GSI data at sites with landslide tended to be lower than at sites without landslides. This means that the sites that have lower GSI data tended to have higher possibility of landslide occurence than the sites that have higher GSI data.

7.1.2. Conclusions from the perspective of research questions

1. a. How is the applicability of outcrop-based GSI system in collecting data in the field?

   GSI system could be applied for the rock mass exposed in outcrops, in surface excavations such as road cuts and in tunnel faces and borehole cores. In the field, collecting data was done in rockmass exposed in outcrops at saplith portion of regolith. GSI data (GSI, UCS, and *mi* values) were collected by using published tables of GSI system. The field experience shows that GSI as a system could be applied well in collecting data based on outcrops but the carefulness and consistency were needed especially in describing regolith portions of weathered rock mass.

   b. Is outcrop-based GSI system suitable to be applied for physical condition in research area?

   GSI as a system can be applied for rock mass that is fresh- weathered, homogenous-heterogenous in lithology, massive-significantly disintegrated. Kayangan cathment has physical condition that varies in geological formations (lithologies), weathering (very poor-very good), and discontinuity (massive-disintegrated), and especially in lithological condition it is dominated by andesitic breccia that covered about a half of the research area. Due to the application conditions of this system and Kayangan cathment physical condition, GSI system could be applied to this research area therefore outcrop-based GSI system was suitable to be applied.

2. a. Can outcrop-based GSI data collected from the field be used in obtaining cohesion and frcition angle as parameters used in slope stability assessment?

   Outcrop-based GSI data collected from the field were GSI, UCS, and *mi*. GSI system provided published tables that relate those data to obtain cohesion and friction angle of rock mass. In slope stability assessment, cohesion and friction angle of rock mass were used as parameters in calculation the safety factor. From the data analysis, it can be concluded that cohesion and friction angle data used as parameters in slope stability assessment can be obtained from outcrop-based GSI data.

3. a. How to perform lanslide hazard zonation based on deterministic method using outcrop-based GSI system?

Landslide hazard zones were based on slope stability assessment processed that were defined from the safety factor values of the area. Slope stability was unstable when safety factor was <1, critical was 1-1.5, and stable was >1.5. This stability domain was modified as landslide hazard domain that were unstable=high, critical=moderate and stable=low. Safety factor values were obtained from infinite slope formula that used some parameters e.g. cohesion and friction angle maps (resulted from outcrop-based GSI data observed), regolith thickness and bulk density maps (resulted from field observation), slope maps (resulted from DEM map), and water saturation scenarios defined and wetness index based water saturation (resulted from DEM map).

b. What is the accuracy of landslide hazard zonation based on deterministic method using outcrop-based GSI system?

Accuracy assessment was performed using using degree of fit (DF) method. The results gave varrying accuracy level from low to moderate. Moderate accuracy level was dominated by landslide hazard maps processed using higher range of GSI data and kriging interpolation method.

c. What kind of scenario does result the best landslide hazard zones based on deterministic method using outcrop-based GSI system?

The best accurate map was landslide hazard map (scenario 24) using higher range of GSI value interpolated by kriging intepolation method that showed moderate performance of accuracy. Its degree of fit (DF) in high hazard was 54.86% and in low hazard 0.70%.

d. Is deterministic method using outcrop-based GSI system reliable in landslide hazard zonation?

The moderate percentages of degree of fit (DF) from validation showed moderate performance of accuracy of landslide hazard maps. Therefore the method can be considered reliable in landslide hazard zonation.

e. Is there any relationship between actual landslides and its GSI data?

The GSI data sites with landslide tended to be lower than at sites without landslide. It could be concluded that the sites that have lower GSI data

qualitatively tended to have higher possibility of landslide occurrence than the sites that have higher GSI data.

7.2. Limitations

This research have some limitations as follows :

1. The failure surface in this research was regolith boundary that was assumed as a slip plane parallel to the surface.
2. Regolith thickness was mapped based on outcrop-based measurement. Some were true regolith thickness and some were called minimum thickness when its regolith boundary was not found.
3. Field GSI data was subjective that depends on researcher kowledge. Researchers based on their knowledge could give different description of rock, blockiness, discontinuity and weathering.
4. The ranging values of GSI data gave the ranging possibility of data that caused the more processes in performing landslide hazard zonation.

7.3. Recommendations

Based on the experiences and conclusions of research, some recomendations are proposed for future landslide hazard zonation :

1. to avoid the subjectivity of researcher in knowledge and experience, the researcher must understand the insight of GSI system about its applications and limitations and try to be careful and consistent in field description.
2. In deterministic method, the sufficiency of data of sites physical parameters was very important therefore sufficient data must be obtained. The more data, the more accurate will be the result.

REFERENCES

Abella, E.A.C. and Van Westen, C.J. 2008. *Qualitative Landslide Susceptibility Assessment by Multicriteria Analysis : A Case Study From San Antonio Del Sur, Guantanamo, Cuba*. Elsevier Science B.V.

Area Profile of Kulon Progo Regency. On-line document; URL: http://www.kulonprogokab.go.id/, accessed on December 13rd, 2010.

Aster GDEM image, ASTGTM S08E110 tile; URL: www.gdem.aster.ersdac.or.jp/, accessed on January 6th, 2010.

Bakosurtanal. Yogyakarta Province Image. URL: http://www.bakosurtanal.go.id, accessed on 2010.

BNPB. 2010. *Landslide data of Indonesia from 1998-2009*. National Disaster Management Agency (BNPB). On-line document; URL: http://dibi.bnpb.go.id.

Case, M., Ardiansyah, F., Spector, E. 2007. *Climate Change in Indonesia: Implications for Humans and Nature*. WWF.

Chung, C.J.F. & Fabbri, A.G. 2003. *Validation of Spatial Prediction Models for Landslide Hazard Mapping*. Natural Hazards 30: 451–472, 2003. Kluwer Academic Publishers. The Netherlands.

Chung, C.J. & Fabbri A.G. 2007. *Predicting landslides for risk analysis-Spatial models tested by a cross-validation technique*. Elsevier B.V.

Colombo R., Voght, J., Bertolo, F. 2001. *Deriving Drainage Networks and Cathment Boundaries at The European Scale: A New Approcah Combining Digital Data and Environmental Characteristics*. European Communities. Italy.

Guzzetti, F.; Carrara, A.; Cardinali, M.; & Reichenbach, P. 1999. *Landslide Hazard Evaluation: a review of current techniques and their application in a multi-scale study, Central Italy*. Elsevier Science B.V.

Guzzetti, F.; Reichenbach, P.; Cardinali, M.; Galli, M.; & Ardizzone F. 2005. *Probabilistic Landslide Hazard Assessment at The Basin Scale*. Elsevier Science B.V.

Hadmoko, D.S.; Saptohadi, J.; Samodra G.; & Christanto, N. 2008. *GIS application for comprehensive spatial landslide analysis in Kayangan Catchment, Menoreh Mountain, Java, Indonesia*. UGM-University Paris 1 Pantheone Sorbonne.

Hadmoko, D.S.; Lavigne, F.; Saptohadi, J.; Hadi, P.; & Winaryo. 2010. *Landslide Hazard and Risk Assessment and Their Application in Risk Management and Landuse Planning in Eastern Flank of Menoreh Mountains, Yogyakarta Province, Indonesia*. Springer Science+Business Media B.V.

Haryono, B. 2001. *Stratigraphy and Sedimentation of Transitional Sediment of Jonggrangan Formation, Kucir Mountain Section, Samigaluh District, Kulon Progo Regency, Yogyakarta Province*. Geological Engineering Department, Gadjah Mada University. Yogyakarta. Student Script. Unpublished.

Hoek, E.; & Brown, E.T. 1997. *Practical estimates of rock mass strength*, International Journal of Rock Mechanics and Mining Sciences, Vol 34, No 8, 1997, pages 1165-1186.

Hoek, E.; Marinos, P.; & Benissi, M. 1998. *Applicability of Geological Strength Index (GSI) Classification for very weak and sheared rock masses: The case of Athens Schist Formation*. Bull Eng Geol Env (1998) 57 : 151–160, Springer-Verlag.

Hoek, E. 2007. *Practical Rock Engineering*, Canada.

Jelinek, R.; & Wagner, P. 2007 *Landslide Hazard Zonation by Deterministic Analysis (Velka Causa Landslide Area, Slovakia)*. Landslides (2007) 4:339–350, DOI 10.1007/s10346-007-0089-9. Springer-Verlag.

Jimenez-Peralvarez, J.D.; Irigaray, C.; El Hamdouni, R.; Chacon, J. 2009. *Building Models for Automatic Landslide-Susceptibility Analysis, Mapping and Validation in ArcGIS*. Nat Hazards (2009) 50:571–590- DOI 10.1007/s11069-008-9305-8. Springer Science+Business Media B.V.

Kusky, T. 2008. *Landslide: Mass Wasting, Soil, and Mineral Hazards*. Facts On Files, Inc. New York.

Marfai, M.A.; King, L.; Singh, L.P.; Mardiatno, D.; Saptohadi, J.; Hadmoko, D.S.; & Dewi, A. 2008. *Natural Hazards in Central Java Province, Indonesia: an overview*. Environmental Geology (2008) 56:335-351 DOI 10.1007/s00254-007-1169-9. Springer – Verlag.

Marinos, P., Hoek, E., Marinos, V. 2006. *Variability of The Engineering Properties of Rock Masses Quantified by The Geological Strength Index: The Case of Ohiolites with Special Emphasis on Tunneling*. Bull Eng Geol Env (2006) 65: 129–142, DOI 10.1007/s10064-005-0018-x. Springer-Verlag.

Marinos, V., Marinos, P., Hoek, E. 2005. *The Geological Strength Index : Applications and Limitations*. Bull Eng Geol Environ (2005) 64: 55–65, DOI 10.1007/s10064-004-0270-5. Springer-Verlag.

Nandy, A.; & Shakoor, A. 2009. *A GIS-based Landslide Susceptibility Evaluation Using Bivariate and Multivariate Statistical Analysis*. Elsevier Science B.v.

Rahardjo, W.; Sukandarrumidi; Rosidi, H.M.D. 1995. *Geological Map of The Yogyakarta Sheet, Jawa*. Geological Research and Development Centre. Bandung.

Scott, Keith M.; & Pain Colin F. 2009. *Regolith Science*. CSIRO Publishing, Australia.

Van Westen, C.J. 1993. *Application of Geographic Information Systems to Landslide Hazard Zonation*. ITC Publication Number 15, International Institute for Aerospace Survey and Earth Sciences (ITC), Enschede, The Netherlands.

Van Westen, C.J. 2006. *Landslide Hazard and Risk Zonation - Why is it still so difficult ?*. Bull Eng Geol Env (2006) 65: 167-184 DOI 10.1007/s10064-005-0023-0. Springer – Verlag.

APPENDIX 1. Sites log form

Sites Log

Date : Oct 22, 2010

No : 113
Location : 113 (407707 9147795) Kebonharjo village, Samigaluh District, Kulon Progo

Regolith Profile		Observation Parameters	
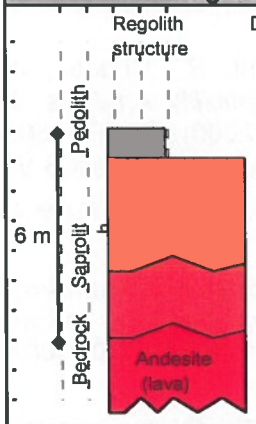		**GSI**	
		SC	VG G F P [VP]
		Structure	I B VB B/D/S [D] L/S
		Value (mean)	13
		UCS (Mpa)	
			R0 [R1] R2 R3 R4 R5 R6
		Value (mean)	3
		mi	Lithology : Andesite (lava)
			C [M] F VF
		Value (mean)	25
		z (m)	6 m
		Photo number	113
Remark : *good site for weathering grade*			

No : 114
Location : 114 (407478 9147874) Kebonharjo village, Samigaluh District, Kulon Progo

Regolith Profile		Observation Parameters	
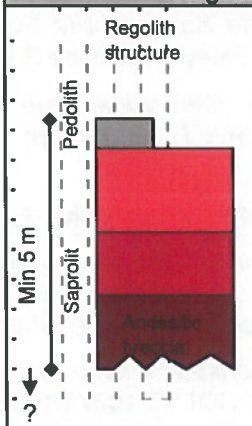		**GSI**	
		SC	VG G F P [VP]
		Structure	I B VB B/D/S [D] L/S
		Value (mean)	13
		UCS (Mpa)	
			R0 [R1] R2 R3 R4 R5 R6
		Value (mean)	3
		mi	Lithology : Andesitic breccia
			[C] M F VF
		Value (mean)	19
		z (m)	min 5 m
		Photo	114
Remark :			

APPENDIX 2. Outcrop-based GSI field data and Calculation of cohesion and internal friction angle

No	Site	Date	Coordinate		GSI			UCS'			*mi*			z	Lithology	c'/UCS'			c'						Φ'			Landslides	
			x	y	lower	mean	higher	lower	mean	higher	lower	mean	higher			lower	mean	higher	lower		mean		higher		mean	higher	lower	Old	2010
								(MPa)	(MPa)	(MPa)				(m)					(MPa)	(KN/m²)	(MPa)	(KN/m²)	(MPa)	(KN/m²)	(...°)	(...°)	(...°)		
1	1	Oct 10, 2010	408832	9147727	6	13	20	1	3	5	18	21	24	min 6	Conglomerate	0.014	0.019	0.026	0.014	13.9565	0.0570	56.8229	0.1300	129.5960	27	30	24		
2	2		408879	9147583	6	13	20	1	3	5	5	7	9	min 3	Siltstone	0.0073	0.013	0.018	0.007	7.2773	0.0390	38.8788	0.0900	89.7203	17	19	13		
3	3		408497	9147746	6	13	20	1	3	5	13	17	21	min 4	Sandstone	0.012	0.018	0.026	0.012	11.9627	0.0540	53.8322	0.1300	129.5960	24	29	18		
4	4		408377	9148105	6	13	20	1	3	5	13	17	21	min 6	Sandstone	0.012	0.018	0.026	0.012	11.9627	0.0540	53.8322	0.1300	129.5960	24	29	18		1
5	5		408848	9148219	14	21	28	1	3	5	14	19	24	min 5	Andesitic breccia	0.018	0.024	0.036	0.018	17.9441	0.0720	71.7762	0.1800	179.4406	28	33	23		
6	6		408838	9147978	6	13	20	1	3	5	5	7	9	min 4	Siltstone	0.0073	0.013	0.018	0.007	7.2773	0.0390	38.8788	0.0900	89.7203	17	19	13		
7	7	Oct 11, 2010	408630	9147867	18	26.5	35	5	15	25	13	17	21	min 10	Sandstone	0.019	0.023	0.038	0.095	94.7048	0.3450	343.9278	0.9500	947.0476	29	32	24		1
8	8		407869	9148545	45	55	65	50	75	100	8	10	12	1	Sparitic limestone	0.032	0.044	0.058	1.600	1595.0275	3.3000	3289.7442	5.8000	5781.9747	33	37	23		
9	9		407634	9148608	6	13	20	1	3	5	14	19	24	min 5	Andesitic breccia	0.013	0.018	0.026	0.013	12.9596	0.0540	53.8322	0.1300	129.5960	25	30	20		
10	10		407264	9148747	27	35.5	44	25	37.5	50	13	17	21	min 6	Sandstone	0.027	0.035	0.043	0.675	672.9022	1.3125	1308.4210	2.1500	2143.3182	33	37	23		
11	11		407386	9148905	27	35.5	44	25	37.5	50	13	17	21	min 4	Sandstone	0.027	0.035	0.043	0.675	672.9022	1.3125	1308.4210	2.1500	2143.3182	33	37	23		
12	12		407280	9149100	6	13	20	1	3	5	20	25	30	min 3	Andesite (lava)	0.015	0.020	0.028	0.015	14.9534	0.0600	59.8135	0.1400	139.5649	28	33	23		
13	13		407193	9149153	6	13	20	1	3	5	20	25	30	min 3	Andesite (lava)	0.015	0.020	0.028	0.015	14.9534	0.0600	59.8135	0.1400	139.5649	28	33	23		
14	14		407398	9148582	6	13	20	1	3	5	20	25	30	min 4	Andesite (lava)	0.015	0.020	0.028	0.015	14.9534	0.0600	59.8135	0.1400	139.5649	28	33	23		
15	15		407386	9148471	6	13	20	1	3	5	20	25	30	min 5	Andesite (lava)	0.015	0.020	0.028	0.015	14.9534	0.0600	59.8135	0.1400	139.5649	28	33	23		
16	16		407348	9148374	6	13	20	1	3	5	20	25	30	9	Andesite (lava)	0.015	0.020	0.028	0.015	14.9534	0.0600	59.8135	0.1400	139.5649	28	33	23		
17	17		407283	9148310	14	21	28	25	37.5	50	20	25	30	min 5	Andesite (lava)	0.019	0.028	0.038	0.475	473.5238	1.0500	1046.7368	1.9000	1894.0952	31	35	26		
18	18		407235	9148108	14	21	28	25	37.5	50	14	19	24	min 5	Andesitic breccia	0.018	0.024	0.036	0.450	448.6015	0.9000	897.2030	1.8000	1794.4059	28	33	23		
19	19		406300	9149245	55	67.5	80	0.25	0.625	1	2	4	6	min 6	Claystone	0.04	0.063	0.110	0.010	9.9689	0.0394	39.2526	0.1100	109.6581	28	31	25		
20	20		405832	9148866	6	13	20	0.25	0.625	1	14	19	24	min 8	Andesitic breccia	0.013	0.018	0.026	0.003	3.2399	0.0113	11.2150	0.0260	25.9192	25	30	20		
21	21	Oct 12, 2010	405473	9149151	6	13	20	0.25	0.625	1	2	4	6	min 4	Claystone	0.007	0.010	0.015	0.002	1.7446	0.0063	6.2306	0.0150	14.9534	14	18	11		
22	22		404918	9149215	6	13	20	1	3	5	14	19	24	min 6	Andesitic breccia	0.013	0.018	0.026	0.013	12.9596	0.0540	53.8322	0.1300	129.5960	25	30	20		
23	23		405016	9149032	6	13	20	1	3	5	14	19	24	min 4	Andesitic breccia	0.013	0.018	0.026	0.013	12.9596	0.0540	53.8322	0.1300	129.5960	25	30	20		
24	24		405073	9148791	6	13	20	5	15	25	14	19	24	min 4	Andesitic breccia	0.013	0.018	0.026	0.065	64.7980	0.2700	269.1609	0.6500	647.9799	25	30	20		
25	25		405216	9148440	6	13	20	5	15	25	14	19	24	min 5	Andesitic breccia	0.013	0.018	0.026	0.065	64.7980	0.2700	269.1609	0.6500	647.9799	25	30	20		
26	26		405410	9148364	14	21	28	25	37.5	50	20	25	30	min 4	Andesite (lava)	0.019	0.028	0.038	0.475	473.5238	1.0500	1046.7368	1.9000	1894.0952	31	35	26		
27	27		405646	9148183	6	13	20	5	15	25	14	19	24	min 5	Andesitic breccia	0.013	0.018	0.026	0.065	64.7980	0.2700	269.1609	0.6500	647.9799	25	30	20		
28	28		405897	9148148	6	13	20	5	15	25	14	19	24	min 5	Andesitic breccia	0.013	0.018	0.026	0.065	64.7980	0.2700	269.1609	0.6500	647.9799	25	30	20		1
29	29		406428	9148078	6	13	20	1	3	5	20	25	30	min 5	Andesite (lava)	0.015	0.020	0.028	0.015	14.9534	0.0600	59.8135	0.1400	139.5649	28	33	23		
30	30		406397	9148151	6	13	20	5	15	25	14	19	24	5	Andesitic breccia	0.013	0.018	0.026	0.065	64.7980	0.2700	269.1609	0.6500	647.9799	28	33	23		
31	31		406384	9148335	6	13	20	1	3	5	20	25	30	min 6	Andesite (lava)	0.015	0.020	0.028	0.015	14.9534	0.0600	59.8135	0.1400	139.5649	28	33	23		
32	32		406248	9148596	6	13	20	1	3	5	14	19	24	min 4	Andesitic breccia	0.013	0.018	0.026	0.013	12.9596	0.0540	53.8322	0.1300	129.5960	25	30	20		
33	33		406307	9148729	6	13	20	1	3	5	14	19	24	min 6	Andesitic breccia	0.013	0.018	0.026	0.013	12.9596	0.0540	53.8322	0.1300	129.5960	25	30	20		
34	34		406346	9148692	14	21	28	25	37.5	50	14	19	24	min 9	Andesitic breccia	0.018	0.024	0.036	0.450	448.6015	0.9000	897.2030	1.8000	1794.4059	28	33	23		
35	35		406501	9148757	6	13	20	1	3	5	14	19	24	min 5	Andesitic breccia	0.013	0.018	0.026	0.013	12.9596	0.0540	53.8322	0.1300	129.5960	25	30	20		
36	36		406592	9148766	18	26.5	35	1	3	5	20	25	30	min 8	Andesite (lava)	0.023	0.033	0.042	0.023	22.9285	0.0990	98.6923	0.2100	209.3474	33	38	28	1	
37	37		405167	9149458	6	13	20	1	3	5	14	19	24	min 3	Andesitic breccia	0.013	0.018	0.026	0.013	12.9596	0.0540	53.8322	0.1300	129.5960	25	30	20		
38	38		404566	9149095	6	13	20	1	3	5	14	19	24	min 6	Andesitic breccia	0.013	0.018	0.026	0.013	12.9596	0.0540	53.8322	0.1300	129.5960	25	30	20		
39	39		404556	9149199	6	13	20	1	3	5	14	19	24	min 3	Andesitic breccia	0.013	0.018	0.026	0.013	12.9596	0.0540	53.8322	0.1300	129.5960	25	30	20		

40	40		404625	9148793	6	13	20	1	3	5	14	19	24	min	3	Andesitic breccia	0.013	0.018	0.026	0.013	12.9596	0.0540	53.8322	0.1300	129.5960	25	30	20										
41	41		404186	9148723	6	13	20	1	3	5	14	19	24	min	6	Andesitic breccia	0.013	0.018	0.026	0.013	12.9596	0.0540	53.8322	0.1300	129.5960	25	30	20										
42	42	Oct 13, 2010	403534	9147298	6	13	20	1	3	5	20	25	30	min	6	Andesite (lava)	0.015	0.020	0.028	0.015	14.9534	0.0600	59.8135	0.1400	139.5649	28	33	23										
43	43		403566	9147110	6	13	20	1	3	5	14	19	24	min	3	Andesitic breccia	0.013	0.018	0.026	0.013	12.9596	0.0540	53.8322	0.1300	129.5960	25	30	20										
44	44		402999	9146956	6	13	20	0.25	0.625	1	5	7	9	min	3	Siltstone	0.0073	0.013	0.018	0.002	1.8193	0.0081	8.0997	0.0180	17.9441	17	19	13										
45	45		403049	9146321	14	21	28	25	37.5	50	13	17	21	min	6	Sandstone	0.015	0.024	0.035	0.375	373.8346	0.9000	897.2030	1.7500	1744.5613	27	33	22										
46	46		403653	9146530	6	13	20	1	3	5	20	25	30	min	4	Andesite (lava)	0.015	0.020	0.028	0.015	14.9534	0.0600	59.8135	0.1400	139.5649	28	33	23										
47	47		403826	9146817	6	13	20	0.25	0.625	1	5	7	9	min	4	Siltstone	0.0073	0.013	0.018	0.002	1.8193	0.0081	8.0997	0.0180	17.9441	17	19	13										
48	48		403948	9146605	6	13	20	1	3	5	20	25	30	min	5	Andesite (lava)	0.015	0.020	0.028	0.015	14.9534	0.0600	59.8135	0.1400	139.5649	28	33	23										
49	49		404016	9146621	6	13	20	1	3	5	20	25	30	min	6	Andesite (lava)	0.015	0.020	0.028	0.015	14.9534	0.0600	59.8135	0.1400	139.5649	28	33	23									1	
50	50		404218	9146552	6	13	20	1	3	5	20	25	30	min	3	Andesite (lava)	0.015	0.020	0.028	0.015	14.9534	0.0600	59.8135	0.1400	139.5649	28	33	23										
51	51		404066	9146664	6	13	20	1	3	5	20	25	30	min	5	Andesite (lava)	0.015	0.020	0.028	0.015	14.9534	0.0600	59.8135	0.1400	139.5649	28	33	23										
52	52		403716	9146423	6	13	20	0.25	0.625	1	20	25	30	min	7	Andesite (lava)	0.015	0.020	0.028	0.004	3.7383	0.0125	12.4612	0.0280	27.9130	28	33	23									1	
53	53		403842	9146369	6	13	20	1	3	5	20	25	30	min	5	Andesite (lava)	0.015	0.020	0.028	0.015	14.9534	0.0600	59.8135	0.1400	139.5649	28	33	23										
54	54	Oct 14, 2010	404329	9146027	6	13	20	1	3	5	20	25	30	min	6	Andesite (lava)	0.015	0.020	0.028	0.015	14.9534	0.0600	59.8135	0.1400	139.5649	28	33	23										
55	55		404668	9146048	27	35.5	44	50	75	100	8	10	12	min	5	Sparitic limestone	0.024	0.031	0.038	1.200	1196.2706	2.3250	2317.7743	3.8000	3788.1903	28	32	23										
56	56		404694	9146266	27	35.5	44	50	75	100	8	10	12	min	6	Sparitic limestone	0.024	0.031	0.038	1.200	1196.2706	2.3250	2317.7743	3.8000	3788.1903	28	32	23										
57	57		404807	9146526	6	13	20	1	3	5	20	25	30	min	4	Andesite (lava)	0.015	0.020	0.028	0.015	14.9534	0.0600	59.8135	0.1400	139.5649	28	33	23										
58	58		404702	9146705	6	13	20	0.25	0.625	1	5	7	9	min	7	Siltstone	0.0073	0.013	0.018	0.002	1.8193	0.0081	8.0997	0.0180	17.9441	17	19	13										
59	59		404658	9146862	6	13	20	1	3	5	20	25	30	min	7	Andesite (lava)	0.015	0.020	0.028	0.015	14.9534	0.0600	59.8135	0.1400	139.5649	28	33	23										
60	60		404810	9147497	6	13	20	1	3	5	20	25	30	min	6	Andesite (lava)	0.015	0.020	0.028	0.015	14.9534	0.0600	59.8135	0.1400	139.5649	28	33	23										
61	61		404692	9147569	44	55.5	67	50	75	100	20	25	30	min	1	Andesite (lava)	0.042	0.055	0.070	2.100	2093.4736	4.1250	4112.1803	7.0000	6978.2453	42	46	36										
62	62		404552	9147806	6	13	20	1	3	5	14	19	24	min	5	Andesitic breccia	0.013	0.018	0.026	0.013	12.9596	0.0540	53.8322	0.1300	129.5960	25	30	20										
63	63		404596	9148032	14	21	28	1	3	5	14	19	24	min	4	Andesitic breccia	0.018	0.024	0.036	0.018	17.9441	0.0720	71.7762	0.1800	179.4406	28	33	23	1									
64	64		404559	9148314	6	13	20	1	3	5	14	19	24	min	4	Andesitic breccia	0.013	0.018	0.026	0.013	12.9596	0.0540	53.8322	0.1300	129.5960	25	30	20										
65	65		404997	9146009	14	21	28	25	37.5	50	8	10	12	min	3	Sparitic limestone	0.014	0.018	0.029	0.350	348.9123	0.6750	672.9022	1.4500	1445.4937	24	27	18										
66	66		405213	9146092	14	21	28	25	37.5	50	8	10	12	min	6	Sparitic limestone	0.014	0.018	0.029	0.350	348.9123	0.6750	672.9022	1.4500	1445.4937	24	27	18										
67	67		405445	9146170	6	13	20	1	3	5	14	19	24	min	4	Andesitic breccia	0.013	0.018	0.026	0.013	12.9596	0.0540	53.8322	0.1300	129.5960	25	30	20										
68	68		405779	9146482	6	13	20	0.25	0.625	1	14	19	24	min	3	Andesitic breccia	0.013	0.018	0.026	0.003	3.2399	0.0113	11.2150	0.0260	25.9192	25	30	20	1								
69	69		406015	9146521	14	21	28	25	37.5	50	8	10	12	min	3	Sparitic limestone	0.014	0.018	0.029	0.350	348.9123	0.6750	672.9022	1.4500	1445.4937	24	27	18										
70	70	Oct 20, 2010	404469	9145877	6	13	20	1	3	5	14	19	24	min	4	Andesitic breccia	0.013	0.018	0.026	0.013	12.9596	0.0540	53.8322	0.1300	129.5960	25	30	20										
71	71		404774	9145544	6	13	20	0.25	0.625	1	2	4	6	min	4	Claystone	0.007	0.010	0.015	0.002	1.7446	0.0063	6.2306	0.0150	14.9534	14	18	11										
72	72		404555	9145422	6	13	20	0.25	0.625	1	14	19	24	min	10	Andesitic breccia	0.013	0.018	0.026	0.003	3.2399	0.0113	11.2150	0.0260	25.9192	25	30	20										
73	73		404484	9145006	6	13	20	1	3	5	14	19	24	min	5	Andesitic breccia	0.013	0.018	0.026	0.013	12.9596	0.0540	53.8322	0.1300	129.5960	25	30	20										
74	74		404711	9144909	6	13	20	0.25	0.625	1	14	19	24	min	3	Andesitic breccia	0.013	0.018	0.026	0.003	3.2399	0.0113	11.2150	0.0260	25.9192	25	30	20										
75	75		404925	9144829	14	21	28	5	15	25	8	10	12	min	6	Sparitic limestone	0.014	0.018	0.029	0.070	69.7825	0.2700	269.1609	0.7250	722.7468	24	27	18										
76	76		405029	9144715	27	35.5	44	50	75	100	8	10	12	min	6	Sparitic limestone	0.024	0.031	0.038	1.200	1196.2706	2.3250	2317.7743	3.8000	3788.1903	28	32	23										
77	77		405087	9144810	27	35.5	44	25	37.5	50	8	10	12	min	3	Sparitic limestone	0.024	0.031	0.038	0.600	598.1353	1.1625	1158.8872	1.9000	1894.0952	28	32	23										
78	78		405084	9145367	6	13	20	0.25	0.625	1	8	10	12	min	2	Sparitic limestone	0.009	0.014	0.019	0.002	2.2430	0.0088	8.7228	0.0190	18.9410	19	24	15										
79	79		405149	9144674	6	13	20	0.25	0.625	1	8	10	12	min	5	Sparitic limestone	0.009	0.014	0.019	0.002	2.2430	0.0088	8.7228	0.0190	18.9410	19	24	15										
80	80		405360	9144469	27	35.5	44	25	37.5	50	8	10	12	min	6	Sparitic limestone	0.024	0.031	0.038	0.600	598.1353	1.1625	1158.8872	1.9000	1894.0952	28	32	23										
81	81		405692	9144376	6	13	20	0.25	0.625	1	8	10	12	min	5	Sparitic limestone	0.009	0.014	0.019	0.002	2.2430	0.0088	8.7228	0.0190	18.9410	19	24	15										
82	82		405720	9144219	14	21	28	5	15	25	5	7	9	min	5	Siltstone	0.011	0.017	0.026	0.055	54.8291	0.2550	254.2075	0.6500	647.9799	21	24	15										
83	83		405764	9143997	6	13	20	0.25	0.625	1	5	7	9	min	4	Siltstone	0.0073	0.013	0.018	0.002	1.8193	0.0081	8.0997	0.0180	17.9441	17	19	13									1	
84	84		405370	9143799	6	13	20	0.25	0.625	1	5	7	9	min	3	Siltstone	0.0073	0.013	0.018	0.002	1.8193	0.0081	8.0997	0.0180	17.9441	17	19	13										
85	85		406067	9146449	6	13	20	0.25	0.625	1	5	7	9	min	8	Siltstone	0.0073	0.013	0.018	0.002	1.8193	0.0081	8.0997	0.0180	17.9441	17	19	13										

86	86		406316	9146705	6	13	20	1	3	5	14	19	24	min	5	Andesitic breccia	0.013	0.018	0.026	0.013	12.9596	0.0540	53.8322	0.1300	129.5960	25	30	20			
87	87		406271	9146851	14	21	28	5	15	25	14	19	24	min	7	Andesitic breccia	0.018	0.024	0.036	0.090	89.7203	0.3600	358.8812	0.9000	897.2030	28	33	23			
88	88		406460	9146990	6	13	20	1	3	5	14	19	24	min	5	Andesitic breccia	0.013	0.018	0.026	0.013	12.9596	0.0540	53.8322	0.1300	129.5960	25	30	20			
89	89		406632	9147043	14	21	28	5	15	25	14	19	24	min	7	Andesitic breccia	0.018	0.024	0.036	0.090	89.7203	0.3600	358.8812	0.9000	897.2030	28	33	23	1		
90	90		406494	9147304	6	13	20	1	3	5	14	19	24	min	7	Andesitic breccia	0.013	0.018	0.026	0.013	12.9596	0.0540	53.8322	0.1300	129.5960	25	30	20		1	
91	91		406514	9147482	6	13	20	5	15	25	20	25	30	min	5	Andesite (lava)	0.015	0.020	0.028	0.075	74.7669	0.3000	299.0677	0.7000	697.8245	28	33	23	1		
92	92		406878	9147860	6	13	20	1	3	5	14	19	24	min	5	Andesitic breccia	0.013	0.018	0.026	0.013	12.9596	0.0540	53.8322	0.1300	129.5960	25	30	20		1	
93	93		406851	9147930	6	13	20	1	3	5	14	19	24	min	6	Andesitic breccia	0.013	0.018	0.026	0.013	12.9596	0.0540	53.8322	0.1300	129.5960	25	30	20		1	
94	94	Oct 21, 2010	406481	9143844	6	13	20	0.25	0.625	1	14	19	24	min	5	Andesitic breccia	0.013	0.018	0.026	0.003	3.2399	0.0113	11.2150	0.0260	25.9192	25	30	20			
95	95		406534	9143666	6	13	20	0.25	0.625	1	14	19	24	min	4	Andesitic breccia	0.013	0.018	0.026	0.003	3.2399	0.0113	11.2150	0.0260	25.9192	25	30	20		1	
96	96		406797	9143320	6	13	20	1	3	5	14	19	24	min	3	Andesitic breccia	0.013	0.018	0.026	0.013	12.9596	0.0540	53.8322	0.1300	129.5960	25	30	20		1	
97	97		406144	9143892	14	21	28	5	15	25	14	19	24	min	5	Andesitic breccia	0.018	0.024	0.036	0.090	89.7203	0.3600	358.8812	0.9000	897.2030	28	33	23			
98	98		406469	9144217	6	13	20	0.25	0.625	1	14	19	24	min	3	Andesitic breccia	0.013	0.018	0.026	0.003	3.2399	0.0113	11.2150	0.0260	25.9192	25	30	20			
99	99		406556	9144334	6	13	20	1	3	5	14	19	24	min	6	Andesitic breccia	0.013	0.018	0.026	0.013	12.9596	0.0540	53.8322	0.1300	129.5960	25	30	20			
100	100		406462	9144575	6	13	20	1	3	5	14	19	24	min	7	Andesitic breccia	0.013	0.018	0.026	0.013	12.9596	0.0540	53.8322	0.1300	129.5960	25	30	20	1		
101	101		406439	9144822	14	21	28	1	3	5	14	19	24	min	4	Andesitic breccia	0.018	0.024	0.036	0.018	17.9441	0.0720	71.7762	0.1800	179.4406	28	33	23			
102	102		406594	9144982	6	13	20	1	3	5	20	25	30	min	4	Andesite (lava)	0.015	0.020	0.028	0.015	14.9534	0.0600	59.8135	0.1400	139.5649	28	33	23			
103	103		406873	9145037	14	21	28	5	15	25	14	19	24	min	4	Andesitic breccia	0.018	0.024	0.036	0.090	89.7203	0.3600	358.8812	0.9000	897.2030	28	33	23			
104	104		406974	9145024	14	21	28	1	3	5	14	19	24	min	5	Andesitic breccia	0.018	0.024	0.036	0.018	17.9441	0.0720	71.7762	0.1800	179.4406	28	33	23		1	
105	105		407277	9145286	6	13	20	1	3	5	14	19	24	min	6	Andesitic breccia	0.013	0.018	0.026	0.013	12.9596	0.0540	53.8322	0.1300	129.5960	25	30	20		1	
106	106		407070	9145134	6	13	20	1	3	5	20	25	30	min	6	Andesite (lava)	0.015	0.020	0.028	0.015	14.9534	0.0600	59.8135	0.1400	139.5649	28	33	23			
107	107		407148	9145391	6	13	20	1	3	5	20	25	30	min	8	Andesite (lava)	0.015	0.020	0.028	0.015	14.9534	0.0600	59.8135	0.1400	139.5649	28	33	23		1	
108	108		407256	9145369	6	13	20	1	3	5	14	19	24	min	8	Andesitic breccia	0.013	0.018	0.026	0.013	12.9596	0.0540	53.8322	0.1300	129.5960	25	30	20			
109	109		407522	9145270	6	13	20	1	3	5	14	19	24	min	4	Andesitic breccia	0.013	0.018	0.026	0.013	12.9596	0.0540	53.8322	0.1300	129.5960	25	30	20			
110	110	Oct 22, 2010	408128	9147793	6	13	20	0.25	0.625	1	14	19	24	min	4	Andesitic breccia	0.013	0.018	0.026	0.003	3.2399	0.0113	11.2150	0.0260	25.9192	25	30	20			
111	111		407968	9147827	6	13	20	0.25	0.625	1	14	19	24	min	4	Andesitic breccia	0.013	0.018	0.026	0.003	3.2399	0.0113	11.2150	0.0260	25.9192	25	30	20			
112	112		407819	9147786	6	13	20	1	3	5	14	19	24		6	Andesitic breccia	0.013	0.018	0.026	0.013	12.9596	0.0540	53.8322	0.1300	129.5960	25	30	20			
113	113		407707	9147795	6	13	20	1	3	5	20	25	30		6	Andesite (lava)	0.015	0.020	0.028	0.015	14.9534	0.0600	59.8135	0.1400	139.5649	28	33	23			
114	114		407478	9147874	6	13	20	1	3	5	14	19	24	min	5	Andesitic breccia	0.013	0.018	0.026	0.013	12.9596	0.0540	53.8322	0.1300	129.5960	25	30	20			
115	115		407174	9147974	6	13	20	1	3	5	18	21	24	min	5	Conglomerate	0.014	0.019	0.026	0.014	13.9565	0.0570	56.8229	0.1300	129.5960	27	30	24			
116	116		407240	9147772	6	13	20	1	3	5	14	19	24	min	6	Andesitic breccia	0.013	0.018	0.026	0.013	12.9596	0.0540	53.8322	0.1300	129.5960	25	30	20			
117	117		407439	9147610	6	13	20	0.25	0.625	1	14	19	24	min	5	Andesitic breccia	0.013	0.018	0.026	0.003	3.2399	0.0113	11.2150	0.0260	25.9192	25	30	20			
118	118		407697	9147476	14	21	28	5	15	25	20	25	30		4	Andesite (lava)	0.019	0.028	0.038	0.095	94.7048	0.4200	418.6947	0.9500	947.0476	31	35	26			
119	119		407959	9147135	14	21	28	5	15	25	14	19	24	min	3	Andesitic breccia	0.018	0.024	0.036	0.090	89.7203	0.3600	358.8812	0.9000	897.2030	28	33	23			
120	120		408033	9147076	6	13	20	1	3	5	20	25	30	min	4	Andesite (lava)	0.015	0.020	0.028	0.015	14.9534	0.0600	59.8135	0.1400	139.5649	28	33	23			
121	121		408361	9146853	6	13	20	1	3	5	5	7	9		4	Siltstone	0.0073	0.013	0.018	0.007	7.2773	0.0390	38.8788	0.0900	89.7203	17	19	13			
122	122		408480	9146695	14	21	28	5	15	25	20	25	30	min	5	Andesite (lava)	0.019	0.028	0.038	0.095	94.7048	0.4200	418.6947	0.9500	947.0476	31	35	26			
123	123	Oct 23, 2010	408427	9147361	6	13	20	1	3	5	14	19	24	min	3	Andesitic breccia	0.013	0.018	0.026	0.013	12.9596	0.0540	53.8322	0.1300	129.5960	25	30	20			
124	124		408558	9147178	37	46	55	1	3	5	14	19	24		3	Andesitic breccia	0.035	0.044	0.053	0.035	34.8912	0.1320	131.5898	0.2650	264.1764	36	41	31			
125	125		408764	9146920	6	13	20	1	3	5	14	19	24	min	4	Andesitic breccia	0.013	0.018	0.026	0.013	12.9596	0.0540	53.8322	0.1300	129.5960	25	30	20			
126	126		409128	9146773	6	13	20	1	3	5	14	19	24		5	Andesitic breccia	0.013	0.018	0.026	0.013	12.9596	0.0540	53.8322	0.1300	129.5960	25	30	20			
127	127		408695	9146694	6	13	20	1	3	5	14	19	24	min	4	Andesitic breccia	0.013	0.018	0.026	0.013	12.9596	0.0540	53.8322	0.1300	129.5960	25	30	20			
128	128		408662	9146470	6	13	20	1	3	5	14	19	24		3	Andesitic breccia	0.013	0.018	0.026	0.013	12.9596	0.0540	53.8322	0.1300	129.5960	25	30	20			
129	129		408849	9146247	6	13	20	1	3	5	14	19	24		4	Andesitic breccia	0.013	0.018	0.026	0.013	12.9596	0.0540	53.8322	0.1300	129.5960	25	30	20			
130	130		408843	9146097	6	13	20	1	3	5	14	19	24		4	Andesitic breccia	0.013	0.018	0.026	0.013	12.9596	0.0540	53.8322	0.1300	129.5960	25	30	20			
131	131		408492	9145993	14	21	28	1	3	5	20	25	30	min	4	Andesite (lava)	0.019	0.028	0.038	0.019	18.9410	0.0840	83.7389	0.1900	189.4095	31	35	26			

132	132		408095	9146219	6	13	20	1	3	5	14	19	24	min	5	Andesitic breccia	0.013	0.018	0.026	0.013	12.9596	0.0540	53.8322	0.1300	129.5960	25	30	20		1
133	133		407938	9146185	6	13	20	1	3	5	14	19	24	min	5	Andesitic breccia	0.013	0.018	0.026	0.013	12.9596	0.0540	53.8322	0.1300	129.5960	25	30	20		1
134	134		407753	9146070	6	13	20	1	3	5	14	19	24		4	Andesitic breccia	0.013	0.018	0.026	0.013	12.9596	0.0540	53.8322	0.1300	129.5960	25	30	20		
135	135		407502	9146144	14	21	28	5	15	25	14	19	24	min	5	Andesitic breccia	0.018	0.024	0.036	0.090	89.7203	0.3600	358.8812	0.9000	897.2030	28	33	23		
136	136		407412	9146021	6	13	20	1	3	5	14	19	24	min	4	Andesitic breccia	0.013	0.018	0.026	0.013	12.9596	0.0540	53.8322	0.1300	129.5960	25	30	20		
137	137		407188	9145866	6	13	20	1	3	5	20	25	30		5	Andesite (lava)	0.015	0.020	0.028	0.015	14.9534	0.0600	59.8135	0.1400	139.5649	28	33	23		
138	138		407271	9145767	6	13	20	1	3	5	14	19	24	min	4	Andesitic breccia	0.013	0.018	0.026	0.013	12.9596	0.0540	53.8322	0.1300	129.5960	25	30	20		1
139	139		407468	9145589	6	13	20	0.25	0.625	1	14	19	24	min	4	Andesitic breccia	0.013	0.018	0.026	0.003	3.2399	0.0113	11.2150	0.0260	25.9192	25	30	20		
140	140		407594	9145431	6	13	20	0.25	0.625	1	14	19	24	min	4	Andesitic breccia	0.013	0.018	0.026	0.003	3.2399	0.0113	11.2150	0.0260	25.9192	25	30	20		
141	141		406885	9145599	6	13	20	0.25	0.625	1	14	19	24	min	7	Andesitic breccia	0.013	0.018	0.026	0.003	3.2399	0.0113	11.2150	0.0260	25.9192	25	30	20		
142	142		406500	9145916	6	13	20	0.25	0.625	1	14	19	24	min	7	Andesitic breccia	0.013	0.018	0.026	0.003	3.2399	0.0113	11.2150	0.0260	25.9192	25	30	20		
143	143		406079	9146037	6	13	20	1	3	5	14	19	24	min	7	Andesitic breccia	0.013	0.018	0.026	0.013	12.9596	0.0540	53.8322	0.1300	129.5960	25	30	20		
144	144		406354	9146350	14	21	28	5	15	25	8	10	12	min	6	Sparitic limestone	0.014	0.018	0.029	0.070	69.7825	0.2700	269.1609	0.7250	722.7468	24	27	18		
145	145		406654	9146404	55	67.5	80	0.25	0.625	1	2	4	6	min	5	Claystone	0.04	0.063	0.110	0.010	9.9689	0.0394	39.2526	0.1100	109.6581	28	31	25		1
146	146		407012	9146319	6	13	20	1	3	5	14	19	24	min	6	Andesitic breccia	0.013	0.018	0.026	0.013	12.9596	0.0540	53.8322	0.1300	129.5960	25	30	20		
147	147		407348	9146231	14	21	28	1	3	5	14	19	24		5	Andesitic breccia	0.018	0.024	0.036	0.018	17.9441	0.0720	71.7762	0.1800	179.4406	28	33	23		
148	148		408924	9145961	14	21	28	1	3	5	14	19	24	min	6	Andesitic breccia	0.018	0.024	0.036	0.018	17.9441	0.0720	71.7762	0.1800	179.4406	28	33	23		
149	149		409262	9145706	6	13	20	1	3	5	14	19	24	min	5	Andesitic breccia	0.013	0.018	0.026	0.013	12.9596	0.0540	53.8322	0.1300	129.5960	25	30	20		
150	150		409051	9146070	6	13	20	1	3	5	14	19	24		8	Andesitic breccia	0.013	0.018	0.026	0.013	12.9596	0.0540	53.8322	0.1300	129.5960	25	30	20		1
151	151		409051	9146070	14	21	28	1	3	5	20	25	30	min	5	Andesite (lava)	0.019	0.028	0.038	0.019	18.9410	0.0840	83.7389	0.1900	189.4095	31	35	26		
152	152	Oct 24, 2010	407142	9144106	6	13	20	0.25	0.625	1	5	7	9	min	4	Siltstone	0.0073	0.013	0.018	0.002	1.8193	0.0081	8.0997	0.0180	17.9441	17	19	13		
153	153		407083	9144188	6	13	20	1	3	5	20	25	30	min	3	Andesite (lava)	0.015	0.020	0.028	0.015	14.9534	0.0600	59.8135	0.1400	139.5649	28	33	23		
154	154		406911	9144293	6	13	20	0.25	0.625	1	20	25	30	min	3	Andesite (lava)	0.015	0.020	0.028	0.004	3.7383	0.0125	12.4612	0.0280	27.9130	28	33	23		
155	155		407461	9144067	14	21	28	1	3	5	14	19	24	min	6	Andesitic breccia	0.018	0.024	0.036	0.018	17.9441	0.0720	71.7762	0.1800	179.4406	28	33	23		
156	156		407672	9144106	6	13	20	0.25	0.625	1	20	25	30	min	3	Andesite (lava)	0.015	0.020	0.028	0.004	3.7383	0.0125	12.4612	0.0280	27.9130	28	33	23		
157	157		407726	9144196	6	13	20	1	3	5	20	25	30	min	3	Andesite (lava)	0.015	0.020	0.028	0.015	14.9534	0.0600	59.8135	0.1400	139.5649	28	33	23		
158	158		407973	9144063	6	13	20	1	3	5	14	19	24	min	4	Andesitic breccia	0.013	0.018	0.026	0.013	12.9596	0.0540	53.8322	0.1300	129.5960	25	30	20		
159	159		407838	9143961	6	13	20	1	3	5	14	19	24	min	7	Andesitic breccia	0.013	0.018	0.026	0.013	12.9596	0.0540	53.8322	0.1300	129.5960	25	30	20		1
160	160		408129	9143982	14	21	28	1	3	5	14	19	24	min	5	Andesitic breccia	0.018	0.024	0.036	0.018	17.9441	0.0720	71.7762	0.1800	179.4406	28	33	23		
161	161		408542	9143672	14	21	28	1	3	5	14	19	24	min	6	Andesitic breccia	0.018	0.024	0.036	0.018	17.9441	0.0720	71.7762	0.1800	179.4406	28	33	23		
162	162		408394	9143818	14	21	28	1	3	5	14	19	24	min	6	Andesitic breccia	0.018	0.024	0.036	0.018	17.9441	0.0720	71.7762	0.1800	179.4406	28	33	23		
163	163		408292	9143745	14	21	28	1	3	5	14	19	24	min	5	Andesitic breccia	0.018	0.024	0.036	0.018	17.9441	0.0720	71.7762	0.1800	179.4406	28	33	23		
164	164		408087	9143406	14	21	28	5	15	25	20	25	30	min	4	Andesite (lava)	0.019	0.028	0.038	0.095	94.7048	0.4200	418.6947	0.9500	947.0476	31	35	26		
165	165		407844	9143652	14	21	28	1	3	5	20	25	30	min	4	Andesite (lava)	0.019	0.028	0.038	0.019	18.9410	0.0840	83.7389	0.1900	189.4095	31	35	26		
166	166		408737	9143657	14	21	28	1	3	5	14	19	24	min	5	Andesitic breccia	0.018	0.024	0.036	0.018	17.9441	0.0720	71.7762	0.1800	179.4406	28	33	23		
167	167		408986	9143498	14	21	28	1	3	5	14	19	24	min	5	Andesitic breccia	0.018	0.024	0.036	0.018	17.9441	0.0720	71.7762	0.1800	179.4406	28	33	23		
168	168		409031	9143618	14	21	28	1	3	5	14	19	24	min	8	Andesitic breccia	0.018	0.024	0.036	0.018	17.9441	0.0720	71.7762	0.1800	179.4406	28	33	23		1
169	169		409077	9143214	6	13	20	1	3	5	14	19	24	min	3	Andesitic breccia	0.013	0.018	0.026	0.013	12.9596	0.0540	53.8322	0.1300	129.5960	25	30	20		
170	170		408937	9143173	14	21	28	0.25	0.625	1	14	19	24	min	5	Andesitic breccia	0.018	0.024	0.036	0.005	4.4860	0.0150	14.9534	0.0360	35.8881	28	33	23		
171	171		409009	9142902	14	21	28	1	3	5	14	19	24	min	6	Andesitic breccia	0.018	0.024	0.036	0.018	17.9441	0.0720	71.7762	0.1800	179.4406	28	33	23		
172	172		409203	9142712	6	13	20	0.25	0.625	1	14	19	24	min	5	Andesitic breccia	0.013	0.018	0.026	0.003	3.2399	0.0113	11.2150	0.0260	25.9192	25	30	20		
173	173		409384	9142386	14	21	28	1	3	5	14	19	24	min	5	Andesitic breccia	0.018	0.024	0.036	0.018	17.9441	0.0720	71.7762	0.1800	179.4406	28	33	23		
174	174		409758	9142030	14	21	28	1	3	5	14	19	24	min	6	Andesitic breccia	0.018	0.024	0.036	0.018	17.9441	0.0720	71.7762	0.1800	179.4406	28	33	23		
175	175		409903	9141267	6	13	20	0.25	0.625	1	14	19	24	min	3	Andesitic breccia	0.013	0.018	0.026	0.003	3.2399	0.0113	11.2150	0.0260	25.9192	25	30	20		
176	176	Oct 25, 2010	409866	9143268	6	13	20	0.25	0.625	1	14	19	24	min	5	Andesitic breccia	0.013	0.018	0.026	0.003	3.2399	0.0113	11.2150	0.0260	25.9192	25	30	20		
177	177		409987	9143147	6	13	20	0.25	0.625	1	14	19	24	min	7	Andesitic breccia	0.013	0.018	0.026	0.003	3.2399	0.0113	11.2150	0.0260	25.9192	25	30	20		

178	178		410006	9143024	14	21	28	1	3	5	14	19	24	min	8	Andesitic breccia	0.018	0.024	0.036	0.018	17.9441	0.0720	71.7762	0.1800	179.4406	28	33	23			
179	179		409896	9143030	14	21	28	1	3	5	14	19	24	min	5	Andesitic breccia	0.018	0.024	0.036	0.018	17.9441	0.0720	71.7762	0.1800	179.4406	28	33	23			
180	180		410146	9143032	6	13	20	0.25	0.625	1	14	19	24	min	6	Andesitic breccia	0.013	0.018	0.026	0.003	3.2399	0.0113	11.2150	0.0260	25.9192	25	30	20			
181	181		410241	9142958	14	21	28	1	3	5	14	19	24	min	5	Andesitic breccia	0.018	0.024	0.036	0.018	17.9441	0.0720	71.7762	0.1800	179.4406	28	33	23			
182	182		410206	9142839	14	21	28	5	15	25	14	19	24	min	4	Andesitic breccia	0.018	0.024	0.036	0.090	89.7203	0.3600	358.8812	0.9000	897.2030	28	33	23			
183	183		410273	9142600	14	21	28	1	3	5	14	19	24	min	5	Andesitic breccia	0.018	0.024	0.036	0.018	17.9441	0.0720	71.7762	0.1800	179.4406	28	33	23			
184	184		410340	9142212	14	21	28	5	15	25	14	19	24	min	4	Andesitic breccia	0.018	0.024	0.036	0.090	89.7203	0.3600	358.8812	0.9000	897.2030	28	33	23			
185	185		410632	9142066	14	21	28	5	15	25	14	19	24	min	3	Andesitic breccia	0.018	0.024	0.036	0.090	89.7203	0.3600	358.8812	0.9000	897.2030	28	33	23			
186	186		410759	9141964	6	13	20	1	3	5	14	19	24	min	5	Andesitic breccia	0.013	0.018	0.026	0.013	12.9596	0.0540	53.8322	0.1300	129.5960	25	30	20			1
187	187		410833	9141745	6	13	20	0.25	0.625	1	14	19	24	min	5	Andesitic breccia	0.013	0.018	0.026	0.003	3.2399	0.0113	11.2150	0.0260	25.9192	25	30	20			
188	188		410679	9141344	6	13	20	0.25	0.625	1	14	19	24	min	4	Andesitic breccia	0.013	0.018	0.026	0.003	3.2399	0.0113	11.2150	0.0260	25.9192	25	30	20			1
189	189		410399	9140929	6	13	20	0.25	0.625	1	14	19	24	min	5	Andesitic breccia	0.013	0.018	0.026	0.003	3.2399	0.0113	11.2150	0.0260	25.9192	25	30	20			
190	190		410529	9140804	14	21	28	1	3	5	14	19	24		7	Andesitic breccia	0.018	0.024	0.036	0.018	17.9441	0.0720	71.7762	0.1800	179.4406	28	33	23			
191	191		411127	9140338	45	55	65	5	15	25	5	7	9		1	Siltstone	0.031	0.042	0.058	0.155	154.5183	0.6300	628.0421	1.4500	1445.4937	29	34	24			
192	192		411793	9139516	44	55.5	67	1	3	5	13	17	21		2	Sandstone	0.038	0.050	0.066	0.038	37.8819	0.1500	149.5338	0.3300	328.9744	38	43	32			
193	193		411228	9139542	14	21	28	1	3	5	5	7	9		2	Siltstone	0.011	0.017	0.026	0.011	10.9658	0.0510	50.8415	0.1300	129.5960	21	24	15			
194	194		411241	9139174	23	30.5	38	1	3	5	5	7	9		2	Siltstone	0.017	0.027	0.028	0.017	16.9472	0.0810	80.7483	0.1400	139.5649	24	25	18			
195	195		411245	9138684	23	30.5	38	1	3	5	5	7	9		1	Siltstone	0.017	0.027	0.028	0.017	16.9472	0.0810	80.7483	0.1400	139.5649	24	25	18			
196	196		411616	9138381	14	21	28	1	3	5	5	7	9		1	Siltstone	0.011	0.017	0.026	0.011	10.9658	0.0510	50.8415	0.1300	129.5960	21	24	15			
197	197		412888	9138822	14	21	28	1	3	5	5	7	9		3	Siltstone	0.011	0.017	0.026	0.011	10.9658	0.0510	50.8415	0.1300	129.5960	21	24	15			
198	198		413146	9138953	14	21	28	1	3	5	5	7	9	min	3	Siltstone	0.011	0.017	0.026	0.011	10.9658	0.0510	50.8415	0.1300	129.5960	21	24	15			
199	199	Oct 26, 2010	409053	9147528	6	13	20	0.25	0.625	1	13	17	21	min	6	Sandstone	0.012	0.018	0.026	0.003	2.9907	0.0113	11.2150	0.0260	25.9192	24	29	18			
200	200		409126	9147423	14	21	28	1	3	5	13	17	21	min	3	Sandstone	0.015	0.024	0.035	0.015	14.9534	0.0720	71.7762	0.1750	174.4561	27	33	22			
201	201		409149	9147287	6	13	20	1	3	5	13	17	21	min	4	Sandstone	0.012	0.018	0.026	0.012	11.9627	0.0540	53.8322	0.1300	129.5960	24	29	18			
202	202		409154	9147380	6	13	20	1	3	5	13	17	21	min	5	Sandstone	0.012	0.018	0.026	0.012	11.9627	0.0540	53.8322	0.1300	129.5960	24	29	18			1
203	203		409150	9147618	6	13	20	0.25	0.625	1	14	19	24	min	4	Andesitic breccia	0.013	0.018	0.026	0.003	3.2399	0.0113	11.2150	0.0260	25.9192	25	30	20			
204	204		409213	9147140	6	13	20	1	3	5	18	21	24	min	5	Conglomerate	0.014	0.019	0.026	0.014	13.9565	0.0570	56.8229	0.1300	129.5960	27	30	24			
205	205		409336	9146953	6	13	20	1	3	5	5	7	9	min	5	Siltstone	0.0073	0.013	0.018	0.007	7.2773	0.0390	38.8788	0.0900	89.7203	17	19	13			
206	206		409861	9146720	6	13	20	1	3	5	14	19	24	min	6	Andesitic breccia	0.013	0.018	0.026	0.013	12.9596	0.0540	53.8322	0.1300	129.5960	25	30	20			
207	207		409974	9146544	14	21	28	0.25	0.625	1	20	25	30		4	Andesite (lava)	0.019	0.028	0.038	0.005	4.7352	0.0175	17.4456	0.0380	37.8819	31	35	26			
208	208		410187	9146607	14	21	28	1	3	5	14	19	24	min	5	Andesitic breccia	0.018	0.024	0.036	0.018	17.9441	0.0720	71.7762	0.1800	179.4406	28	33	23			
209	209		409916	9145959	6	13	20	1	3	5	14	19	24	min	5	Andesitic breccia	0.013	0.018	0.026	0.013	12.9596	0.0540	53.8322	0.1300	129.5960	25	30	20			
210	210		409880	9145920	14	21	28	1	3	5	14	19	24	min	4	Andesitic breccia	0.018	0.024	0.036	0.018	17.9441	0.0720	71.7762	0.1800	179.4406	28	33	23			1
211	211		409837	9146065	6	13	20	0.25	0.625	1	14	19	24	min	5	Andesitic breccia	0.013	0.018	0.026	0.003	3.2399	0.0113	11.2150	0.0260	25.9192	25	30	20			1
212	212		409728	9145957	6	13	20	0.25	0.625	1	14	19	24	min	6	Andesitic breccia	0.013	0.018	0.026	0.003	3.2399	0.0113	11.2150	0.0260	25.9192	25	30	20			
213	213		409752	9145599	6	13	20	1	3	5	14	19	24	min	4	Andesitic breccia	0.013	0.018	0.026	0.013	12.9596	0.0540	53.8322	0.1300	129.5960	25	30	20			
214	214		409742	9145486	14	21	28	5	15	25	14	19	24		6	Andesitic breccia	0.018	0.024	0.036	0.090	89.7203	0.3600	358.8812	0.9000	897.2030	28	33	23			1
215	215		409976	9145458	14	21	28	1	3	5	14	19	24	min	4	Andesitic breccia	0.018	0.024	0.036	0.018	17.9441	0.0720	71.7762	0.1800	179.4406	28	33	23			
216	216		410061	9145438	6	13	20	1	3	5	14	19	24	min	5	Andesitic breccia	0.013	0.018	0.026	0.013	12.9596	0.0540	53.8322	0.1300	129.5960	25	30	20			1
217	217		410217	9145326	6	13	20	0.25	0.625	1	14	19	24	min	8	Andesitic breccia	0.013	0.018	0.026	0.003	3.2399	0.0113	11.2150	0.0260	25.9192	25	30	20			
218	218		410155	9144999	6	13	20	1	3	5	14	19	24	min	8	Andesitic breccia	0.013	0.018	0.026	0.013	12.9596	0.0540	53.8322	0.1300	129.5960	25	30	20			
219	219		410174	9144735	6	13	20	1	3	5	14	19	24	min	8	Andesitic breccia	0.013	0.018	0.026	0.013	12.9596	0.0540	53.8322	0.1300	129.5960	25	30	20			
220	220		410458	9144263	6	13	20	1	3	5	5	7	9	min	3	Siltstone	0.0073	0.013	0.018	0.007	7.2773	0.0390	38.8788	0.0900	89.7203	17	19	13	1		
221	221		410113	9144229	6	13	20	1	3	5	5	7	9	min	3	Siltstone	0.0073	0.013	0.018	0.007	7.2773	0.0390	38.8788	0.0900	89.7203	17	19	13			
222	222		410012	9144256	6	13	20	0.25	0.625	1	14	19	24	min	5	Andesitic breccia	0.013	0.018	0.026	0.003	3.2399	0.0113	11.2150	0.0260	25.9192	25	30	20			
223	223		409758	9144325	6	13	20	1	3	5	14	19	24	min	4	Andesitic breccia	0.013	0.018	0.026	0.013	12.9596	0.0540	53.8322	0.1300	129.5960	25	30	20			1

224	224		409517	9144499	23	30.5	38	5	15	25	14	19	24		7	Andesitic breccia	0.024	0.035	0.040	0.120	119.6271	0.5250	523.3684	1.0000	996.8922	32	33	26		
225	225		409267	9144602	6	13	20	1	3	5	14	19	24		5	Andesitic breccia	0.013	0.018	0.026	0.013	12.9596	0.0540	53.8322	0.1300	129.5960	25	30	20		
226	226		409319	9144890	6	13	20	1	3	5	14	19	24	min	5	Andesitic breccia	0.013	0.018	0.026	0.013	12.9596	0.0540	53.8322	0.1300	129.5960	25	30	20		
227	227		409169	9145137	14	21	28	1	3	5	14	19	24	min	5	Andesitic breccia	0.018	0.024	0.036	0.018	17.9441	0.0720	71.7762	0.1800	179.4406	28	33	23		
228	228		409120	9145252	6	13	20	0.25	0.625	1	14	19	24	min	5	Andesitic breccia	0.013	0.018	0.026	0.003	3.2399	0.0113	11.2150	0.0260	25.9192	25	30	20		1
229	229		409033	9145270	14	21	28	1	3	5	14	19	24	min	5	Andesitic breccia	0.018	0.024	0.036	0.018	17.9441	0.0720	71.7762	0.1800	179.4406	28	33	23		
230	230		408582	9144990	6	13	20	1	3	5	14	19	24	min	5	Andesitic breccia	0.013	0.018	0.026	0.013	12.9596	0.0540	53.8322	0.1300	129.5960	25	30	20		1
231	231		408791	9144581	6	13	20	0.25	0.625	1	14	19	24	min	5	Andesitic breccia	0.013	0.018	0.026	0.003	3.2399	0.0113	11.2150	0.0260	25.9192	25	30	20		
232	232		409329	9144174	6	13	20	1	3	5	14	19	24	min	3	Andesitic breccia	0.013	0.018	0.026	0.013	12.9596	0.0540	53.8322	0.1300	129.5960	25	30	20		
233	233		409212	9144075	14	21	28	1	3	5	14	19	24		3	Andesitic breccia	0.018	0.024	0.036	0.018	17.9441	0.0720	71.7762	0.1800	179.4406	28	33	23		
234	234		409070	9144108	14	21	28	1	3	5	14	19	24		3	Andesitic breccia	0.018	0.024	0.036	0.018	17.9441	0.0720	71.7762	0.1800	179.4406	28	33	23		
235	235		408825	9144176	14	21	28	1	3	5	14	19	24		4	Andesitic breccia	0.018	0.024	0.036	0.018	17.9441	0.0720	71.7762	0.1800	179.4406	28	33	23		
236	236		408450	9144157	6	13	20	0.25	0.625	1	14	19	24	min	5	Andesitic breccia	0.013	0.018	0.026	0.003	3.2399	0.0113	11.2150	0.0260	25.9192	25	30	20		
237	237		408652	9143923	6	13	20	1	3	5	14	19	24	min	6	Andesitic breccia	0.013	0.018	0.026	0.013	12.9596	0.0540	53.8322	0.1300	129.5960	25	30	20		
238	238		408885	9143889	14	21	28	1	3	5	14	19	24	min	5	Andesitic breccia	0.018	0.024	0.036	0.018	17.9441	0.0720	71.7762	0.1800	179.4406	28	33	23		
239	239		409191	9143784	14	21	28	1	3	5	14	19	24	min	5	Andesitic breccia	0.018	0.024	0.036	0.018	17.9441	0.0720	71.7762	0.1800	179.4406	28	33	23		
240	240		409381	9143682	6	13	20	0.25	0.625	1	14	19	24	min	5	Andesitic breccia	0.013	0.018	0.026	0.003	3.2399	0.0113	11.2150	0.0260	25.9192	25	30	20		
241	241		409527	9143718	14	21	28	1	3	5	14	19	24		4	Andesitic breccia	0.018	0.024	0.036	0.018	17.9441	0.0720	71.7762	0.1800	179.4406	28	33	23		
242	242	Oct 27, 2010	410668	9142277	14	21	28	1	3	5	14	19	24	min	8	Andesitic breccia	0.018	0.024	0.036	0.018	17.9441	0.0720	71.7762	0.1800	179.4406	28	33	23		
243	243		410817	9142226	14	21	28	1	3	5	14	19	24	min	5	Andesitic breccia	0.018	0.024	0.036	0.018	17.9441	0.0720	71.7762	0.1800	179.4406	28	33	23		
244	244		410942	9142159	14	21	28	1	3	5	14	19	24	min	5	Andesitic breccia	0.018	0.024	0.036	0.018	17.9441	0.0720	71.7762	0.1800	179.4406	28	33	23		
245	245		409674	9143490	14	21	28	1	3	5	14	19	24	min	5	Andesitic breccia	0.018	0.024	0.036	0.018	17.9441	0.0720	71.7762	0.1800	179.4406	28	33	23		
246	246		409387	9143574	37	46	55	25	37.5	50	14	19	24	min	3	Andesitic breccia	0.035	0.044	0.053	0.875	872.2807	1.6500	1644.8721	2.6500	2641.7643	37	41	31		
247	247		409512	9146701	37	46	55	25	37.5	50	20	25	30	min	3	Andesite (lava)	0.039	0.047	0.058	0.975	971.9699	1.7625	1757.0225	2.9000	2890.9874	39	43	34		
248	248		409384	9146744	14	21	28	1	3	5	14	19	24		4	Andesitic breccia	0.018	0.024	0.036	0.018	17.9441	0.0720	71.7762	0.1800	179.4406	28	33	23		
249	249		409348	9146776	14	21	28	1	3	5	14	19	24		6	Andesitic breccia	0.018	0.024	0.036	0.018	17.9441	0.0720	71.7762	0.1800	179.4406	28	33	23	1	1
250	250		408117	9147632	6	13	20	0.25	0.625	1	14	19	24		5	Andesitic breccia	0.013	0.018	0.026	0.003	3.2399	0.0113	11.2150	0.0260	25.9192	25	30	20		1
251	251	Oct 31, 2010	405947	9143054	6	13	20	0.25	0.625	1	20	25	30	min	4	Andesite (lava)	0.015	0.020	0.028	0.004	3.7383	0.0125	12.4612	0.0280	27.9130	28	33	23		
252	252	Nov 01, 2010	414804	9137634	27	35.5	44	1	3	5	5	7	9	min	3	Siltstone	0.02	0.028	0.031	0.020	19.9378	0.0840	83.7389	0.1550	154.5183	25	26	20		
253	253		413236	9143891	14	21	28	0.25	0.625	1	13	17	21	min	3	Sandstone	0.015	0.024	0.035	0.004	3.7383	0.0150	14.9534	0.0350	34.8912	27	33	22		
254	254		413223	9144663	14	21	28	0.25	0.625	1	13	17	21	min	3	Sandstone	0.015	0.024	0.035	0.004	3.7383	0.0150	14.9534	0.0350	34.8912	27	33	22		
255	255		411327	9143972	6	13	20	1	3	5	14	19	24	min	4	Andesitic breccia	0.013	0.018	0.026	0.013	12.9596	0.0540	53.8322	0.1300	129.5960	25	30	20		
256	256		410358	9143737	6	13	20	0.25	0.625	1	14	19	24	min	5	Andesitic breccia	0.013	0.018	0.026	0.003	3.2399	0.0113	11.2150	0.0260	25.9192	25	30	20		
257	257		409812	9143934	6	13	20	0.25	0.625	1	14	19	24	min	4	Andesitic breccia	0.013	0.018	0.026	0.003	3.2399	0.0113	11.2150	0.0260	25.9192	25	30	20		
258	258		410503	9142937	6	13	20	1	3	5	14	19	24	min	6	Andesitic breccia	0.013	0.018	0.026	0.013	12.9596	0.0540	53.8322	0.1300	129.5960	25	30	20		1
259	259		410414	9142808	6	13	20	1	3	5	14	19	24	min	6	Andesitic breccia	0.013	0.018	0.026	0.013	12.9596	0.0540	53.8322	0.1300	129.5960	25	30	20		1

APPENDIX 3. Calculation of regolith bulk density

No	Code	Site	Shape	Dimension (m)				Volume	Weight	Bulk Density		Lithology	Formation	Sum of each formation	Regolith Bulk Density (Average)
				Length	Width	Height	Diameter	(m^3)	kg	kg/m^3	(KN/m^3)				
1	AB1	245	Cilinder	-	-	0.122	0.055	0.000290	0.35532	1225.377197	12.016845	Andesitic breccia	Kebobutak		Colluvium ≈ Young Volc. Deposits of Merapi Volc.≈ Kebobutak =
2	AB2	96	Cilinder	-	-	0.122	0.055	0.000290	0.34132	1177.095984	11.543368	Andesitic breccia	Kebobutak		11.790
3	AB3	73	Cilinder	-	-	0.122	0.055	0.000290	0.35732	1232.274513	12.084485	Andesitic breccia	Kebobutak	Sentolo =	Sentolo =
4	AB4	41	Cilinder	-	-	0.122	0.055	0.000290	0.3722	1283.590546	12.587723	Andesitic breccia	Kebobutak	32.728812	10.910
5	AB5	256	Cilinder	-	-	0.122	0.055	0.000290	0.3058	1054.599648	10.342090	Andesitic breccia	Kebobutak	Jonggrangan =	Jonggrangan =
6	AL1	152	Cilinder	-	-	0.122	0.055	0.000290	0.35317	1217.962582	11.944133	Andesite (lava)	Kebobutak	86.796888	17.359
7	AL2	251	Cilinder	-	-	0.122	0.055	0.000290	0.38322	1321.594758	12.960417	Andesite (lava)	Kebobutak	Kebobutak =	Kebobutak =
8	CL1	204	Cilinder	-	-	0.122	0.055	0.000290	0.33247	1146.575359	11.244063	Conglomerate	Jonggrangan	94.318978	11.790
9	CL2	1	Cilinder	-	-	0.122	0.055	0.000290	0.43067	1485.233585	14.565166	Conglomerate	Jonggrangan		Nanggulan ≈ Sentolo =
10	SS1	10	Cube	0.045	0.045	0.036	-	0.000073	0.1145	1570.644719	15.402763	Sandstone	Jonggrangan		10.910
11	SL1	84	Cilinder	-	-	0.122	0.055	0.000290	0.2332	804.227070	7.886773	Siltstone	Sentolo		
12	SL2	82	Cube	0.042	0.034	0.03	-	0.000043	0.06728	1570.494865	15.401293	Siltstone	Sentolo		
13	SL3	252	Cube	0.07	0.063	0.055	-	0.000243	0.2335	962.688106	9.440745	Siltstone	Sentolo		
14	CS1	21	Cilinder	-	-	0.122	0.055	0.000290	0.32052	1105.363895	10.839917	Claystone	Kebobutak		
15	LS1	76	Cube	0.05	0.045	0.023	-	0.000052	0.07552	1459.323671	14.311076	Limestone	Jonggrangan		
16	LS2	8	Cube	0.038	0.037	0.029	-	0.000041	0.13003	3189.042037	31.273819	Limestone	Jonggrangan		

APPENDIX 4. Validation using Degree of Fit (DF)

No	Scenario	Landslide Hazard Map Scenarios	Hazardous Area (m squared)						Degree of Fit (DF)						Accuracy	Rangking			Rank of Total
			High		Moderate		Low		High		Moderate		Low			High	Low	Total	
			mi	*ti*	*mi*	*ti*	*mi*	*ti*	(normal)	(%)	(normal)	(%)	(normal)	(%)					
1	24	HGSI, KI, WI-based water saturation	16200	7809400	500	298600	1194	36506200	0.5486	54.86	0.4428	44.28	0.0086	0.86	Moderate	1	4		1
2	22	HGSI, KI, 50% water saturation	12900	7386600	800	273500	1224	36954100	0.3712	37.12	0.6217	62.17	0.0070	0.70	Moderate	2	1		2
3	23	HGSI, KI, 100% water saturation	6300	4225400	700	277300	1291	40111500	0.3684	36.84	0.6237	62.37	0.0080	0.80	Moderate	3	3		3
4	15	MGSI, KI, 100% water saturation	5200	4886000	3000	967500	1279	38760700	0.2535	25.35	0.7386	73.86	0.0079	0.79	Low	4	2		4
5	2	LGSI, NPI, 50% water saturation	2500	5263400	0	512100	3000	38838700	0.8601	86.01	0.0000	0.00	0.1399	13.99	Low	5	5	10	5
6	1	LGSI, NPI, 0% water saturation	4000	5349900	0	313400	13210	38950900	0.6879	68.79	0.0000	0.00	0.3121	31.21	Low	6	12	18	6
7	19	HGSI, NPI, 100% water saturation	67200	16162700	700	385900	68000	28061700	0.4953	49.53	0.2161	21.61	0.2887	28.87	Low	10	11	21	7
8	20	HGSI, NPI, WI-based water saturation	105000	29242200	0	116400	30900	15251700	0.6393	63.93	0.0000	0.00	0.3607	36.07	Low	7	14	21	8
9	18	HGSI, NPI, 50% water saturation	104900	29024600	100	284500	30900	15301200	0.6039	60.39	0.0587	5.87	0.3374	33.74	Low	9	13	22	9
10	3	LGSI, NPI, 100% water saturation	19400	5130000	26300	6835300	90400	32648900	0.3637	36.37	0.3700	37.00	0.2663	26.63	Low	14	9	23	10
11	17	HGSI, NPI, 0% water saturation	105000	29316900	0	75200	30900	15218200	0.6382	63.82	0.0000	0.00	0.3618	36.18	Low	8	15	23	11
12	8	LGSI, KI, WI-based water saturation	46500	13894600	13500	1159200	76100	29560400	0.1905	19.05	0.6629	66.29	0.1465	14.65	Low	22	6	28	12
13	5	LGSI, KI, 0% water saturation	52000	14196000	10300	946200	73800	29472000	0.2148	21.48	0.6384	63.84	0.1468	14.68	Low	21	7	28	13
14	18	MGSI, NPI, 50% water saturation	21100	6140900	1400	1282900	113600	37190400	0.4532	45.32	0.1439	14.39	0.4029	40.29	Low	11	18	29	14
15	7	LGSI, KI, 100% water saturation	30800	11658500	15800	3273700	89500	29682000	0.2520	25.20	0.4604	46.04	0.2876	28.76	Low	20	10	30	15
16	11	MGSI, NPI, 100% water saturation	18900	5259500	2000	1285800	115200	38068900	0.4396	43.96	0.1903	19.03	0.3702	37.02	Low	13	17	30	16
17	6	LGSI, KI, 50% water saturation	41300	13748600	16600	1379100	78200	29486500	0.1698	16.98	0.6803	68.03	0.1499	14.99	Low	23	8	31	17
18	16	MGSI, KI, WI-based water saturation	20100	7149700	2400	906100	113600	36558400	0.3281	32.81	0.3092	30.92	0.3627	36.27	Low	16	16	32	18
19	12	MGSI, NPI, WI-based water saturation	21100	6307400	1500	1392900	113500	36913900	0.4462	44.62	0.1436	14.36	0.4101	41.01	Low	12	20	32	19
20	13	MGSI, KI, 0% water saturation	25300	9932800	1400	846200	109400	33835200	0.3426	34.26	0.2225	22.25	0.4349	43.49	Low	15	21	36	20
21	14	MGSI, KI, 50% water saturation	16800	6658500	2000	924700	117300	37031000	0.3213	32.13	0.2754	27.54	0.4033	40.33	Low	18	19	37	21
22	21	HGSI, KI, 0% water saturation	19300	8590100	400	283000	116400	35741100	0.3248	32.48	0.2043	20.43	0.4708	47.08	Low	17	22	39	22
23	9	MGSI, NPI, 0% water saturation	21100	9649900	2400	1541700	112600	33422600	0.3074	30.74	0.2189	21.89	0.4737	47.37	Low	19	23	42	23
24	4	LGSI, NPI, WI-based water saturation	2800	5286600	600	420200	132700	38907400	0.0987	9.87	0.2660	26.60	0.6353	63.53	Low	24	24	48	24

Note :
LGSI : Lower GSI data
MGSI : Mean GSI data
HGSI : Higher GSI data
NPI : Nearest point interpolation
KI : Kriging interpolation

: High
: Moderate
: Low

APPENDIX 5. Descriptions of some landslides

Landslide at site 63

This landslide was located at Purwosari village, Girimulyo district. This was an old landslide that occured in rainy season 2009.
According to Kusky's landslide type (2008), this landslide was a debris flow that involved the downslope movement of unconsolidated regolith and most of which was coarser than sand. It involved andesitic breccia rock mass at slope 19.00°.
Its GSI data showed low data of GSI value (6-20 MPa), low ucs value (1-5), and *mi* (andesitic breccia) (14-24), that resulted cohesion (12.96-129.60 KN/m^2) and friction angle (20-30°).

Landslide at site 93

This landslide was located at Kebonharjo village, Samigaluh district. This was a new landslide that occured on February 2010 and damaged 1 house.
According to Kusky's landslide type (2008), this landslide was a slump that a type of sliding slope failure in which a downward and outward rotational movement of rock or regolith occurs along a concave up slip surface. It involved andesitic breccia rock mass at slope 17.23°.
Its GSI data showed low data of GSI value (6-20 MPa), low ucs value (1-5), and *mi* (andesitic breccia) (14-24), that resulted cohesion (12.96-129.60 KN/m^2) and friction angle (20-30°).

Landslide at site 100

This landslide was located at Giripurwo village, Girimulyo district. This was an old landslide that occured in 2007 and damaged 1 house.
According to Kusky's landslide type (2008), this landslide was a debris flow that involved the downslope movement of unconsolidated regolith and most of which was coarser than sand. It involved andesitic breccia rock mass at slope 19.00°.
Its GSI data showed data of GSI value (6-20 MPa), UCS value (1-5), and *mi* (andesitic breccia) (14-24), that resulted cohesion (12.96-129.60 KN/m^2) and friction angle (20-30°).

Landslide at site 104

This small landslide was located at Purwosari village, Girimulyo district. This was a new landslide that occured on October 17, 2010 when the heavy rain happened in the night.
According to Kusky's landslide type (2008), this landslide was a debris flow that involved the downslope movement of unconsolidated regolith and most of which was coarser than sand. It involved andesitic breccia rock mass at slope 19.80°.
Its GSI data showed data of GSI value (14-28 MPa), UCS value (5-25), and *mi* (andesitic breccia) (14-24), that resulted cohesion (17.94-179.44 KN/m^2) and friction angle (23-33°).

Landslide at site 105

This landslide was located at Purwosari village, Girimulyo district. This was a new landslide that accured on October 17, 2010 when the heavy rain happened in the night.
According to Kusky's landslide type (2008), this landslide was a debris flow that involved the downslope movement of unconsolidated regolith and most of which was coarser than sand. It involved andesitic breccia rock mass at slope 26.61°.
Its GSI data showed data of GSI value (6-20 MPa), UCS value (1-5), and *mi* (andesitic breccia) (14-24), that resulted cohesion (12.96-129.60 KN/m^2) and friction angle (20-30°).

Landslide at site 132

This landslide was located at Purwosari village, Girimulyo district. This was an old landslide that occured in about July 2010.
According to Kusky's landslide type (2008), this landslide was a debris flow that involved the downslope movement of unconsolidated regolith and most of which was coarser than sand. It involved andesitic breccia rock mass at slope 16.71°.
Its GSI data showed data of GSI value (6-20 MPa), UCS value (1-5), and *mi* (andesitic breccia) (14-24), that resulted cohesion (12.96-129.60 KN/m^2) and friction angle (20-30°).

Landslide at site 133

This small landslide was located at Purwosari village, Girimulyo district. This was a new landslide that occured in October 2010.
According to Kusky's landslide type (2008), this landslide was a debris flow that involved the downslope movement of unconsolidated regolith and most of which was coarser than sand. It involved andesitic breccia rock mass at slope 12.42°.
Its GSI data showed data of GSI value (6-20 MPa), UCS value (1-5), and *mi* (andesitic breccia) (14-24), that resulted cohesion (12.96-129.60 KN/m^2) and friction angle (20-30°).

Landslide at site 145

This landslide was located at Purwosari village, Girimulyo district. This was a new landslide that occured in August 2010.
According to Kusky's landslide type (2008), this landslide was a mud flow that resembles debris flows, except that they have higher concentrations of water (up to 30 percent) that make them more fluid, with a consistency ranging from soup to wet concrete. It involved claystone at slope 15.07°.
Its GSI data showed data of GSI value (55-80 MPa), UCS value (0.25-1), and *mi* (andesitic breccia) (2-6), that resulted cohesion (9.97-109.67 KN/m^2) and friction angle (25-31°).

Landslide at site 159

This landslide was located at Giripurwo village, Girimulyo district. This was a new landslide that occured in October 2010.
According to Kusky's landslide type (2008), this landslide was a debris flow that involved the downslope movement of unconsolidated regolith and most of which was coarser than sand. It involved andesitic breccia rock mass at slope 20.39°.
Its GSI data showed data of GSI value (6-20 MPa), UCS value (1-5), and *mi* (andesitic breccia) (14-24), that resulted cohesion (12.96-129.60 KN/m^2) and friction angle (20-30°).

Landslide at site 168

This small landslide was located at Pendoworejo village, Girimulyo district. This was a new landslide that occured in October 2010.
According to Kusky's landslide type (2008), this landslide was a debris flow that involved the downslope movement of unconsolidated regolith and most of which was coarser than sand. It involved andesitic breccia rock mass at slope 34.38°.
Its GSI data showed data of GSI value (14-28 MPa), UCS value (1-5), and *mi* (andesitic breccia) (14-24), that resulted cohesion (17.94-179.44 KN/m^2) and friction angle (23-33°).

Landslide at site 186

This landslide was located at Pendoworejo village, Girimulyo district. This was a new landslide that occured in about April 2010 (*Setu wage*). The dike was built to strengthen the slope.
According to Kusky's landslide type (2008), this landslide was a debris flow that involved the downslope movement of unconsolidated regolith and most of which was coarser than sand. It involved andesitic breccia rock mass at slope 24.75°.
Its GSI data showed data of GSI value (6-20 MPa), UCS value (1-5), and *mi* (andesitic breccia) (14-24), that resulted cohesion (12.96-129.60 KN/m^2) and friction angle (20-30°).

Landslide at site 211

This small landslide was located at Pendoworejo village, Girimulyo district. This was a new landslide that occured in October 2010.
According to Kusky's landslide type (2008), this landslide was a debris flow that involved the downslope movement of unconsolidated regolith and most of which was coarser than sand. It involved andesitic breccia rock mass at slope 21.31°.
Its GSI data showed data of GSI value (6-20 MPa), UCS value (0.25-1), and *mi* (andesitic breccia) (14-24), that resulted cohesion (3.24-25.92 KN/m^2) and friction angle (20-30°).

Landslide at site 230

This small landslide was located at Purwosari village, Girimulyo district. This was a new landslide that occured in October 2010.
According to Kusky's landslide type (2008), this landslide was a debris flow that involved the downslope movement of unconsolidated regolith and most of which was coarser than sand. It involved andesitic breccia rock mass at slope 17.55°.
Its GSI data showed data of GSI value (6-20 MPa), UCS value (1-5), and *mi* (andesitic breccia) (14-24), that resulted cohesion (12.96-129.60 KN/m^2) and friction angle (20-30°).

Landslide at site 228

This small landslide was located at Pendoworejo village, Girimulyo district. This was a new landslide that occured in October 2010.
According to Kusky's landslide type (2008), this landslide was a debris flow that involved the downslope movement of unconsolidated regolith and most of which was coarser than sand. It involved andesitic breccia rock mass at slope 9.76°.
Its GSI data showed data of GSI value (6-20 MPa), UCS value (0.25-1), and *mi* (andesitic breccia) (14-24), that resulted cohesion (3.24-25.92 KN/m^2) and friction angle (20-30°).

Landslide at site 249

This landslide was located at Purwosari village, Girimulyo district. This was an old landslide that moved again as new landslide that occured twice in October 17 and 18, 2010.
According to Kusky's landslide type (2008), this landslide was a debris flow that involved the downslope movement of unconsolidated regolith and most of which was coarser than sand. It involved andesitic breccia rock mass at slope 23.42°.
Its GSI data showed data of GSI value (14-28 MPa), UCS value (1-5), and *mi* (andesitic breccia) (14-24), that resulted cohesion (17.94-179.44 KN/m^2) and friction angle (23-33°).

Landslide at site 250

This landslide was located at Banjarsari village, Samigaluh district. This was a new landslide that occured in 2010 and damaged 1 house.
According to Kusky's landslide type (2008), this landslide was a debris flow that involved the downslope movement of unconsolidated regolith and most of which was coarser than sand. It involved andesitic breccia rock mass at slope 16.71°.
Its GSI data showed data of GSI value (6-20 MPa), UCS value (0.25-1), and *mi* (andesitic breccia) (14-24), that resulted cohesion (3.24-25.92 KN/m^2) and friction angle (20-30°).